NASA CONTRACTOR REPORT

NASA CR-2696

REFLECTION-PLANE TESTS OF SPOILERS ON AN ADVANCED TECHNOLOGY WING WITH A LARGE FOWLER FLAP

W. H. Wentz, Jr., and C. G. Volk, Jr.

Prepared by
WICHITA STATE UNIVERSITY
Wichita, Kans. 67208
for Langley Research Center

NATIONAL AERONAUTICS AND SPACE ADMINISTRATION • WASHINGTON, D. C. • JULY 1976

1. Report No.	2. Government Accession No.	3. Recipient's Catalog No.
NASA CR-2696		

4. Title and Subtitle	5. Report Date
Reflection-Plane Tests of Spoilers on an Advanced Technology Wing with a Large Fowler Flap	July 1976
	6. Performing Organization Code
7. Author(s) W. H. Wentz, Jr., and C. G. Volk, Jr.	8. Performing Organization Report No. WSU AR 75-2
9. Performing Organization Name and Address Wichita State University Wichita, KS 67208	10. Work Unit No.
	11. Contract or Grant No. NSG 1118
12. Sponsoring Agency Name and Address National Aeronautics and Space Administration Washington, D.C. 20546	13. Type of Report and Period Covered Contractor Report
	14. Sponsoring Agency Code

15. Supplementary Notes

Langley technical monitor: Harold Crane

16. Abstract

Wind tunnel experiments have been conducted to determine the effectiveness of spoilers applied to a finite-span wing which utilizes the GA(W)-1 airfoil section and a 30% chord full-span Fowler flap. A series of spoiler cross-sectioned shapes were tested utilizing a reflection-plane model. Five-component force characteristics and hinge moment measurements were obtained. Results confirm earlier two-dimensional tests which had shown that spoilers could provide large lift increments at any flap setting, and that spoiler control reversal tendencies could be eliminated by providing a vent path from lower surface to upper surface. Performance penalties due to spoiler leakage airflow were measured in the present tests.

17. Key Words (Suggested by Author(s))	18. Distribution Statement
Spoilers, with Fowler Flap, reflection plane	Unclassified - unlimited Subject Category 02

19. Security Classif. (of this report)	20. Security Classif. (of this page)	21. No. of Pages	22. Price*
Unclassified	Unclassified	88	$4.75

* For sale by the National Technical Information Service, Springfield, Virginia 22161

SUMMARY

Wind tunnel experiments have been conducted to determine the effectiveness of spoilers applied to a finite-span wing which utilizes the GA(W)-1 airfoil section and a 30% chord full-span Fowler flap. A series of spoiler cross-sectioned shapes were tested utilizing a reflection-plane model. Five-component force characteristics and hinge moment measurements were obtained. Results confirm earlier two-dimensional tests which had shown that spoilers could provide large lift increments at any flap setting, and that spoiler control reversal tendencies could be eliminated by providing a vent path from lower surface to upper surface. Performance penalties due to spoiler leakage airflow were measured in the present tests.

INTRODUCTION

Earlier reports (refs. 1,2) have documented the results of two-dimensional wind tunnel tests of spoilers applied to the GA(W)-1 airfoil section. These tests show that for certain spoiler configurations applied to an airfoil with a large Fowler flap, a control dead-band or reversal occurs for small spoiler deflections. These characteristics had also been reported in earlier NACA spoiler research with large Fowler flaps (ref. 3).

The purpose of the present wind tunnel research is to obtain experimental information as to the effectiveness of spoilers applied to a three-dimensional wing utilizing the GA(W)-1 airfoil with a large Fowler flap and to obtain spoiler hinge moment measurements. For this purpose, a reflection-plane model was selected for the test configuration. The model was designed to represent a wing panel of the Advanced Technology Light Twin (ATLIT) research vehicle currently undergoing flight evaluation at NASA Langely Research Center (refs. 4,5). The model was designed to permit testing of various spoiler configurations, and flap settings from 0° to 40°.

SYMBOLS

The lift, drag, and pitching moment data have been referred to the mean .25c location of the exposed planform. Reference area for these data is exposed planform area. Rolling moment and yawing moment measurements have been referred to an equivalent airplane centerline location (beneath the tunnel floor), and are non-dimensionalized with respect to total equivalent wing area and total equivalent span, including the portion of the wing covered by the fuselage. Figure 1 illustrates the reference points, lengths and areas described above.

Dimensional quantities are given in both International (S.I.) units and in U.S. Customary units. Conversion factors between the various units may be found in reference 6. The symbols used in the present report are defined as follows:

A	aspect ratio, $(\text{span})^2/\text{area}$
b_t	model reference span, including image
c	model chord at spoiler mid-span
$\bar{c}$	model mean aerodynamic chord, based upon exposed area, flap nested
c_{sp}	spoiler chord
C_D	model drag coefficient, drag/(dynamic pressure x S_e)
C_H	spoiler hinge moment coefficient, hinge moment/(dynamic pressure x S_{sp} x c_{sp}) (opening moment is positive)
C_l	section lift coefficient
C_L	model lift coefficient, lift/(dynamic pressure x S_e)
C_M	model pitching moment coefficient, pitching moment/(dynamic pressure x S_e x c)
$C_{l\alpha}$	section lift curve slope, per degree
$C_{L\alpha}$	wing lift curve slope, per degree
C_{ℓ}	model rolling moment coefficient, rolling moment/(dynamic pressure x S_t x b_t)
C_N	model yawing moment coefficient, yawing moment/(dynamic pressure x S_t x b_t)
e	span efficiency factor
Δh	spoiler trailing edge projection height
RN	Reynolds number based on mean aerodynamic chord

S_e	model exposed planform area
S_t	full-span planform area, including fuselage carryover
α	angle of attack of wing root chord, degrees
Δ	increment
δ	rotation of surface from nested position, degrees

Subscripts

f	flap
i	induced
sp	spoiler
t	total

EXPERIMENTAL INVESTIGATIONS

Wind Tunnel Models and Instrumentation

All tests were conducted using a 1/4 scale reflection-plane model representative of the exposed right-hand wing of the ATLIT airplane, without nacelles (ref. 5). The model (figs. 1,2) was milled from solid aluminum to provide maximum flexibility in machining spoiler and flap cutouts and attaching brackets, etc. The ATLIT wing utilizes the 17% thick GA(W)-1 airfoil section (ref. 1) at root and tip, with a taper ratio of 0.53, unswept 50% chord, 3° twist (washout) and 7° dihedral.

All testing was conducted in the WSU 2.13m x 3.05m (7' x 10') low speed tunnel. An aluminum disk of 0.76m (2.5') diameter was fitted at the wing root to act as an end-plate seal. This plate provided an offset of 1.27cm (0.50 inches) above the tunnel floor to minimize tunnel wall boundary layer effects. The model spar attached directly to the tunnel main balance for direct force measurements. All data have been corrected for end plate drag, and for wall effects as outlined in reference 7. Detailed computer program listings and sample calculations are given in the Appendices.

The model was fitted with a 30% chord Fowler flap, attached at four spanwise locations. A series of brackets were fabricated to provide various flap settings. A cavity was milled in the wing to simulate the spoiler cutout and approximate rib structure of the airplane. Two strain-gaged flexures were designed to provide for spoiler attachment and hinge moment measurement. Each flexure utilized a full four-gage bridge. A series of wedge blocks were fabricated to provide for spoiler deflections from -5° to +60°. Several spoiler cross-sectional shapes were fabricated (fig. 3). Tests were conducted at a Reynolds number of 1.0×10^6, based upon the wing mean aerodynamic chord length of 29.21 cm (11.50 inches).

Flap-Nested Performance

Predictions of finite-span wing performance may be made from two-dimensional data by applying the following corrections:

(a) Adjust the angle of zero lift to account for wing twist at the M.A.C. For this model the M.A.C. twist is -1.4° relative to the wing root chord reference.

(b) Correct the lift-curve slope according to the following formula from reference 8:

$$C_{L\alpha} = \frac{C_{l\alpha}}{1 + \frac{57.3\ C_{l\alpha}}{\pi e A}} \qquad (1)$$

(c) Correct the drag by adding an induced drag term given by the following formula from reference 8:

$$C_{D_i} = \frac{C_L^{\,2}}{\pi e A} \qquad (2)$$

In these equations, e is the span efficiency factor, taken as 0.8.

Applying the offset and slope change calculated as described in (a) and (b), the experimental C_l vs. α relationship gives the predicted three-dimensional relationship shown in figure 4. It is seen that this prediction agrees well with the experimental three-dimensional data, even through the stall.

Table 1 illustrates comparisons of some predicted and experimental aerodynamic parameters. The two-dimensional values are from reference 9.

Table 1 - Predicted and Experimental Three-Dimensional Aerodynamic Parameters

Parameter	2-D Value (ref. 9)	Predicted 3-D Value	Experimental 3-D Value
Zero lift angle	-3.8°	-2.4°	-2.6°
Lift curve slope	0.112/deg.	.0883/deg.	.087/deg.
Maximum lift coefficient	1.57	1.35	1.36

A predicted drag polar for the flap-nested case is developed from two-dimensional data, with the added induced drag based upon an 80% span efficiency factor. As shown in the figure, the experimental three-dimensional relationship agrees well with the prediction, except for lift coefficients near stall.

Two- and three-dimensional pitching moment data are also compared in figure 4. In this case the pitching moment values are compared directly, based upon measurements referred to the 25% mean aerodynamic chord of the three-dimensional planform. The comparison shows good agreement.

Flap-Extended Performance

A series of baseline runs were made to obtain the aerodynamic characteristics of the basic reflection-plane wing for various flap settings, with spoilers closed and sealed. These data (figs. 5, 6, and 7) show the basic lift, drag and pitching moment characteristics of the reflection-plane model. Tabulated flap gap and overlap are shown for each flap deflection. These settings, with the exception of the 40° case, are the same as those developed from the two-dimensional GA(W)-1 tests reported in reference 9.

During initial force tests of the wing with 40° flap deflection, it was discovered that expected values for $C_{L_{MAX}}$ were not being attained. Tuft studies revealed that the flow over the flap was separated at all angles of attack. The flap brackets were then modified to provide for gap and overlap adjustment. Figure 8 illustrates definitions of gap and overlap. From the tuft studies it was determined that attached flow on the flap could be achieved with modified settings. Table 2 compares the best gap and overlap values for the present three-dimensional tests and the earlier two-dimensional tests.

Table 2 - Best Flap Settings for 40° Deflection

Source	Gap	Overlap	Reynolds Number
2-D (ref. 9 tests)	2.7%c	-0.7%c	2.2×10^6
3-D (Present tests)	2.2%c	+0.8%c	1.0×10^6

The results of the revised gap and overlap settings (fig. 8) show substantial improvement in linearity of the lift curve as well as in $C_{L_{MAX}}$ performance. All subsequent 40° flap testing was done with the revised gap and overlap settings.

The discrepancy in optimum flap settings between two-dimensional and three-dimensional tests merits discussion. Both tests utilized models of rigid construction to avoid possible aero-elastic deflection problems. The Reynolds numbers of the tests do differ, but only by a factor of 2. The tunnel balance load limits prohibited testing the reflection plane model at $C_{L_{MAX}}$ with 40° flap at RN = 2×10^6. It was possible to test this model at RN = 2×10^6 at zero angle of attack, however. This testing showed that the flap flow was not attached, indicating that the Reynolds number change is probably not responsible for the change in separation observed.

Three-dimensional effects on the flap slot flow are difficult to assess. However, for a wing with zero sweep (at 50% chord) little spanwise flow is to be expected. Tuft patterns tend to substantiate this, at least in the absence of separation. The reasons for the discrepancy in gap and overlap between two-dimensional and three-dimensional tests remain unexplained.

It is noted that the lift curves with flap extended have steeper slopes than the flap-nested case. This is expected, since the Fowler action provides an increase in effective chord. By accounting for the increase in wing area for each flap deflection it is possible to predict lift curve slopes for the flap extended cases. Results of calculations of this type are shown in figure 9, along with the experimental values. Agreement between experiment and prediction is good.

Flap effectiveness in producing increments in $C_{L_{MAX}}$ and in C_L at $\alpha = 0°$ is also shown in figure 9, along with corresponding data from the two-dimensional tests. These data show that the three-dimensional flap effectiveness is 70% to 80% of the two-dimensional values. For 40° flap, the present tests yield a $C_{L_{MAX}}$ value of 3.0 compared to a section $C_{l_{max}}$ of 3.8 from two-dimensional tests.

Using the method of reference 10, it is possible to calculate a correction factor relating two-dimensional flap effectiveness to three-dimensional effectiveness. For the ATLIT reflection-plane model, this parameter is 93% which compares unfavorably with the measurements as related above. The reasons for this discrepancy are not clear.

Theoretical drag polars for various flap settings have been calculated utilizing the experimental zero lift drag and span efficiency factors of 1.0 and 0.8. For this analysis no accounting has been made of section drag increases with lift coefficient, since in principle an optimum flap and slot can minimize separation drag. Results of this analysis are compared with experimental data in figure 6, which shows that a span efficiency of 0.8 gives a reasonably accurate assessment of optimum lift-drag performance available at any lift coefficient.

Spoiler Effectiveness and Hinge Moment Tests

In order to evaluate the influence of spoiler cross-sectional shape on control effectiveness, a series of five spoilers were tested. These shapes are shown in figure 3. They are similar to shapes evaluated in earlier two-dimensional spoiler tests (ref. 2).

Flap Nested Results. - Results of flap-nested tests are presented in figures 10 through 14. These data reflect good roll control characteristics, with rolling moment varying approximately in a linear fashion with spoiler projection height for all configurations. At the higher angles of attack, all configurations reflect some non-linearity for small deflections. This is an expected trend, on the basis that the boundary layer thickens near the trailing edge at high angles of attack. No cases of control reversal or hysteresis were observed, and control response is evidently satisfactory for all configurations. Yawing moment data indicate proverse (favorable) yawing which is characteristic of spoilers. The drag data show increases in drag with spoiler deflection, as expected. This drag force, of course, is responsible for the proverse yawing characteristic of spoiler lateral control systems.

The pitching moment data reflect a tendency to pitch nose-up as spoilers are deflected. This tendency is attributed to loss of lift over the aft portion of the wing resulting from the aft-mounted spoilers.

The hinge-moment characteristics show a nearly linear aerodynamic moment generated in opposition to the spoiler deflection. For zero deflection a substantial opening hinge moment is observed. This moment is generated by the pressure difference between upper and lower surfaces at zero spoiler deflection.

These tests show that all configurations produce satisfactory rolling characteristics with flap nested, and that all parameters, (rolling, yawing, etc.) are essentially independent of spoiler cross-section.

5° and 10° Flap Results - Limited runs with the triangle spoiler were conducted for small spoiler deflections at low flap settings. These runs were designed to determine whether control reversals observed for 40% flap would occur with low flap settings. The data (figs. 15 and 16) show that no reversal tendency is present for these cases.

30° Flap Results - Spoiler characteristics for the 30° flap setting are shown in figures 17 through 21. These data show non-linear rolling moment characteristics similar to data obtained from earlier two-dimensional tests (ref. 2). Even though substantial non-linearities are present, no cases of control reversal are observed.

The hinge-moment data with flap extended are characterized by a large opening hinge moment for zero spoiler deflection and by greater sensitivity to angle of attack than the flap-nested data. Both of these effects are attributed to the greater pressure difference across the spoilers resulting from the added lift carried by the wing trailing edge region with flap extended.

All spoilers except the flat plate and MU-2 configurations have a parabolic hinge moment curve with zero slope for small spoiler deflections. The flat plate and MU-2, on the other hand, have more nearly linear hinge moment characteristics, even for small deflections.

40° Flap Results - Results of spoiler tests with 40° flap deflection are shown in figures 22 through 26. These data show a greater tendency for non-linear control than the 30° flap configuration. The triangle, flat plate, and sharp triangle show no reversal. The MU-2 and TEE spoilers, on the other hand, show slight control reversals at high angles of attack for small deflections.

The hinge moment data for these configurations are similar to hinge moment trends observed with 30° flap, with the flat plate and MU-2 spoilers again providing more linear hinge moment trends. Unfortunately, even though the MU-2 configuration gives a nearly linear hinge moment characteristic, it suffers from control reversal at high-α, small deflections conditions.

Effects of Sealing the Spoiler Cavity - Earlier two-dimensional tests revealed that control reversal would occur with large flap deflections and small spoiler deflections, without cavity venting (ref. 2). These tests and earlier NACA data, (ref. 3) revealed that providing a vent path from the flap cavity lower surface would alleviate the reversal problem. A special run was made in the present test series to determine whether the reversal problem would be present in a three-dimensional case. For this run a sheet metal plate was fabricated to close the cavity vent lower surface. The edges of this plate were carefully sealed with tape to prevent leakage flow from acting on the spoiler.

Results of this run are shown in figure 27. These data show that the sealed configuration suffers from control reversal, just as observed in the two-dimensional case. The hinge moment data show zero hinge-moment at zero deflection, as would be expected for a sealed cavity.

Effects of a sealed spoiler cavity on flap nested performance were obtained by testing with a tape seal applied along the flap leading edge. Results of this test (fig. 28) show that adequate control response for the flap nested configuration can be obtained without venting. Again, the hinge moment data show zero moment at zero spoiler deflection.

Effects of Spoiler Gap Leaks on Wing Performance

In both the present tests and earlier two-dimensional tests, it has been demonstrated that providing lower surface ventilation to the spoilers is a key to insuring positive control for small deflections. Unfortunately, a vent path also permits some leakage airflow around spoiler leading and trailing edges with zero deflection.

This leakage flow results in large penalties in both lift and drag performance. A measure of these penalties was obtained in the present tests by conducting runs with the spoiler gaps sealed with tape, and with "normal" gaps. Results of these runs are shown in figures 29, 30 and 31. It should be noted that the proper cruising performance penalty is determined as a drag increment at constant lift coefficient, not at constant angle of attack.

A second problem with vented spoilers is that the wing lifting pressure difference provides a large opening hinge moment at zero spoiler deflection. This effect is magnified by operation with Fowler flaps extended. Thus vented spoilers will tend to float open if any of the control system linkage elements are poorly fitted or have inadequate stiffness. Drag penalties for various amounts of spoiler "float open" deflection at constant lift coefficient may be evaluated from figures 32 and 33.

Two methods seem possible for alleviating the gap leak problem. One method would be to seal the flap cavity with flap nested. This would eliminate the cruise drag penalty, and the data show that venting is not necessary with flap nested. The flap extended configuration must have venting, however, and the $C_{L_{MAX}}$ penalties noted for venting will still be present.

A second method would be to relocate the spoiler aft to the wing trailing edge. Such a "slot-lip" configuration seems to eliminate control reversal problems (ref. 2) and should be easier to seal than the present configuration.

Flow Visualization

Stall patterns with flap nested are shown in figure 34. These photos show that the flow separation begins at the wing trailing edge and progresses gradually forward as angle of attack is increased. The forward progression of the separation region begins at about the 20% semispan location. Even when $C_{L_{MAX}}$ is achieved, the flow is attached at the root and the tip. The two photos at 20° angle of attack indicate unsteady flow, with separation at mid-semispan ranging from 50% chord to the leading edge. Root and tip regions remain attached even at this extreme post-stall condition.

The initial separation patterns are quite similar to the patterns predicted by McVeigh and Kisielowski (ref. 11) for a wing with 0.5 taper ratio, 2.5° washout and NACA 44xx sections.

Stall patterns for 5° flap setting are shown in figure 35. These photos show that separation begins on the main airfoil section at the trailing edge, and progresses gradually forward, beginning at about 20% semispan. The flap flow remains attached through stall. Stall patterns for 10° and 30° flap settings (figs. 36 and 37) are similar to the 5° flap case.

Tuft photos for 40° flap are shown in figure 38. These photos were obtained with the three-dimensional optimized gap and overlap. Separation patterns are quite similar to those observed with lower flap settings. The flap flow remains attached at all angles of attack. Separation begins at about 20% semispan on the main airfoil section and shows gradual progression forward.

With the original gap and overlap based upon two-dimensional tests, tuft patterns (not recorded) showed flap separation over the entire angle of attack range.

CONCLUSIONS

1. Reflection plane tests of a 1/4 scale advanced technology wing show that flap-nested performance characteristics are very close to values predicted from two-dimensional data. Flaps down data, however, show that lift increments due to flaps are somewhat less than predicted values.

2. Reflection-plane wind tunnel tests of spoiler control effectiveness correlate well with earlier two-dimensional data.

3. Control dead-band and reversal tendencies are observed for large flap deflections. Control reversal is eliminated by lower surface venting, but non-linear control response remains.

4. Spoiler cross-sectional shape variations have relatively minor effects on control effectiveness.

5. Hinge moment measurements show that vented configurations are subject to rather large opening moments for zero spoiler with large flap deflections. These opening moments are attributed to wing lifting pressure distribution.

6. Tests of spoiler gap leak effects show that relatively small clearance gaps result in large penalties in $C_{L_{MAX}}$ and drag.

7. It is recommended that studies be conducted of slot-lip spoilers applied to the GA(W)-1 airfoil with a large Fowler flap to determine whether more linear control response can be obtained, without gap leak penalties.

REFERENCES

1. Wentz, W. H. Jr., Seetharam, H. C. and Calhoun, J. T.: Wind Tunnel and Flight Development of Spoilers for General Aviation Aircraft. SAE Paper 750523, 1975.

2. Wentz, W. H. Jr.: Effectiveness of Spoilers on the GA(W)-1 Airfoil with a High Performance Fowler Flap. NASA CR-2538, 1975.

3. Wenzinger, C. J. and Rogallo, R. M.: Wind-Tunnel Investigation of Spoiler, Deflector and Slot Lateral-Control Devices on Wings with Full-Span Split and Slotted Flaps. NACA TR706, 1940.

4. Crane, H. L., McGhee, R. J. and Kohlman, D. L.: Applications of Advanced Aerodynamic Technology to Light Aircraft. SAE Paper 730318, 1973.

5. Kohlman, D. L., Holmes, B. J. and Crane, H. L.: Preliminary Flight-Test Results of an Advanced Technology Light Twin-Engine Airplane. SAE Paper 750525, 1975.

6. Mechtly, E. A.: The International System of Units--Physical Constants and Conversion Factors (revised). NASA SP-7012, 1969.

7. Pope, A., and Harper, J. J.: Low-Speed Wind Tunnel Testing. John Wiley and Sons, Inc., 1966.

8. Dommasch, D. O., Sherby, S. S. and Connolly, T. F.: Airplane Aerodynamics. Pitman Publishing Corp., 1967.

9. Wentz, W. H. Jr., and Seetharam, H. C.: Development of a Fowler Flap System for a High Performance General Aviation Airfoil. NASA CR-2443, 1974.

10. Callaghan, J. G.: Aerodynamic Prediction Methods for Aircraft at Low Speeds with Mechanical High Lift Devices. AGARD Lecture Series No. 67, Von Karman Institute, Brussels, Belgium, 1974.

11. McVeigh, M. A. and Kisielowski, E.: A Design Summary of Stall Characteristics of Straight Wings. NASA CR-1646, 1971.

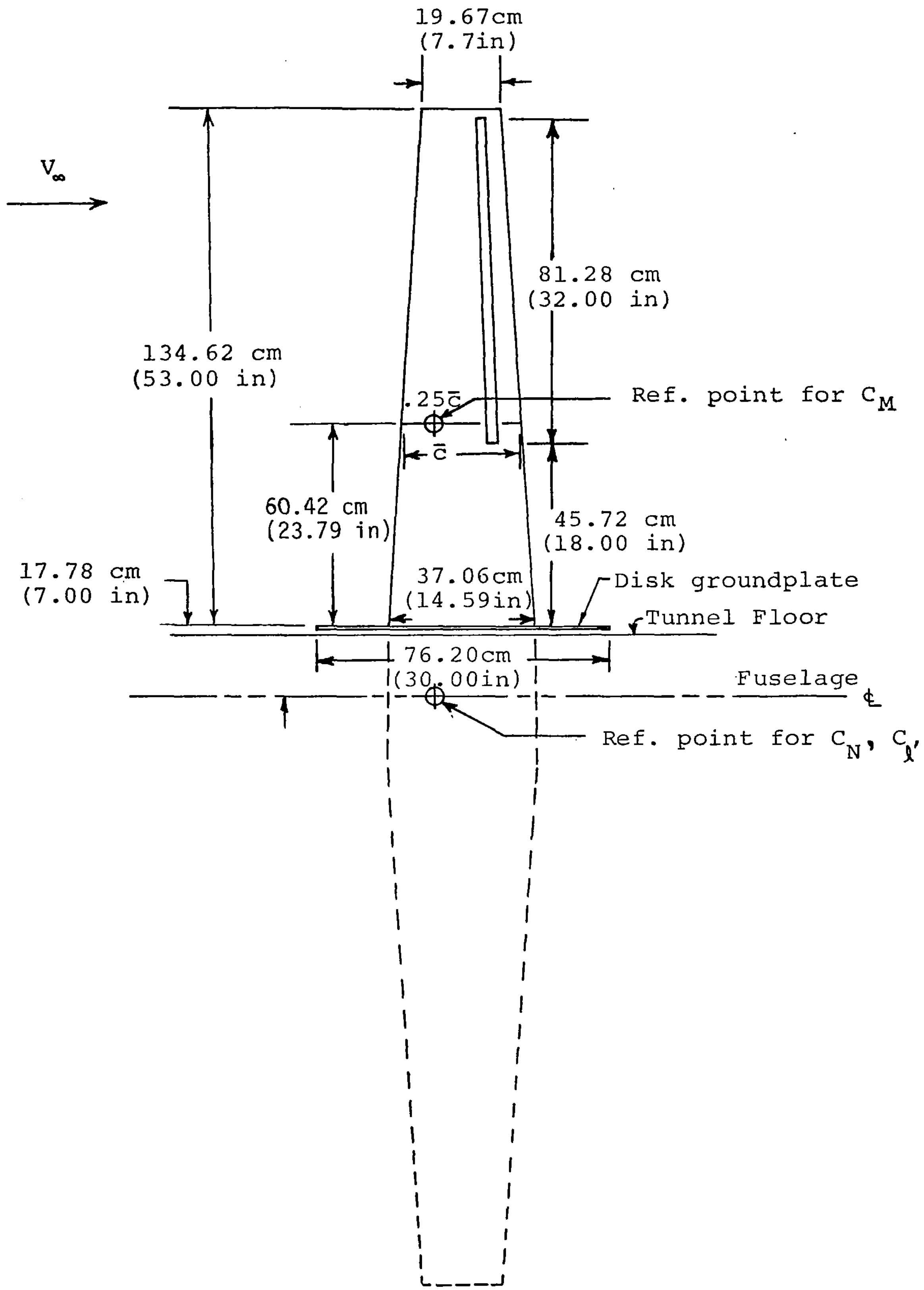

Figure 1 - Reflection Plane Experimental Set-up

REFLECTION PLANE MODEL CONSTANTS

S_e,	Exposed Wing Area	3818 cm^2	(4.11 $ft.^2$)
$\bar{c}$,	M.A.C.	29.21 cm.	(11.5 in.)
S_{sp},	Spoiler Area	210.58 cm^2	(32.64 $in.^2$)
c,	Wing Chord at Spoiler Midspan	25.91 cm.	(10.2 in.)
c_{sp},	Spoiler Reference Chord	2.591 cm.	(1.02 in.)
S_t,	Total Wing Area	9002 cm^2	(9.69 $ft.^2$)
b_e,	Exposed Wingspan	24.20 cm.	(53.0 in.)
b_t,	Total Wingspan	304.8 cm.	(120.0 in.)
	Twist	3^o (washout)	
	Dihedral	7^o (positive)	

DEFINITION OF AERODYNAMIC COEFFICIENTS

$C_L = L/qS_e$

$C_D = D/qS_e$

$C_M = M/qS_e\bar{c}$

$C_\ell = \ell/qS_t b_t$

$C_N = N/qS_t b_t$

$C_H = H/qS_{sp}c_{sp}$ (Opening moment is positive)

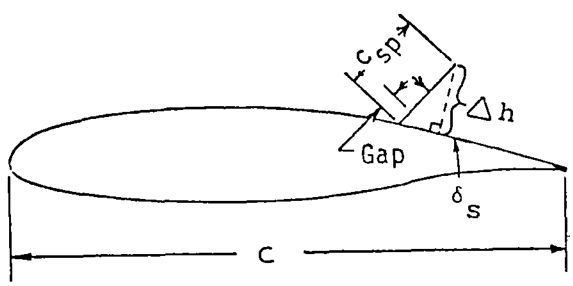

(c = Wing Chord at mid-spoiler span)

Figure 2 - Model Geometry

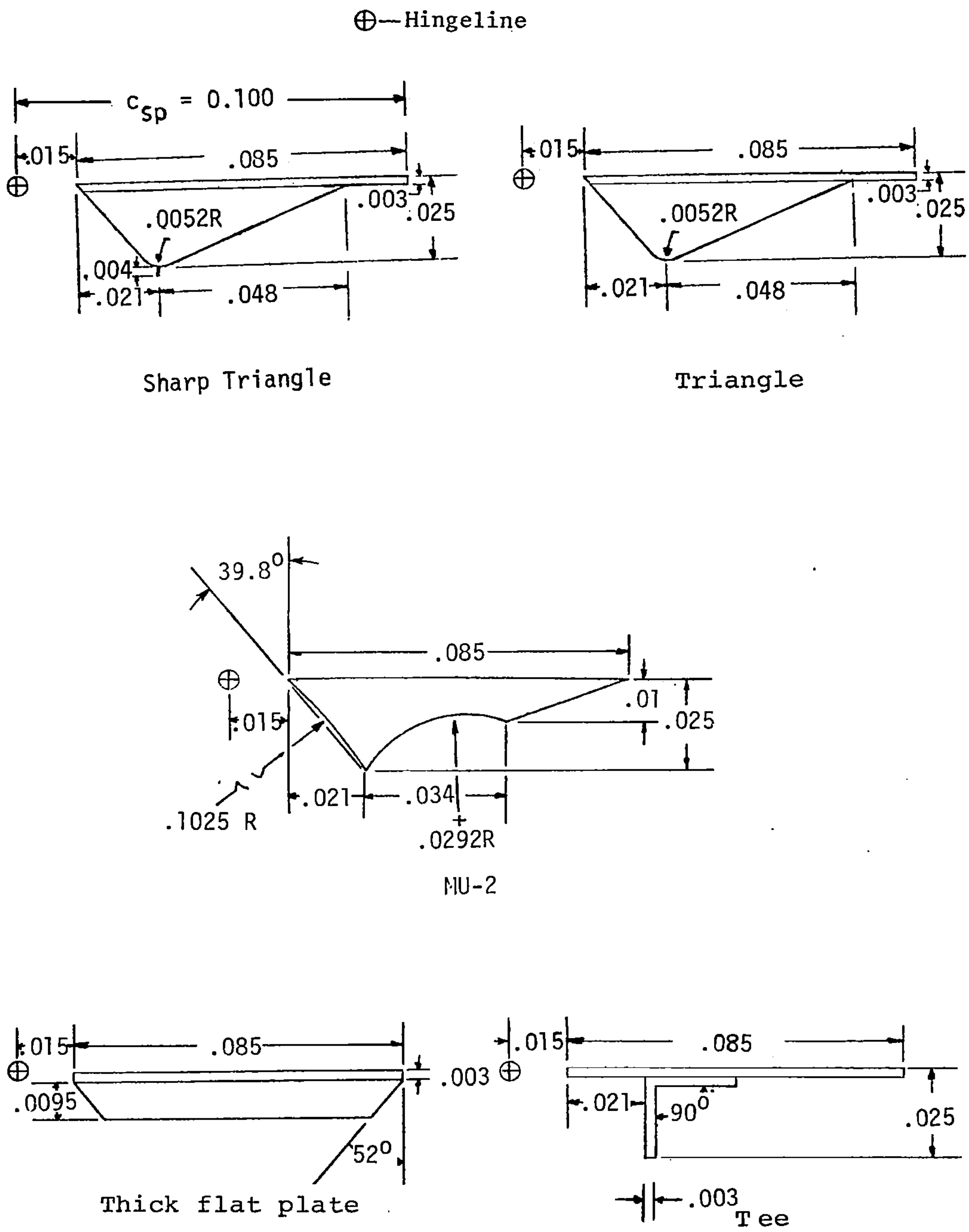

Note: All lengths are non-dimensionalized with respect to wing chord at spoiler midspan.

Figure 3 - Spoiler geometry

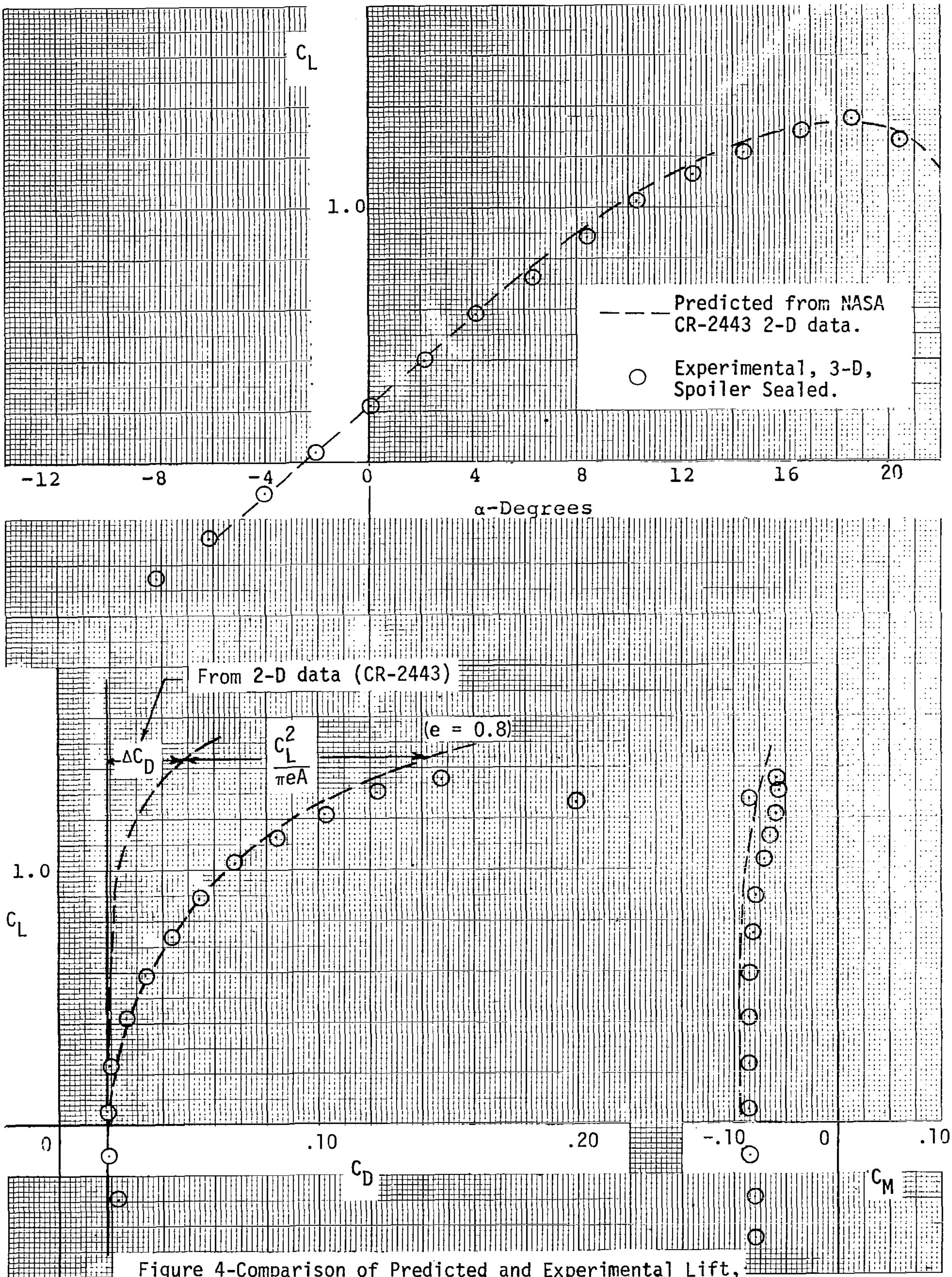

Figure 4-Comparison of Predicted and Experimental Lift, Drag and Pitching Moments, Flap Nested.

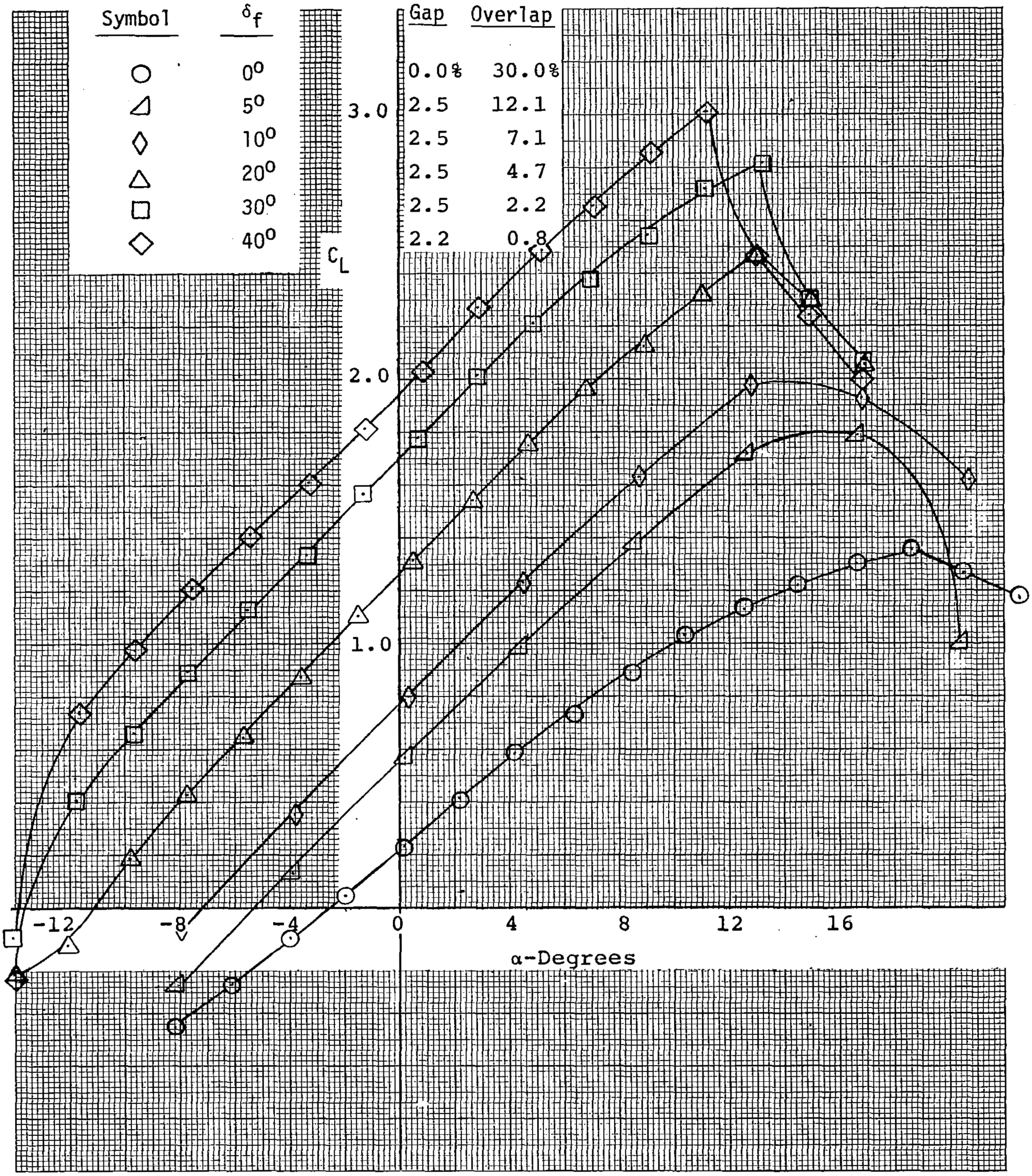

Figure 5 - Lift for various flap settings. Spoiler Sealed.

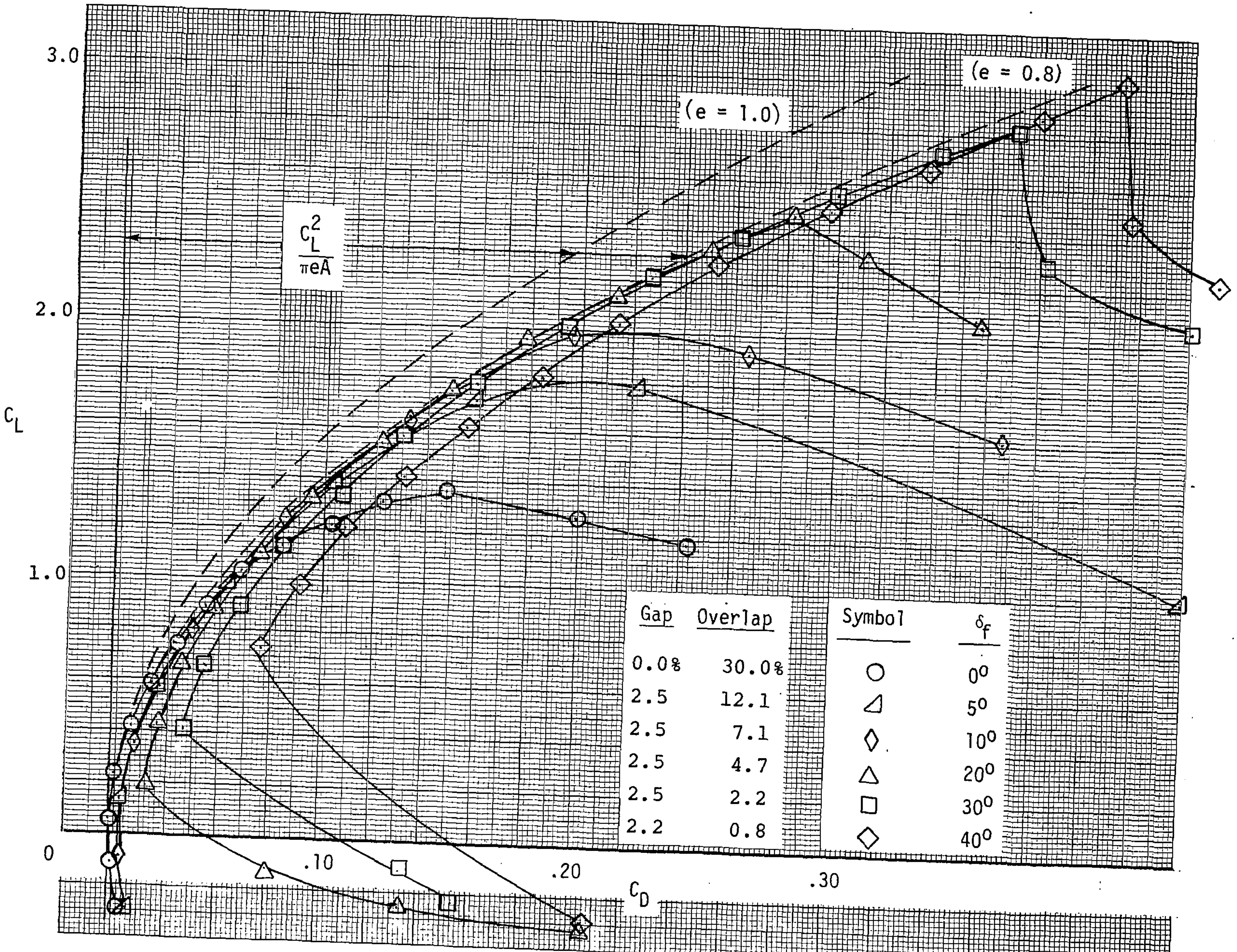

Figure 6 - Drag Polars. Spoiler Sealed.

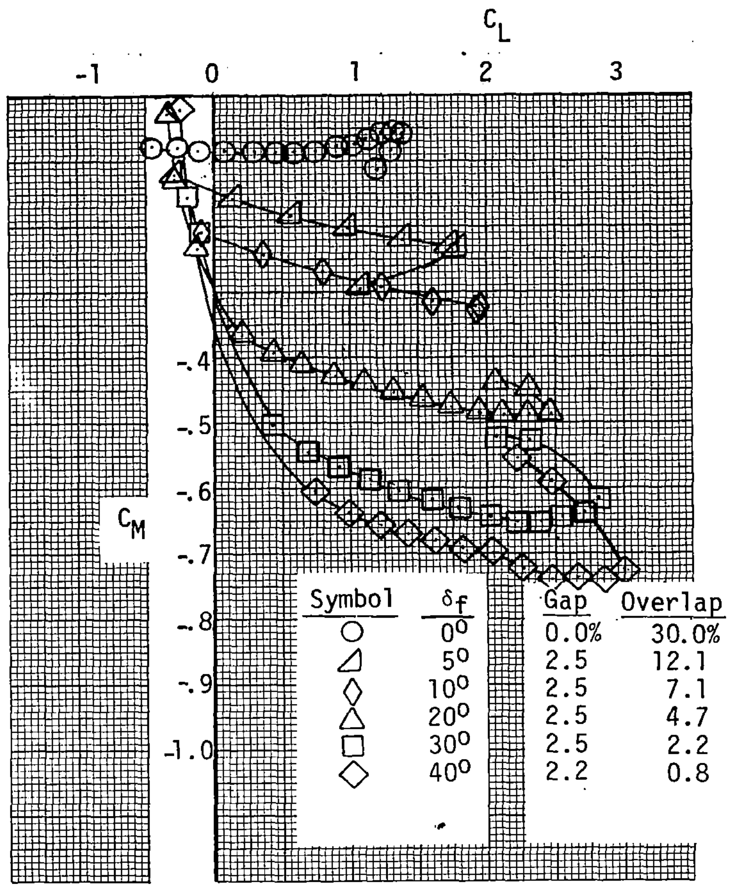

Figure 7 - Pitching Moments. Spoiler Sealed.

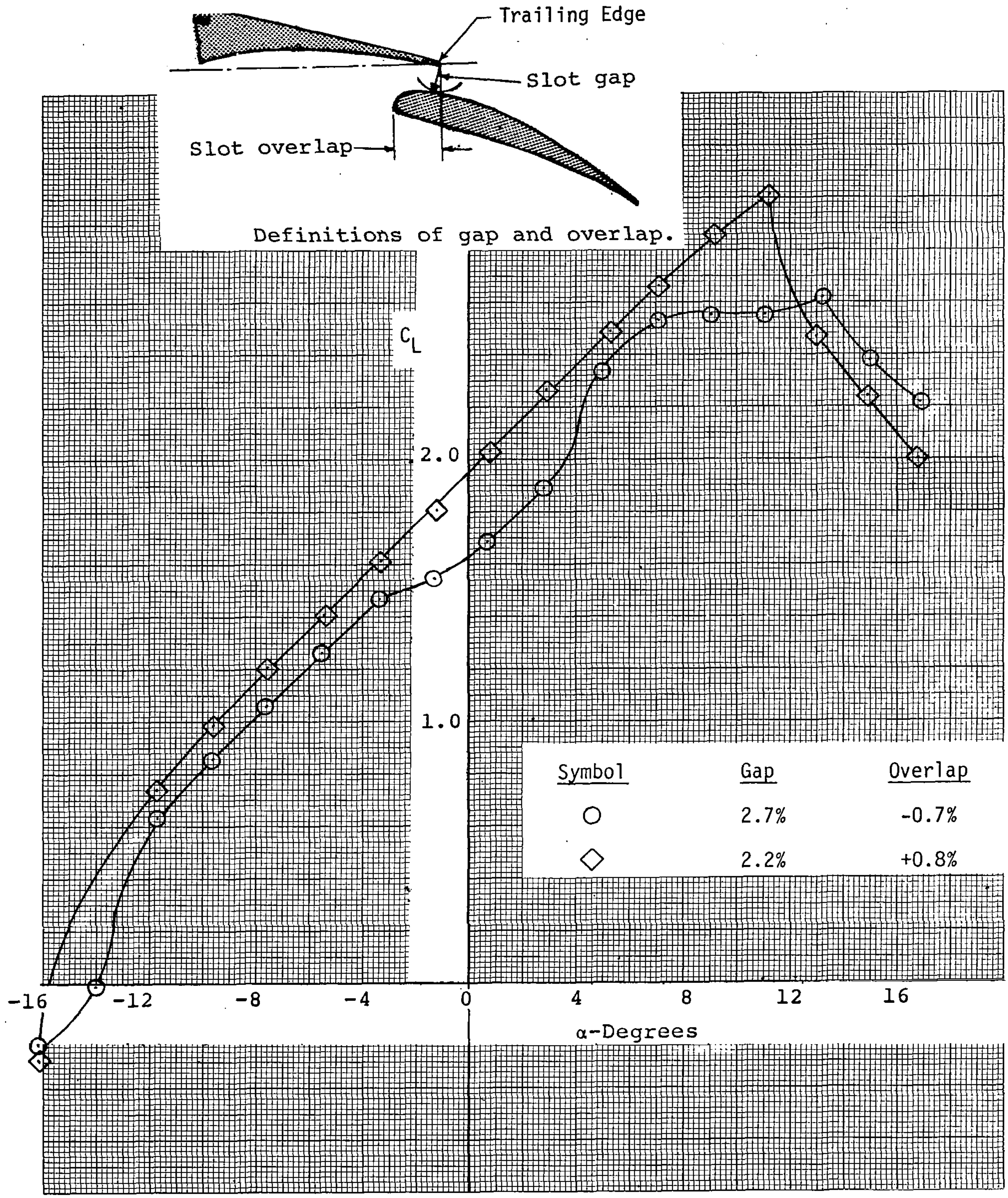

Figure 8 - Lift Curves for 2-D optimum and 3-D optimum gap and overlap. Spoiler Sealed. 40° Flap.

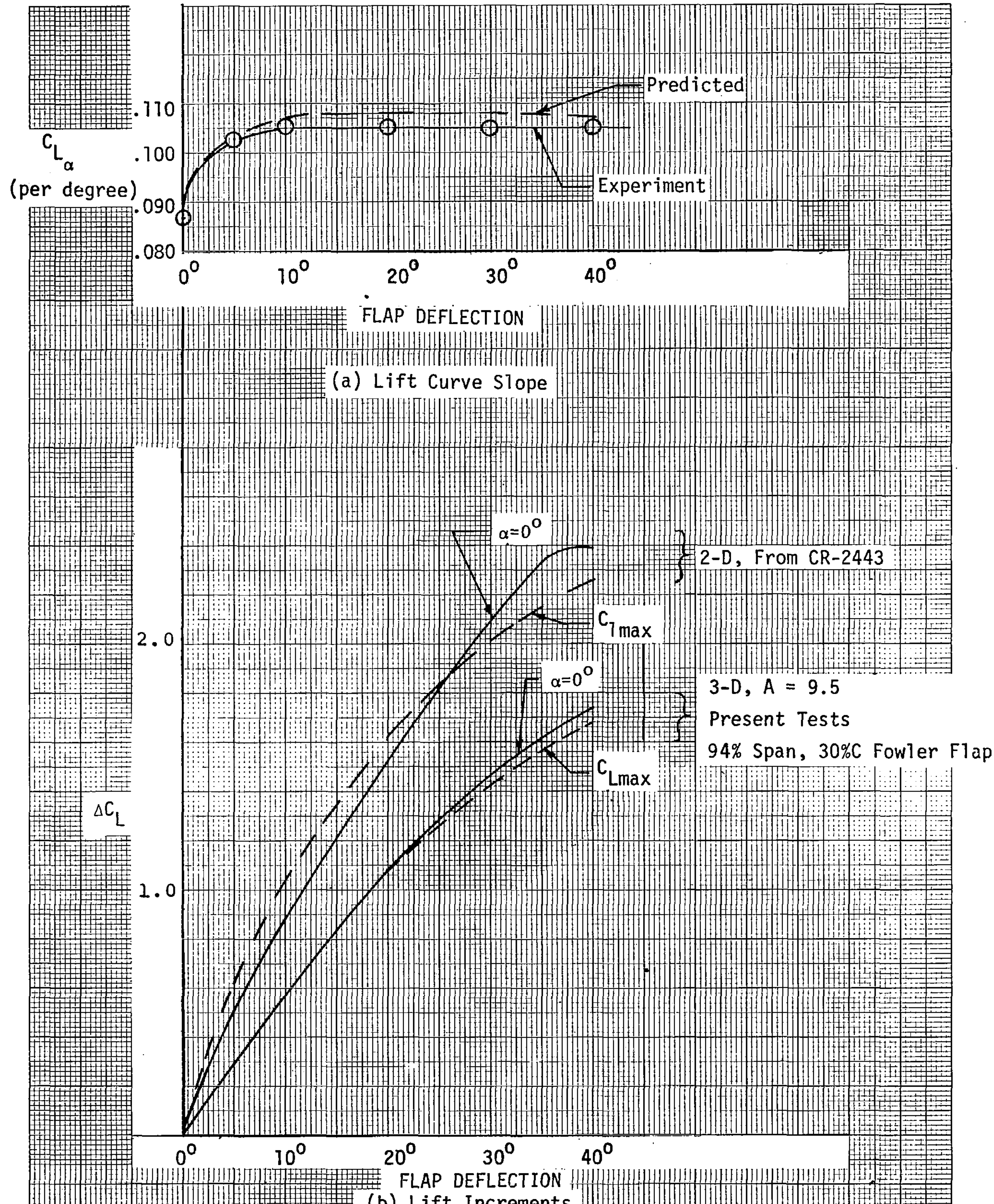

Figure 9 - Flap Effectiveness. Spoiler Sealed.

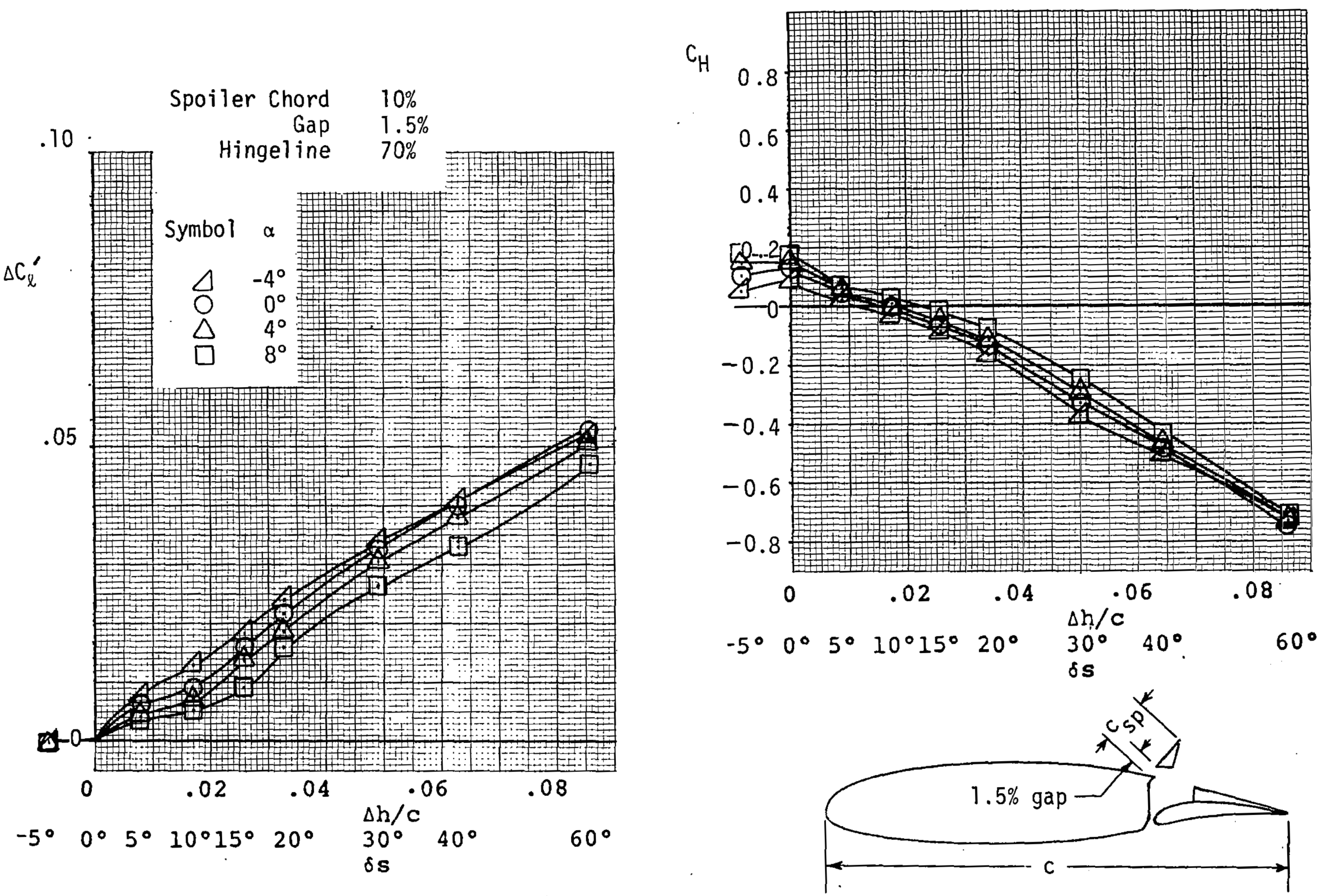

(a) Rolling Moments and Hinge Moments

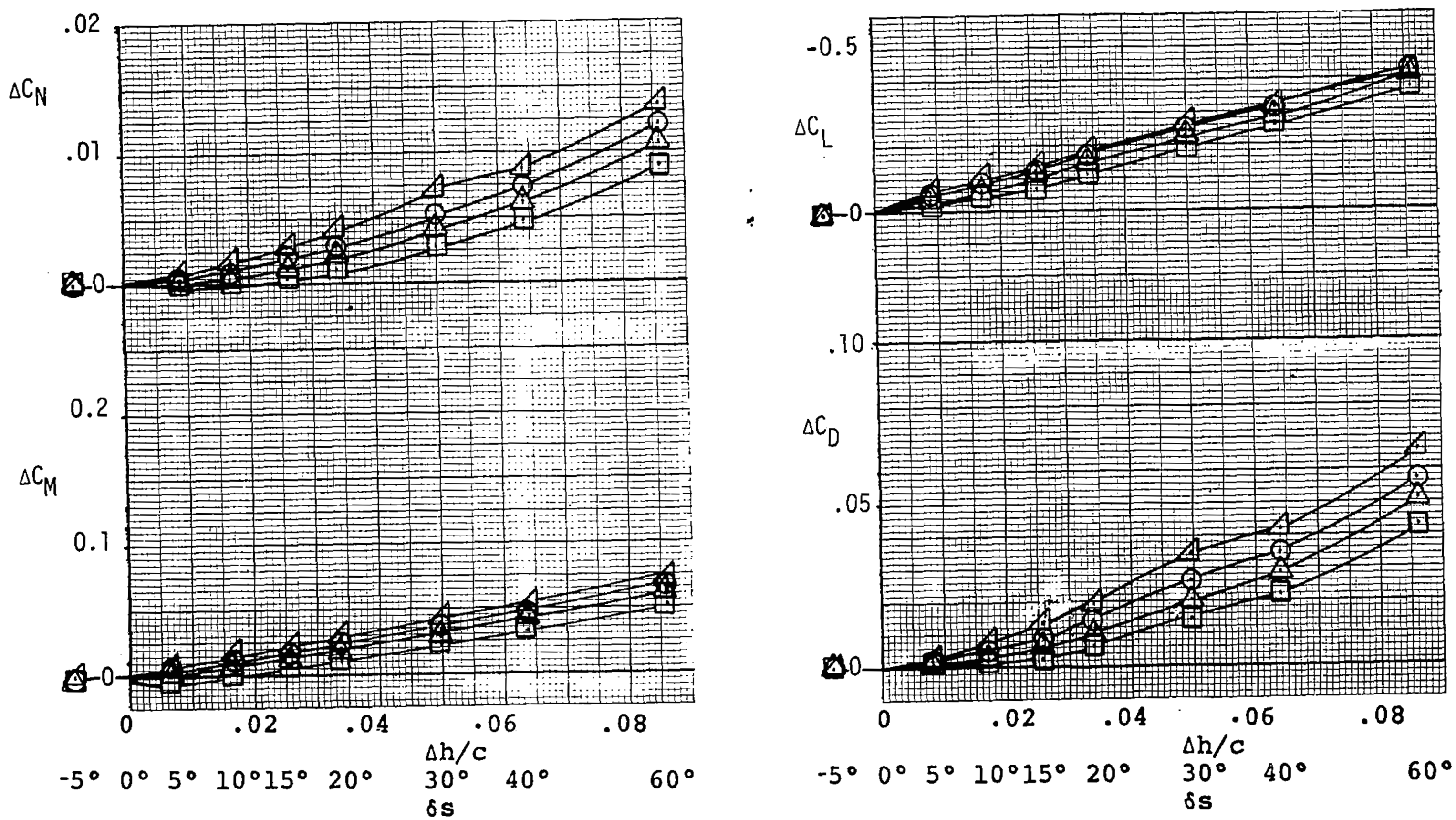

(b) Yawing Moments, Pitching Moments, Lift, and Drag.

Figure 10 -Effects of Triangle Spoiler. Flap 0^{0}.

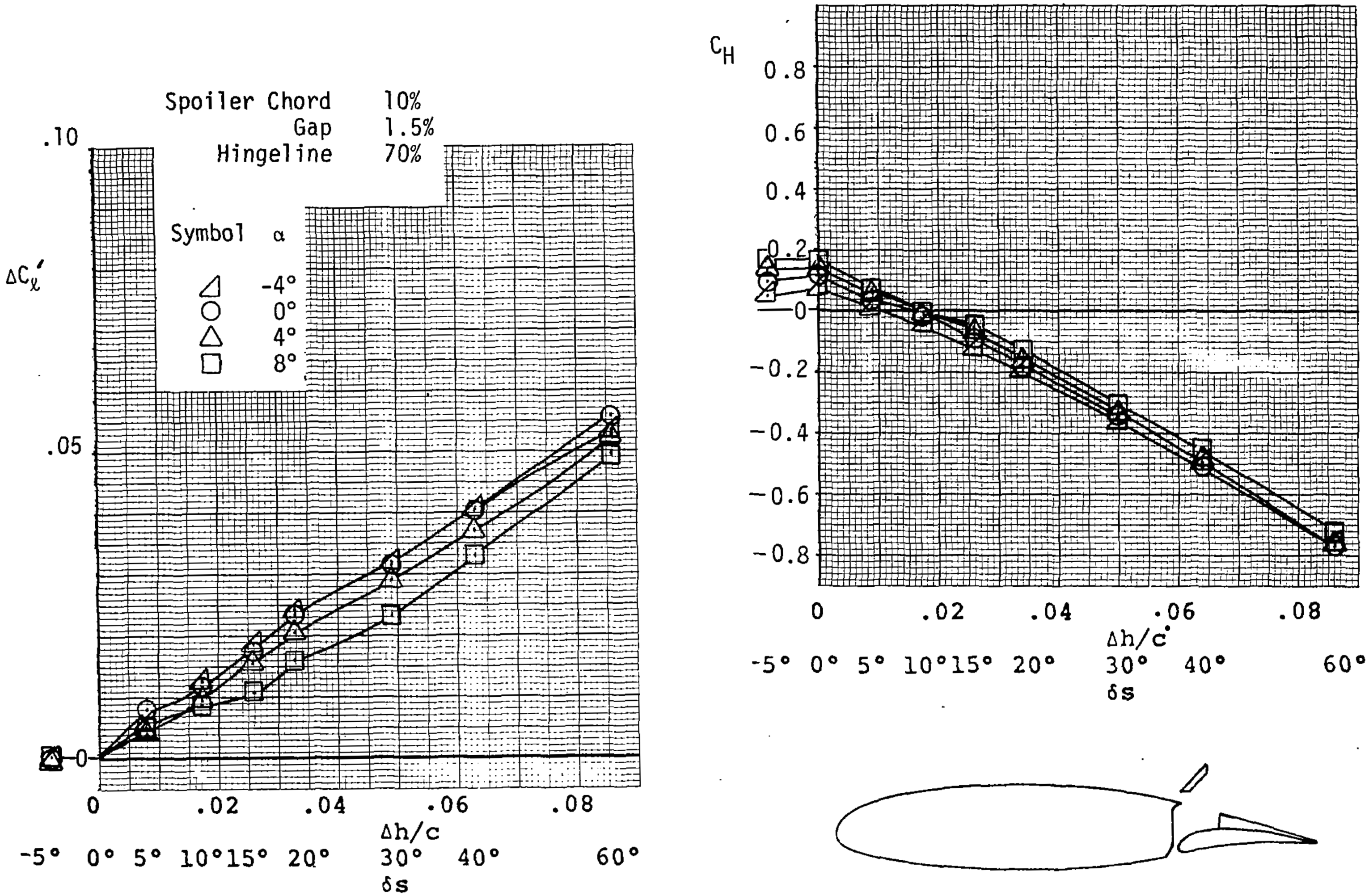

(a) Rolling Moments and Hinge Moments

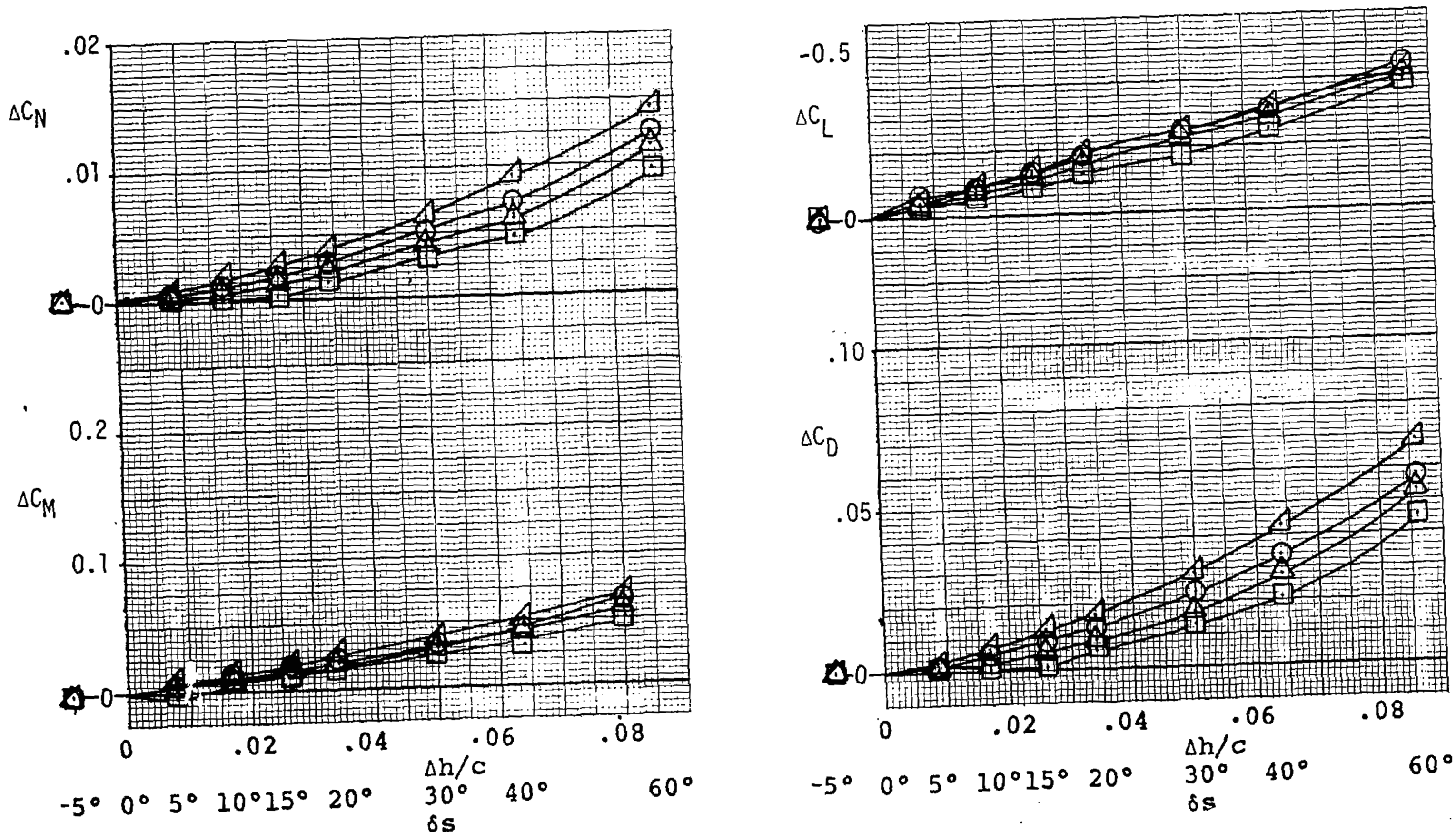

(b) Yawing Moments, Pitching Moments, Lift, and Drag.

Figure 11 - Effects of Flat Plate Spoiler. Flap 0^{o}.

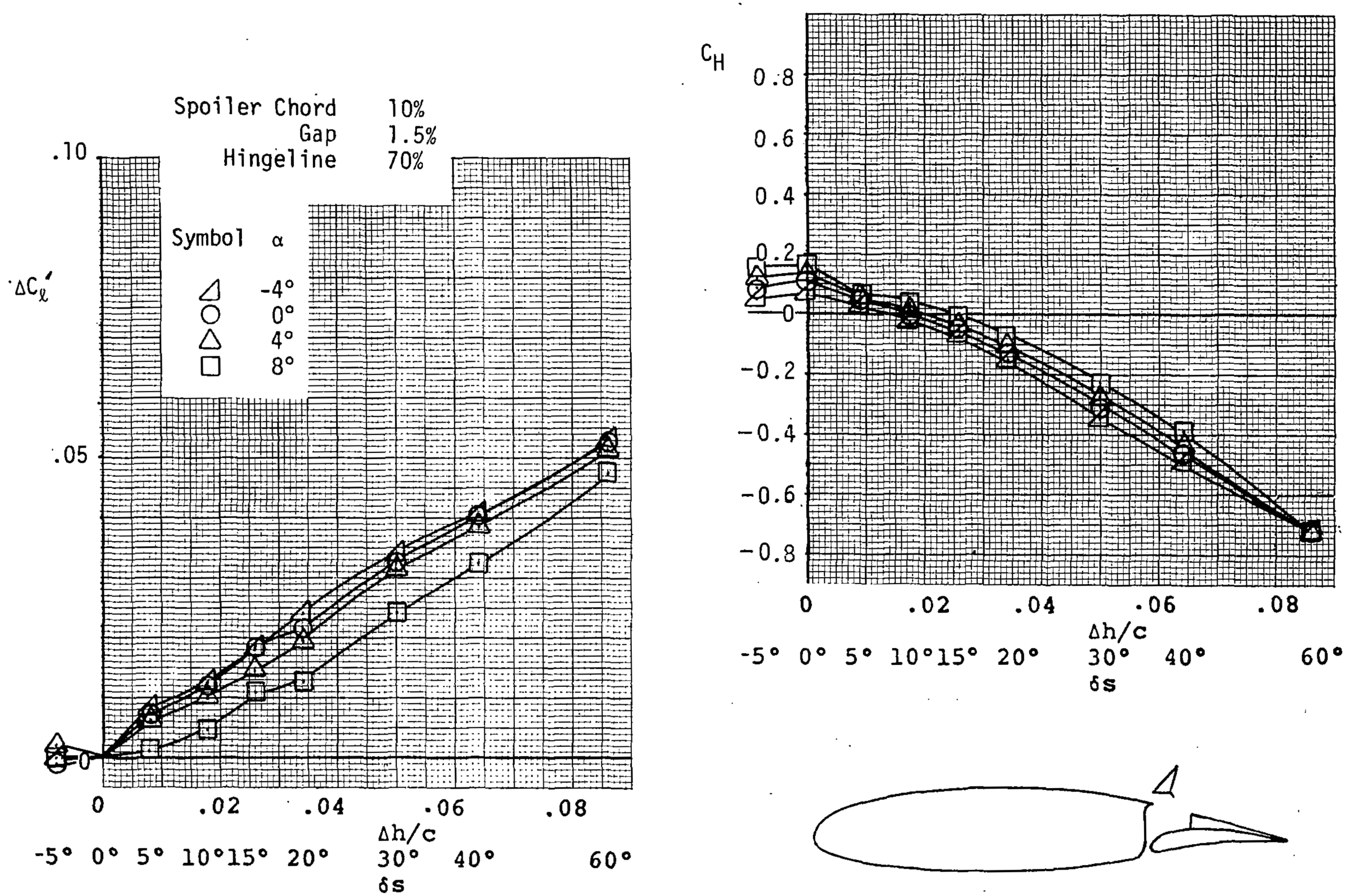

(a) Rolling Moments and Hinge Moments

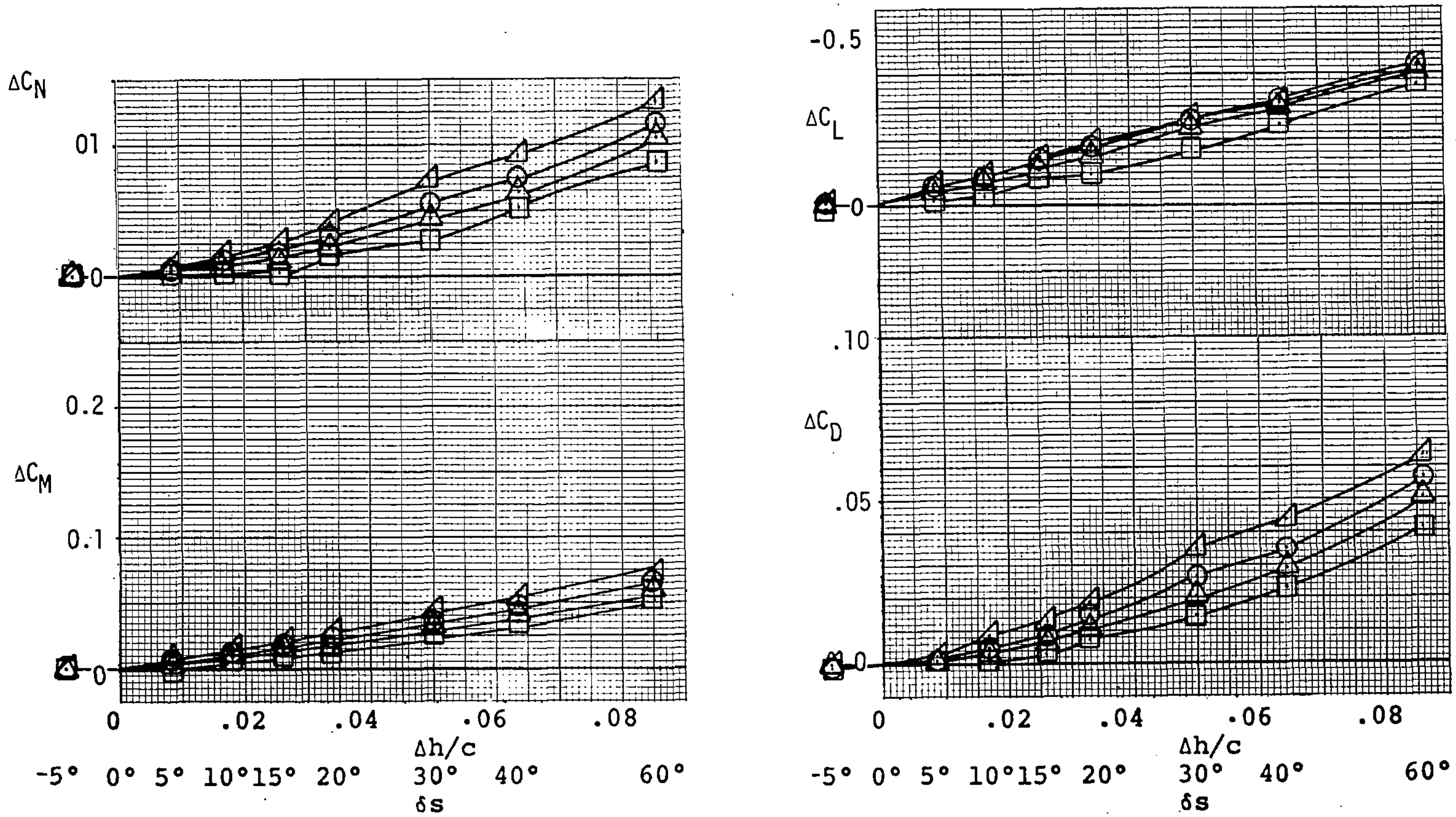

(b) Yawing Moments, Pitching Moments, Lift, and Drag.

Figure 12 - Effects of Sharp Triangle Spoiler. Flap 0°.

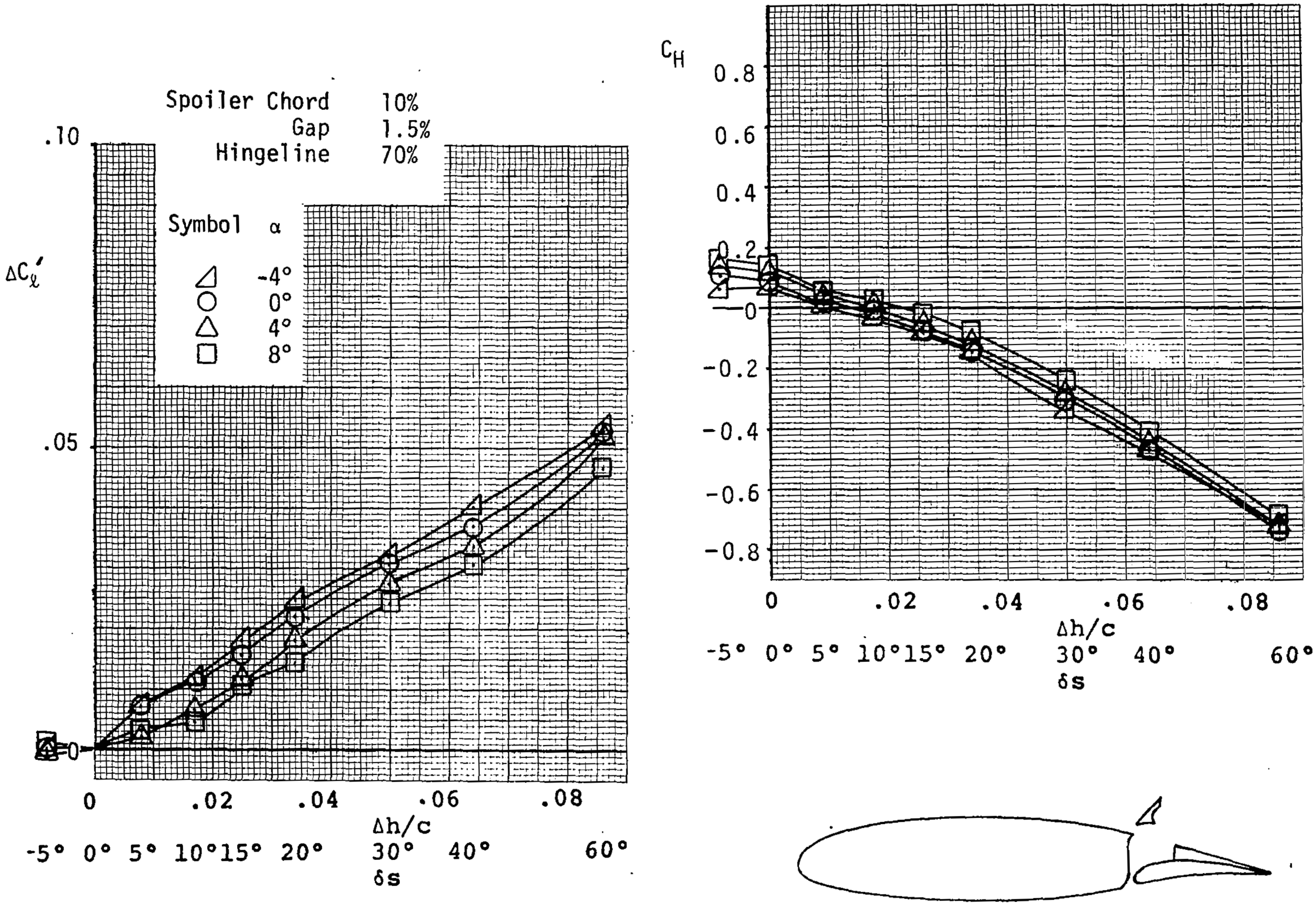

(a) Rolling Moments and Hinge Moments

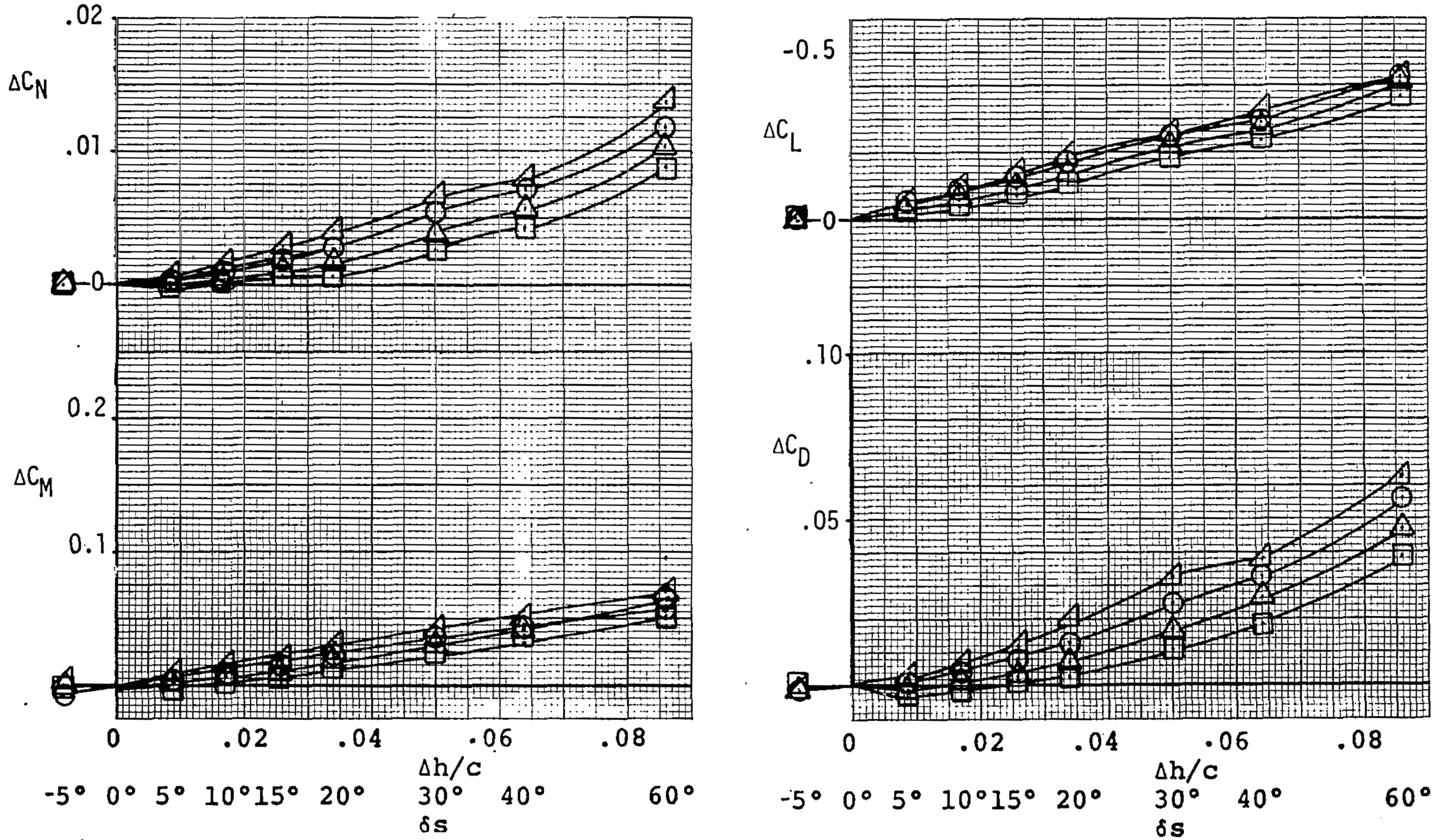

(b) Yawing Moments, Pitching Moments, Lift, and Drag.

Figure 13 - Effects of MU-2 Spoiler. Flap 0^{o}.

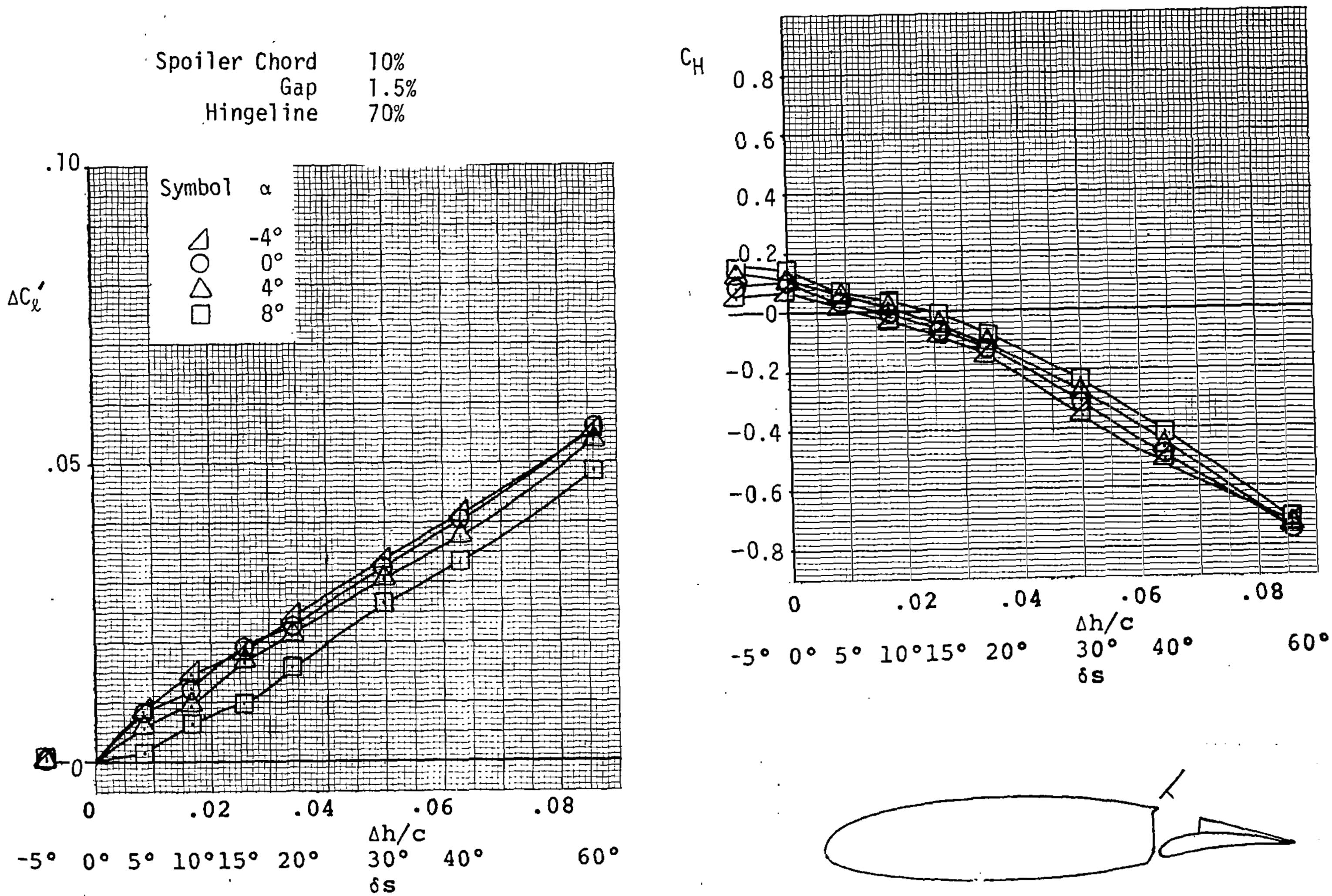

(a) Rolling Moments and Hinge Moments

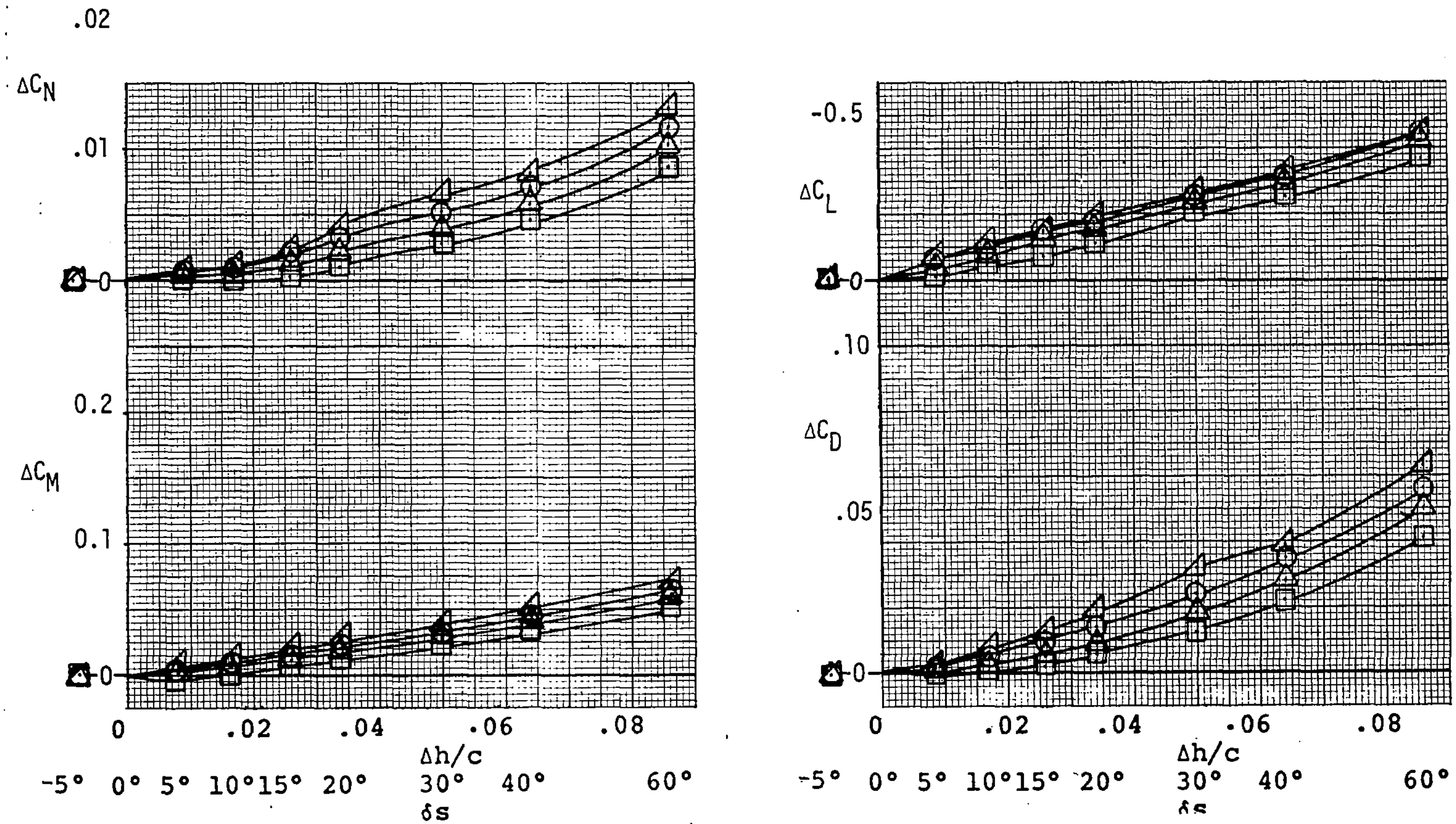

(b) Yawing Moments, Pitching Moments, Lift, and Drag.

Figure 14 - Effects of Tee Spoiler. Flap 0^{o}.

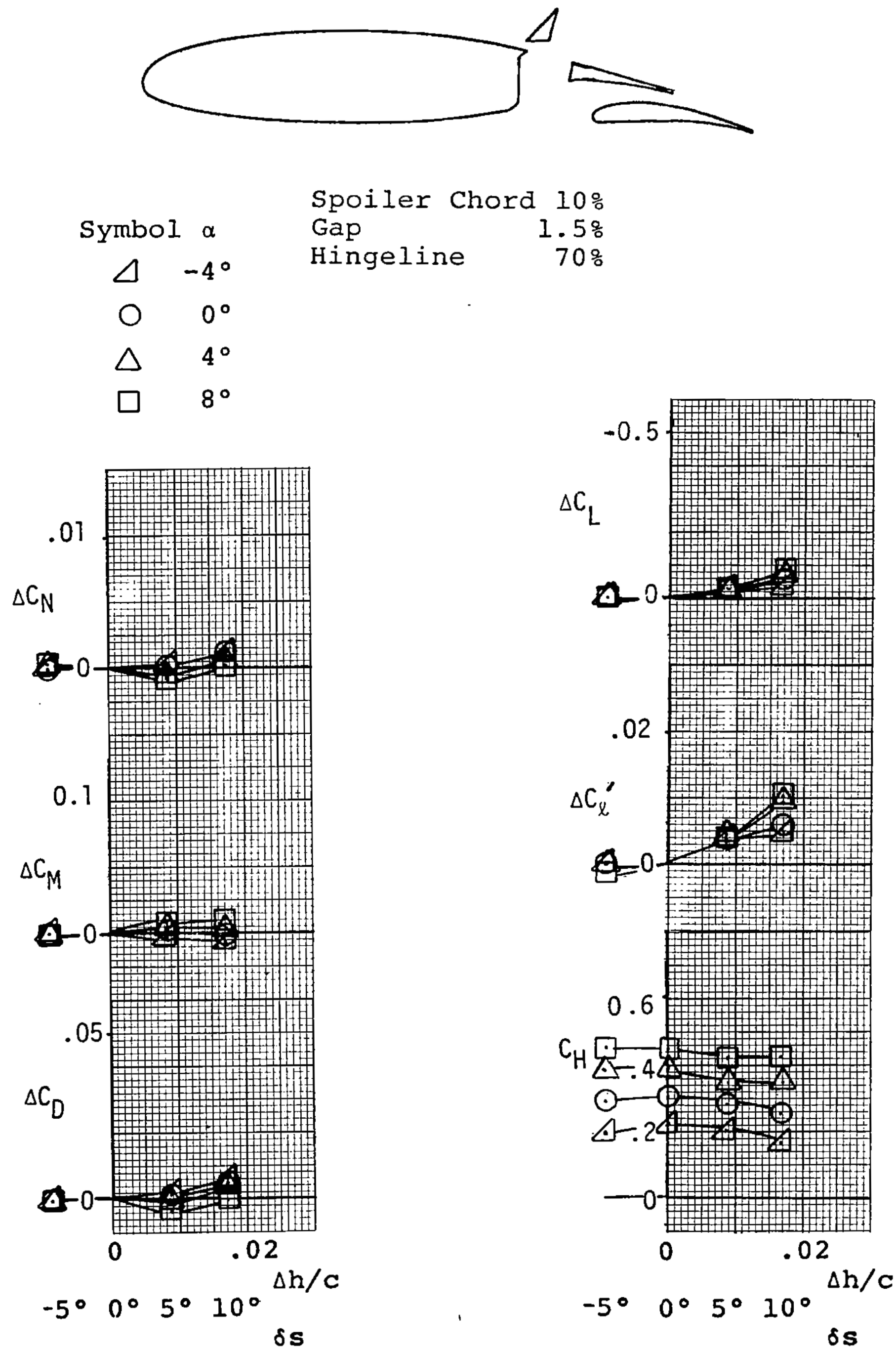

Figure 15 - Effects of Triangle Spoiler. Flap 5°.

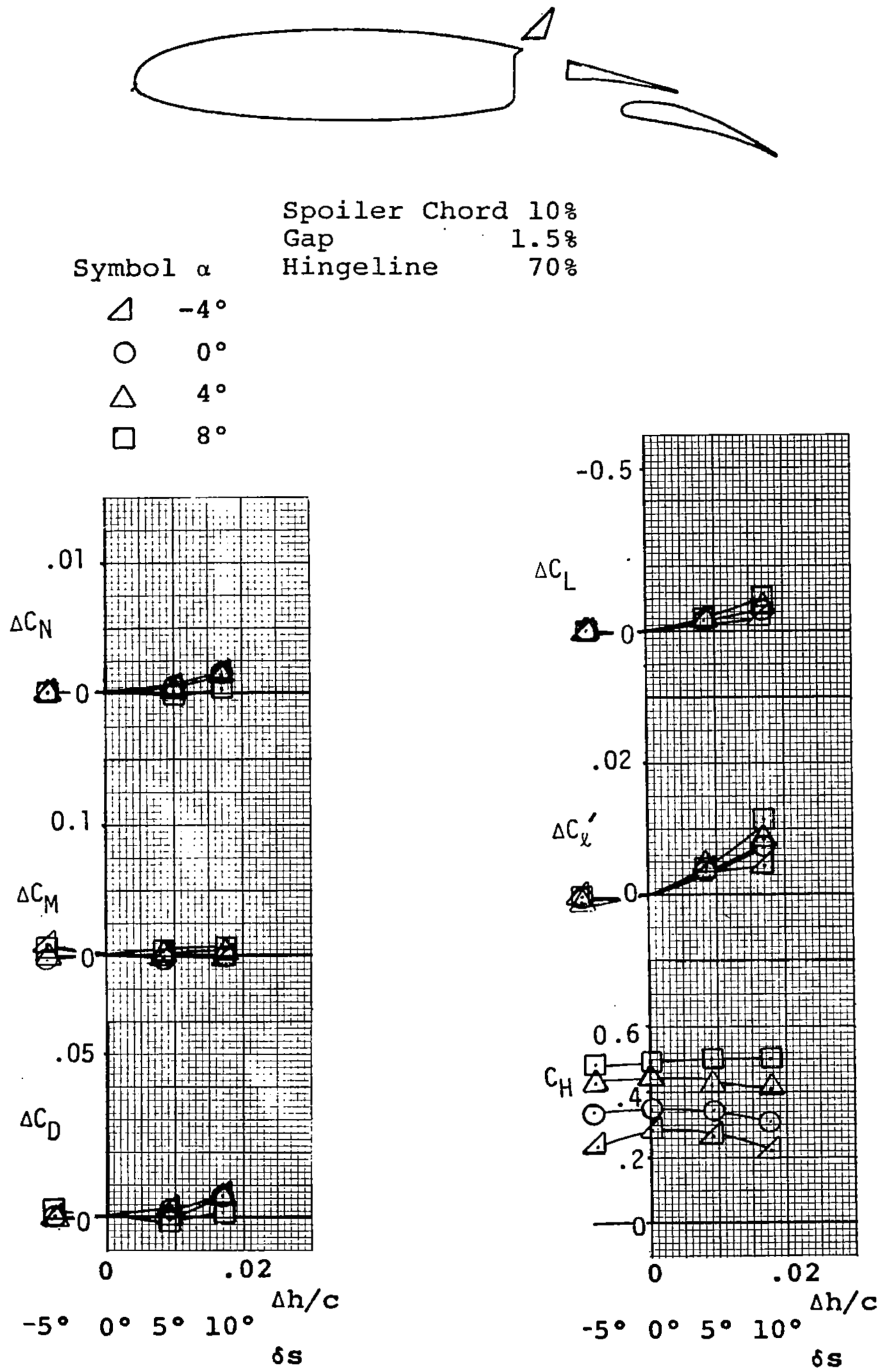

Figure 16 - Effects of Triangle Spoiler. Flap 10^{0}.

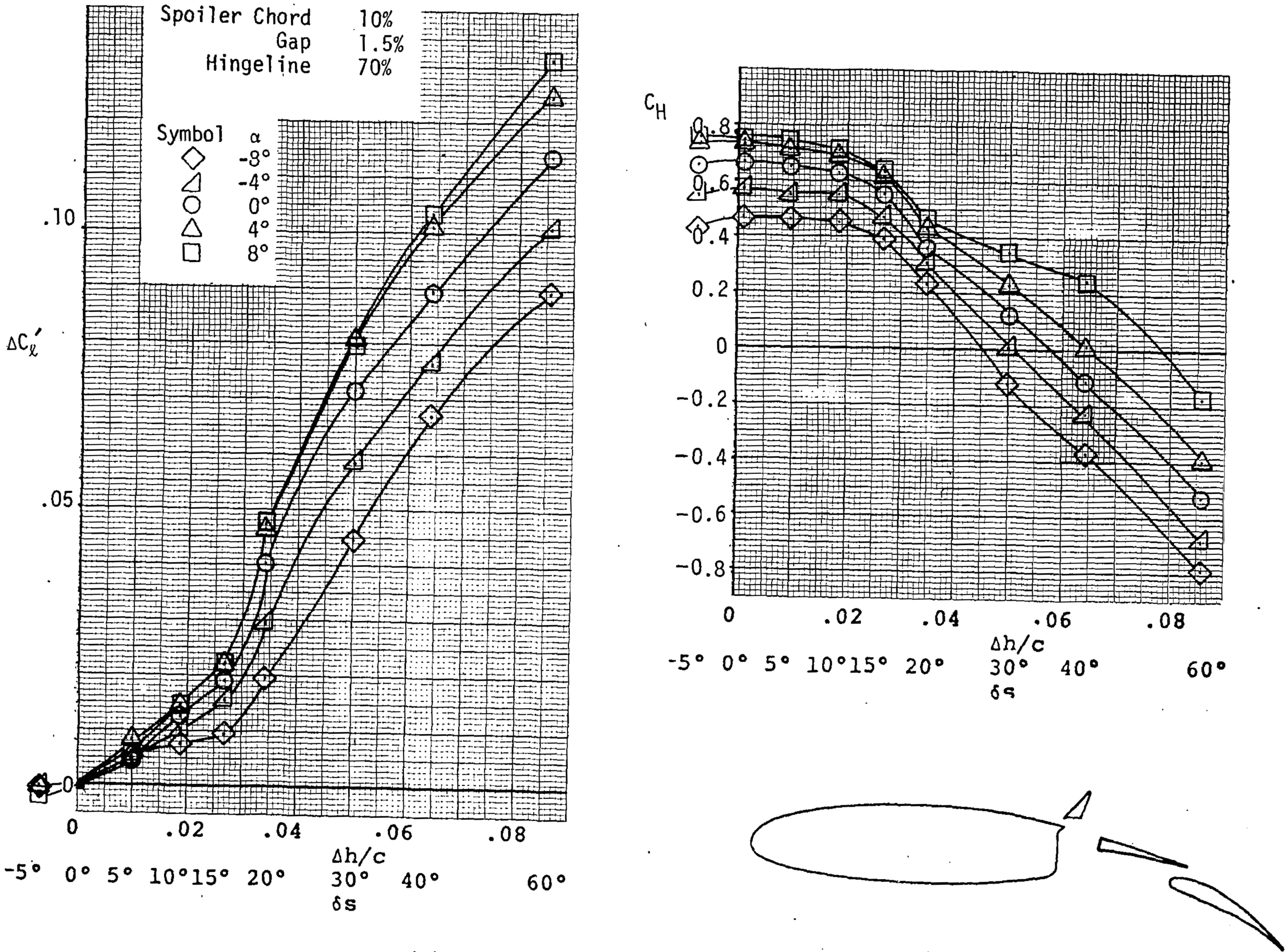

(a) Rolling Moments and Hinge Moments

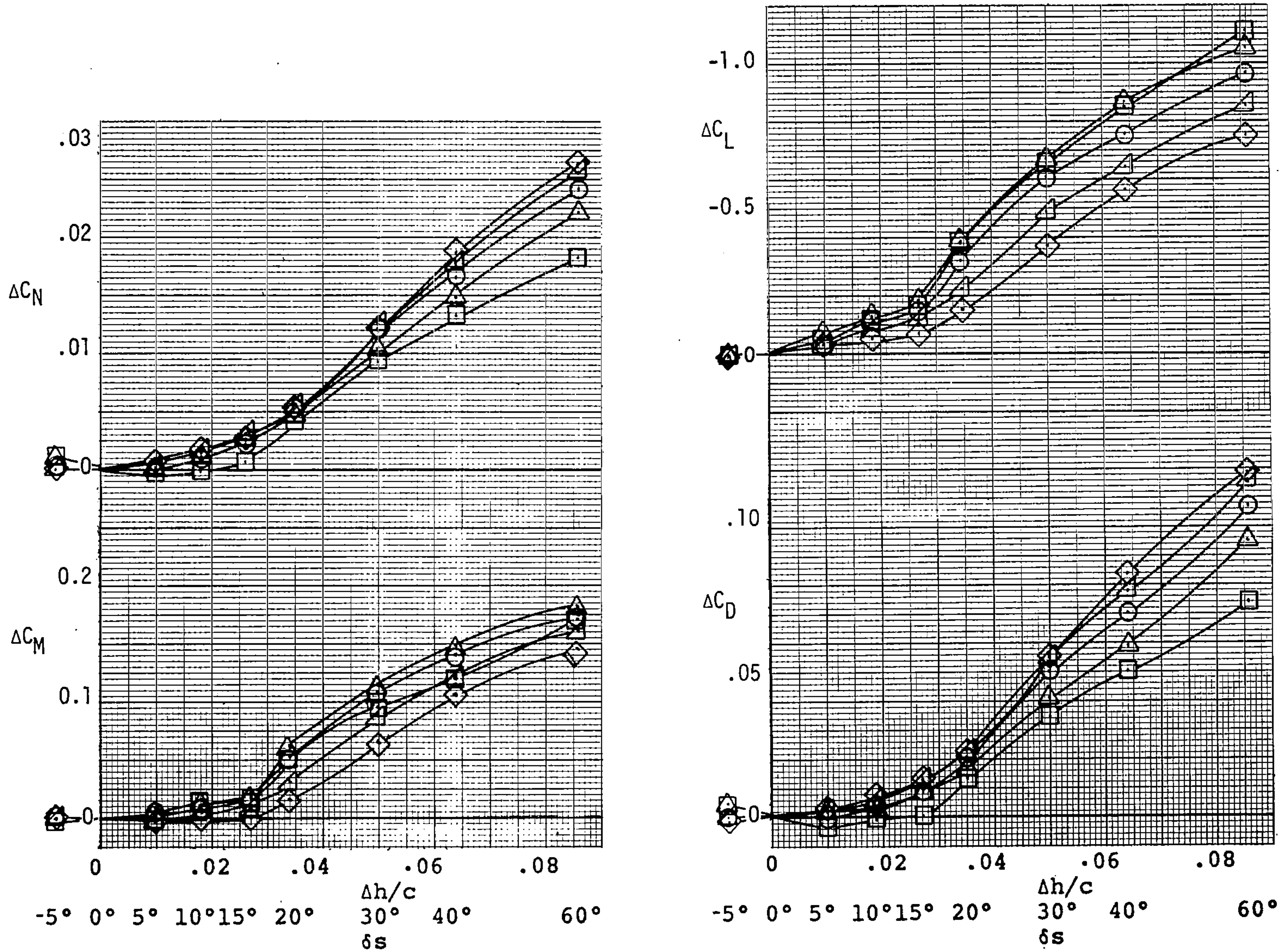

(b) Yawing Moments, Pitching Moments, Lift, and Drag.

Figure 17 - Effects of Triangle Spoiler. Flap 30°

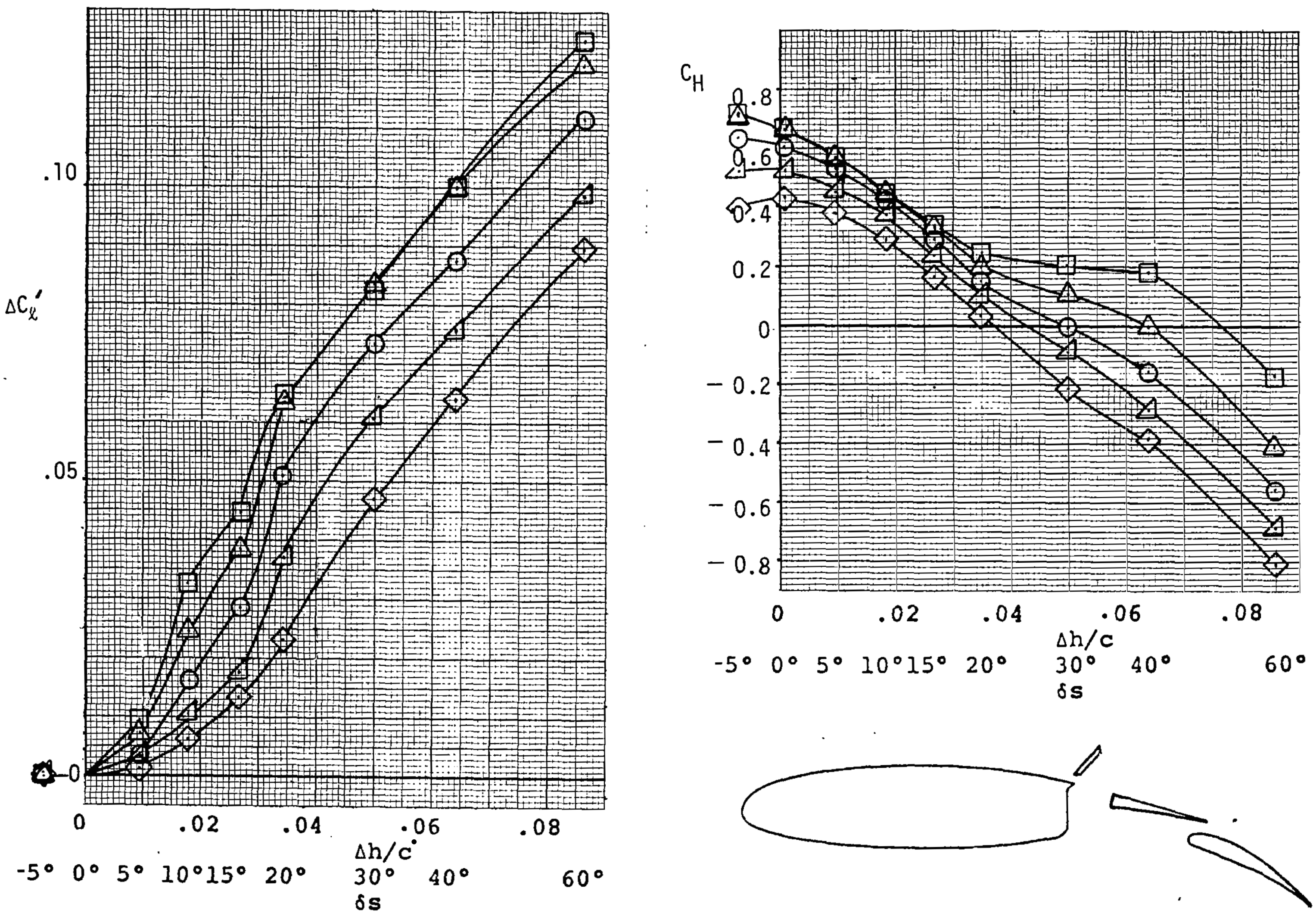

(a) Rolling Moments and Hinge Moments

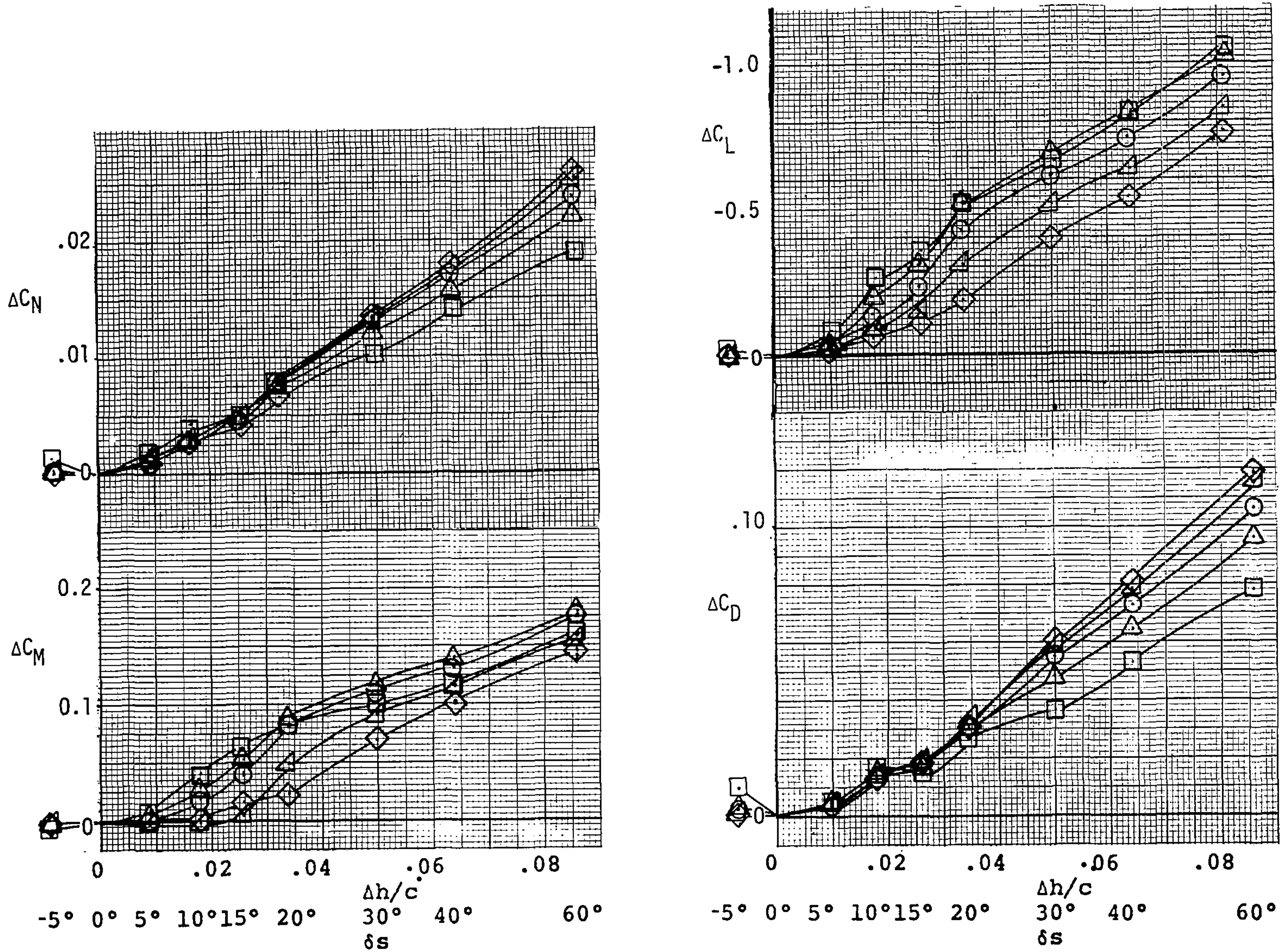

(b) Yawing Moments, Pitching Moments, Lift, and Drag.

Figure 18 - Effects of Flat Plate Spoiler. Flap 30°.

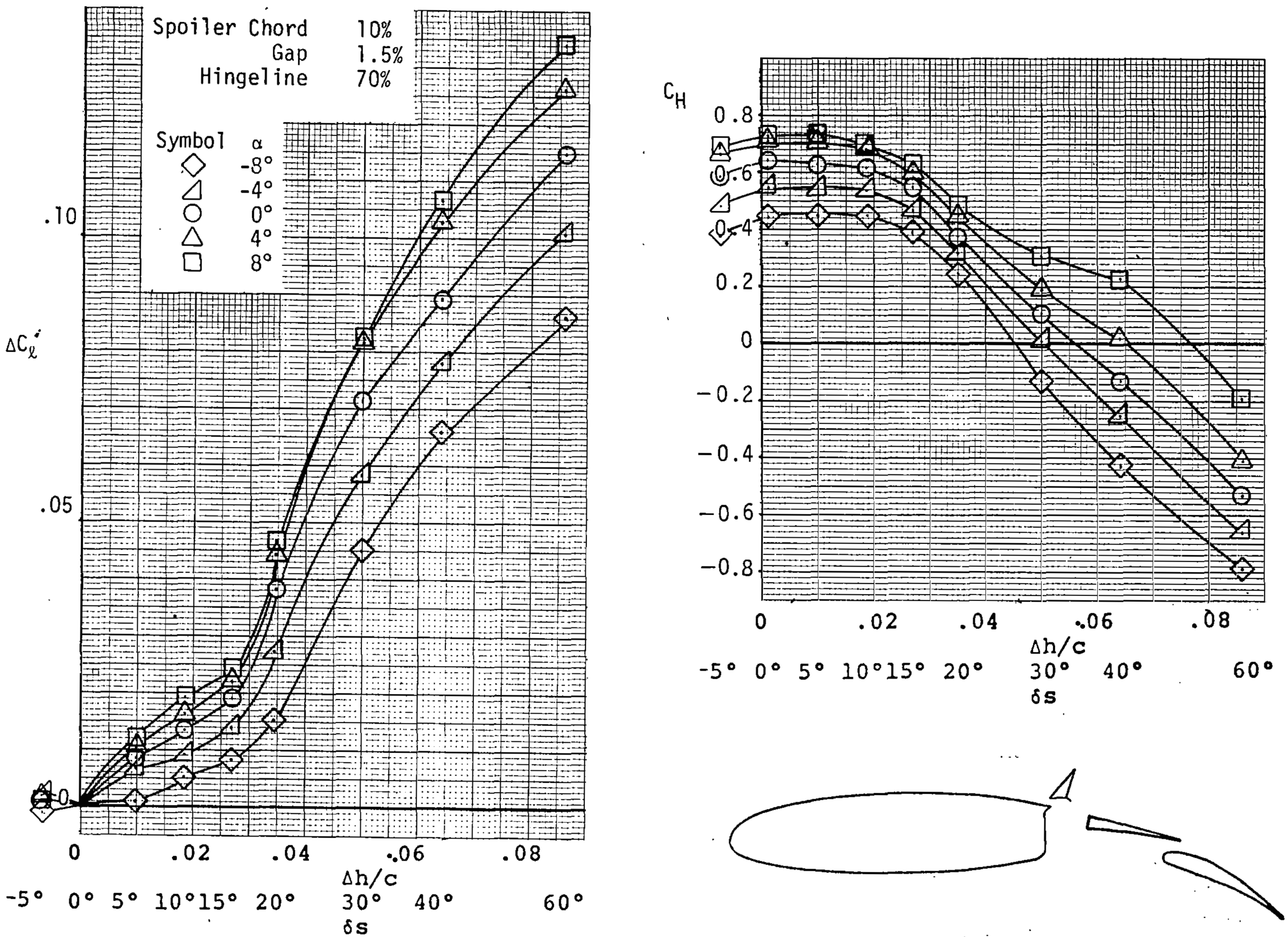

(a) Rolling Moments and Hinge Moments

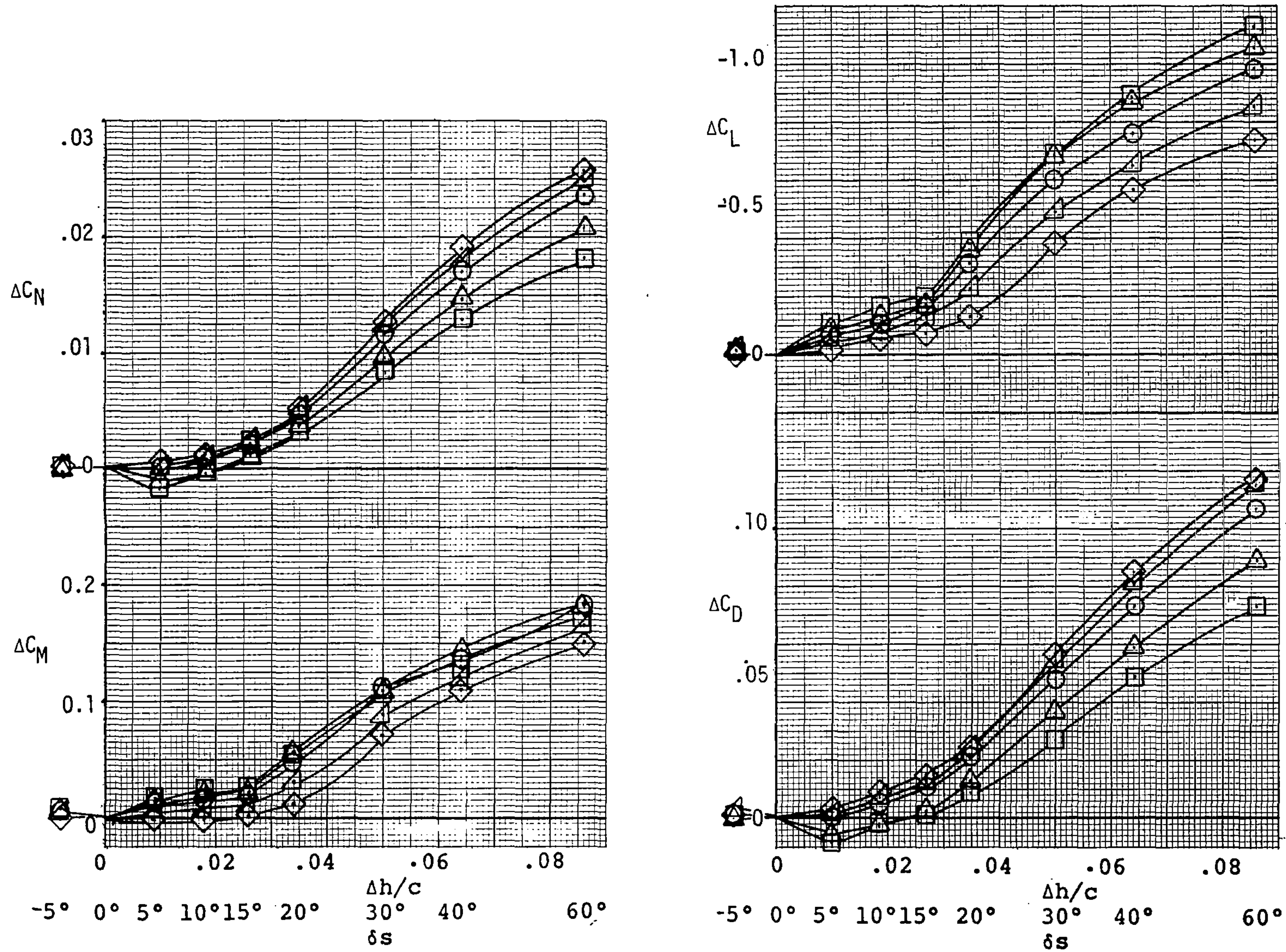

(b) Yawing Moments, Pitching Moments, Lift, and Drag.

Figure 19. – Effects of Sharp Triangle Spoiler. Flap 30^{0}.

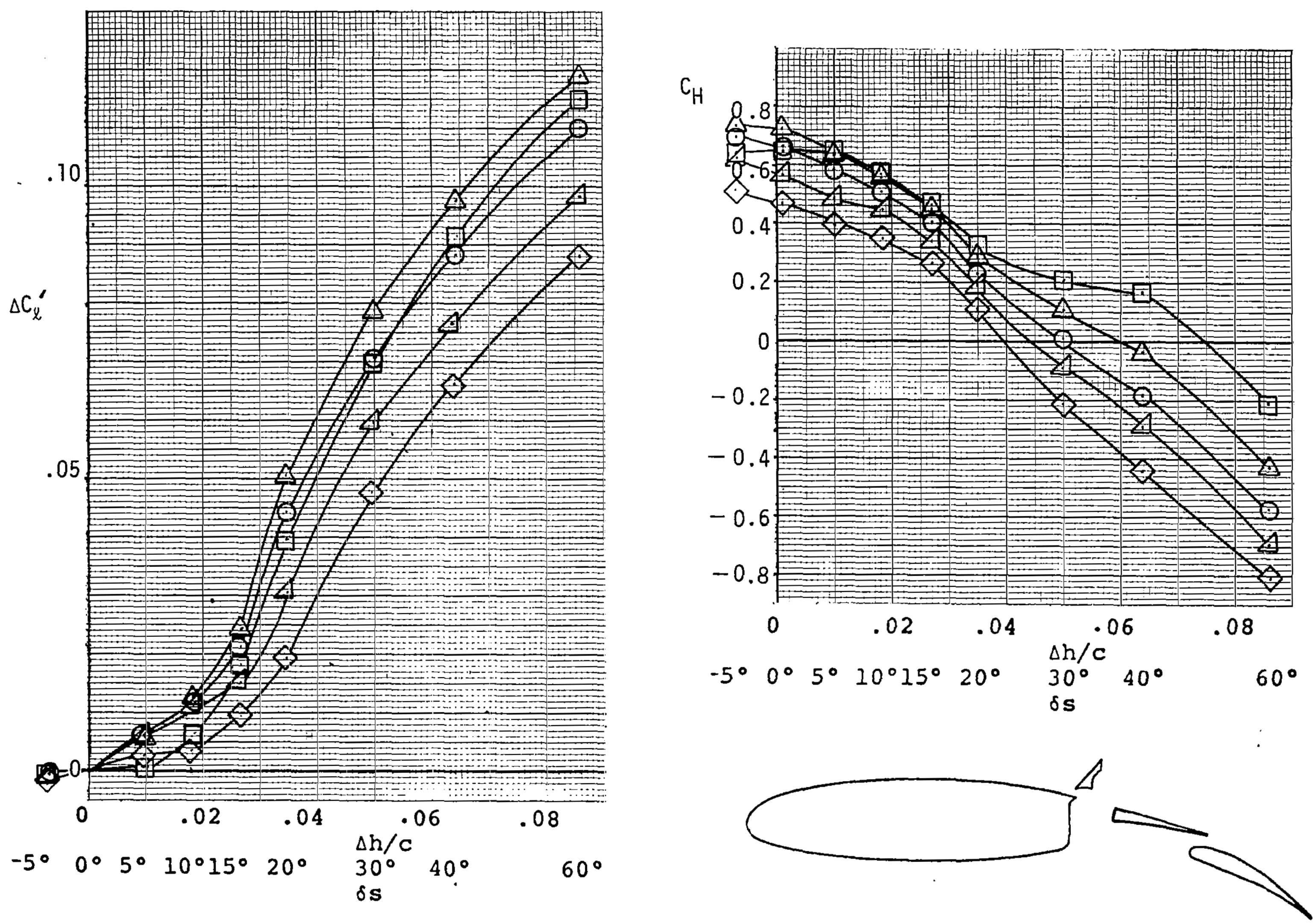

(a) Rolling Moments and Hinge Moments

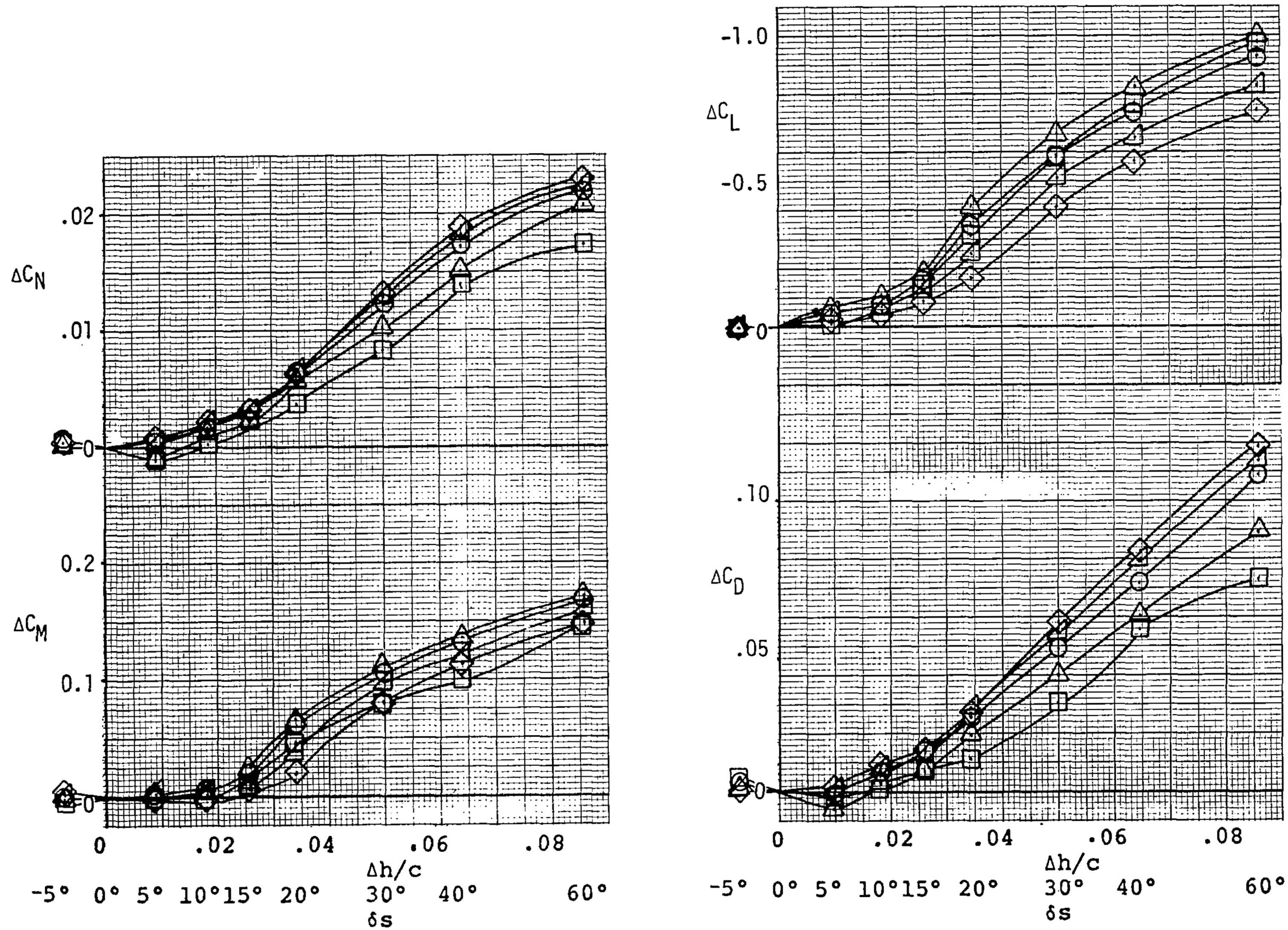

(b) Yawing Moments, Pitching Moments, Lift, and Drag.

Figure 20 - Effects of MU-2 Spoiler. Flap 30°.

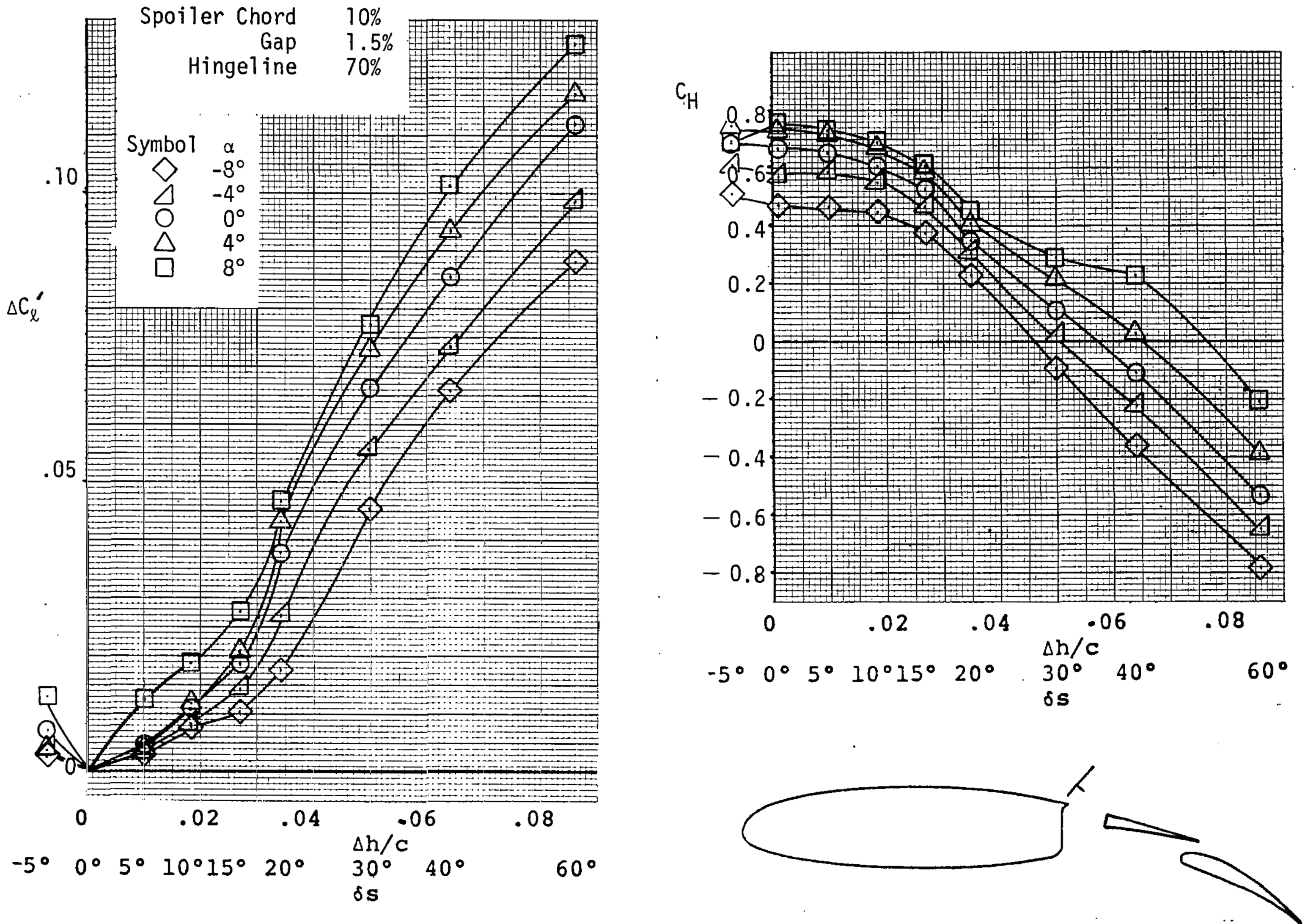

(a) Rolling Moments and Hinge Moments

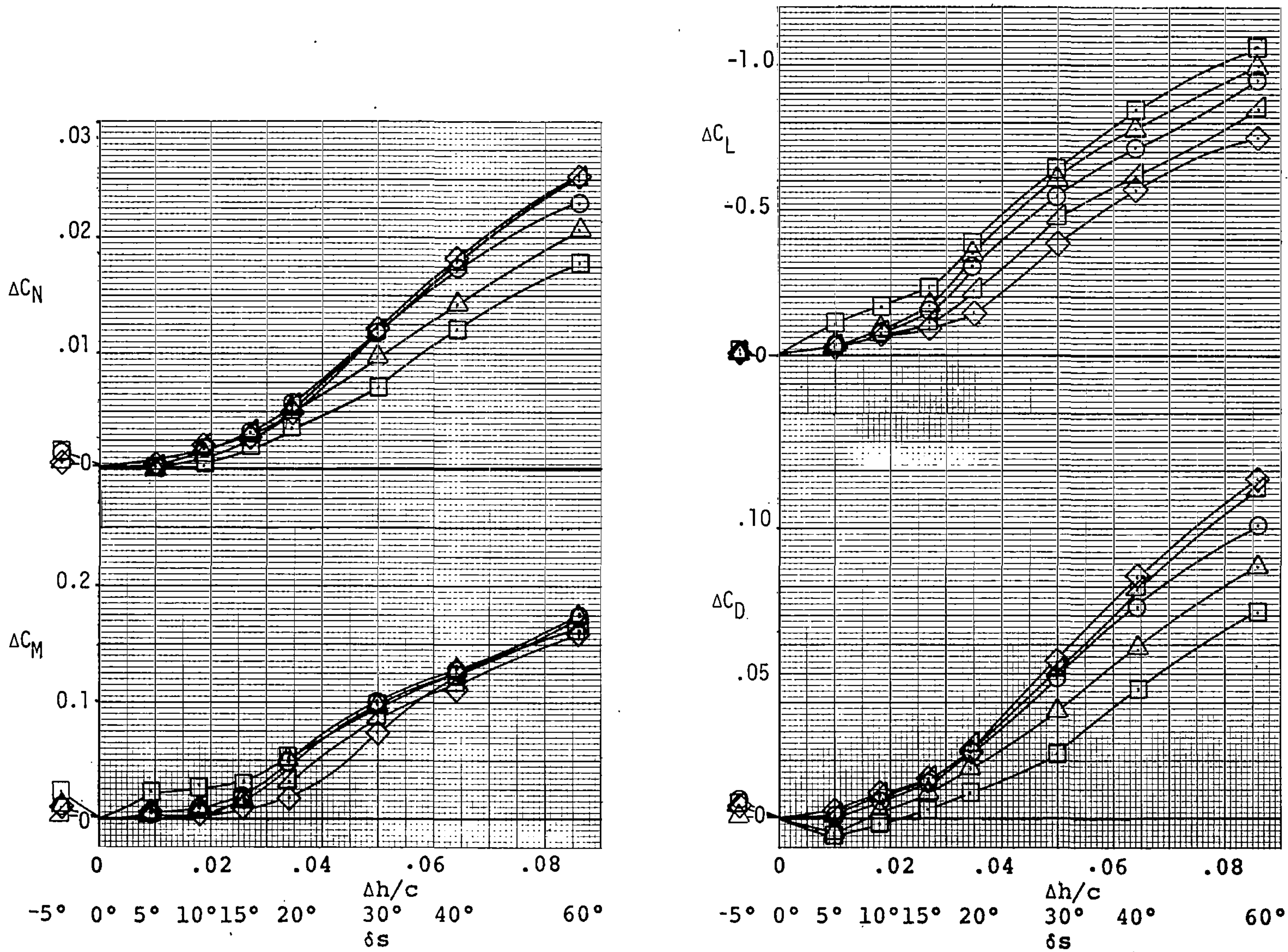

(b) Yawing Moments, Pitching Moments, Lift, and Drag.

Figure 21 - Effects of Tee Spoiler. Flap 30°.

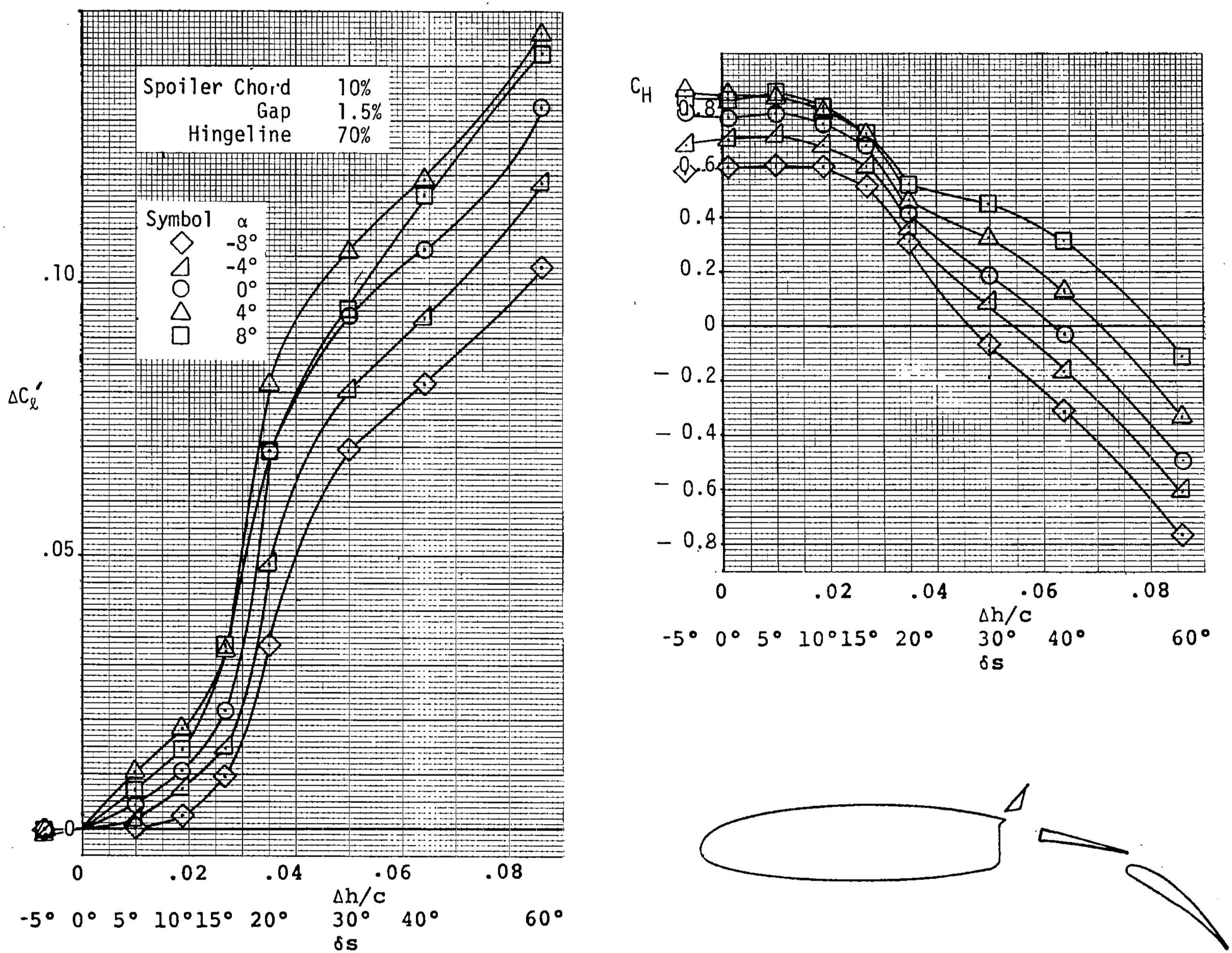

(a) Rolling Moments and Hinge Moments

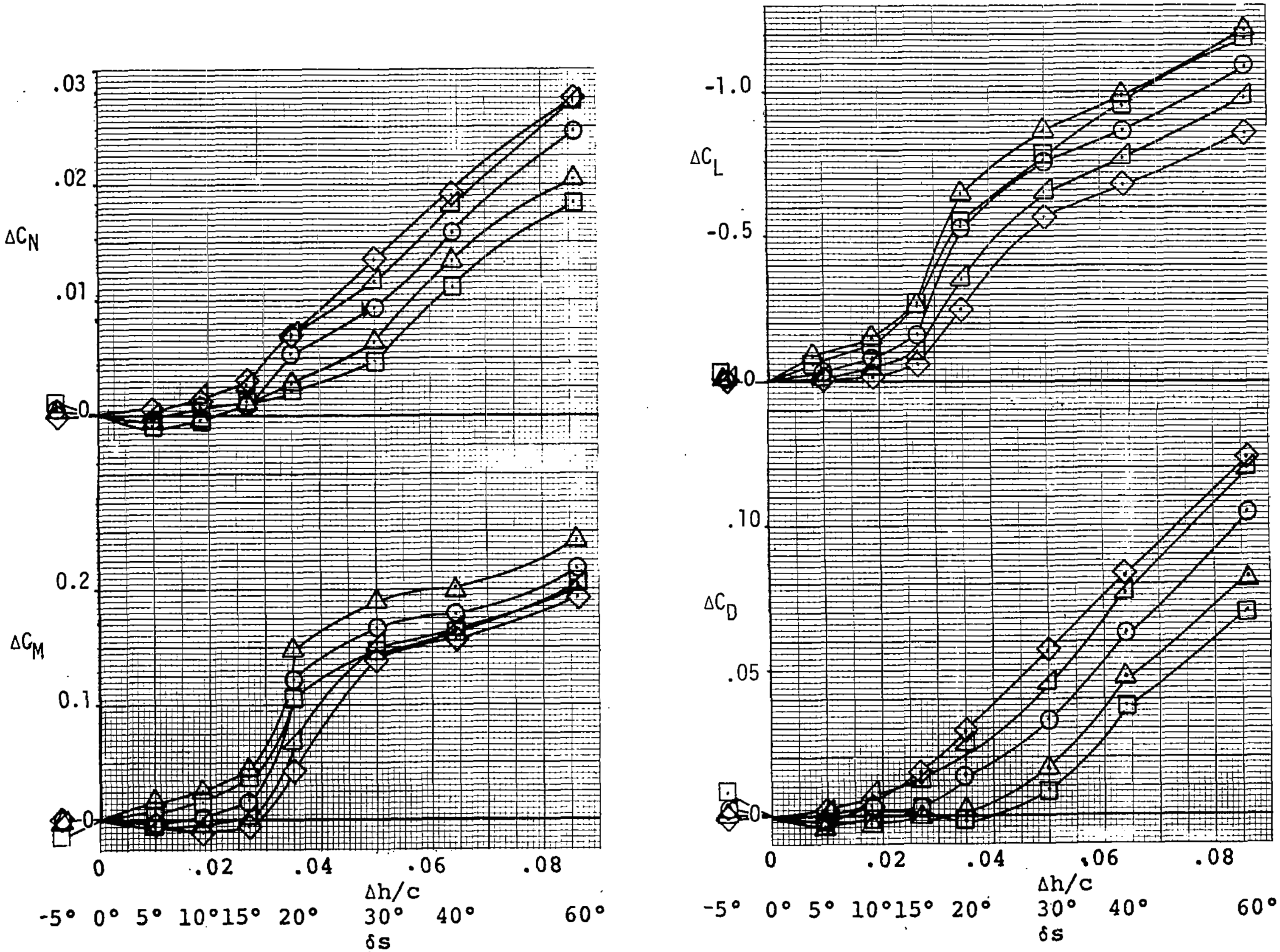

(b) Yawing Moments, Pitching Moments, Lift, and Drag.

Figure 22 - Effects of Triangle Spoiler. Flap 40°.

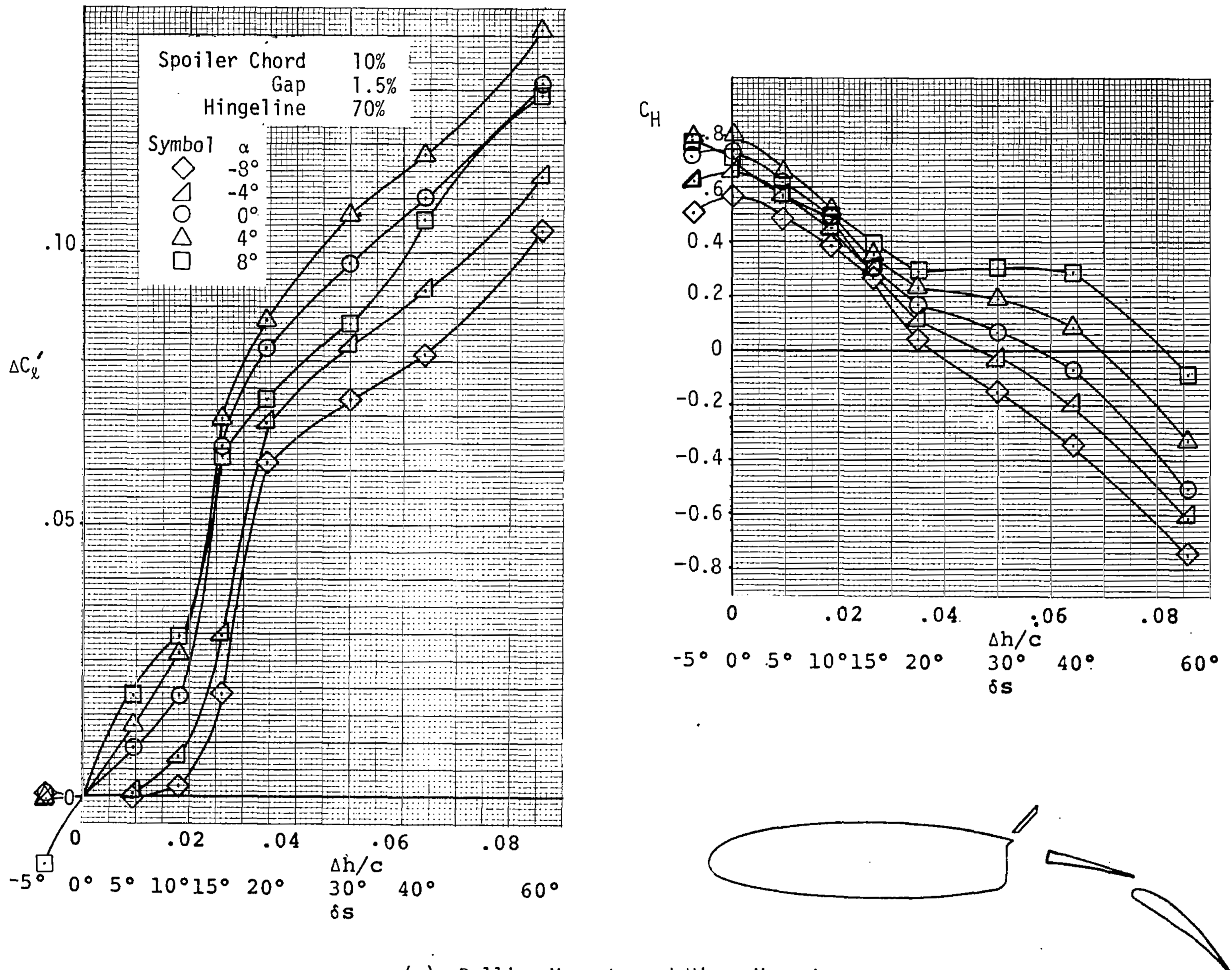

(a) Rolling Moments and Hinge Moments

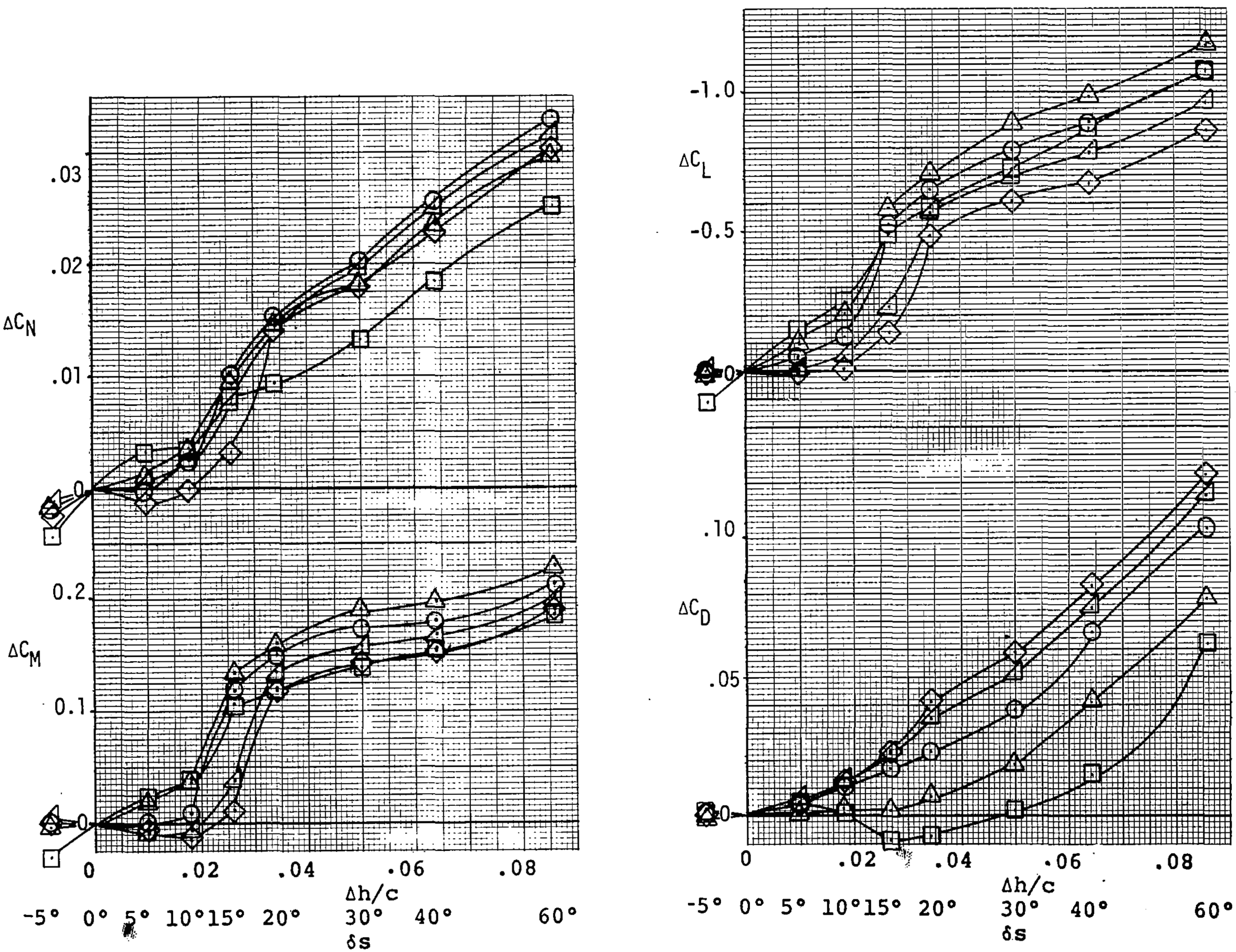

(b) Yawing Moments, Pitching Moments, Lift, and Drag.

Figure 23 - Effects of Flat Plate Spoiler. Flap 40°.

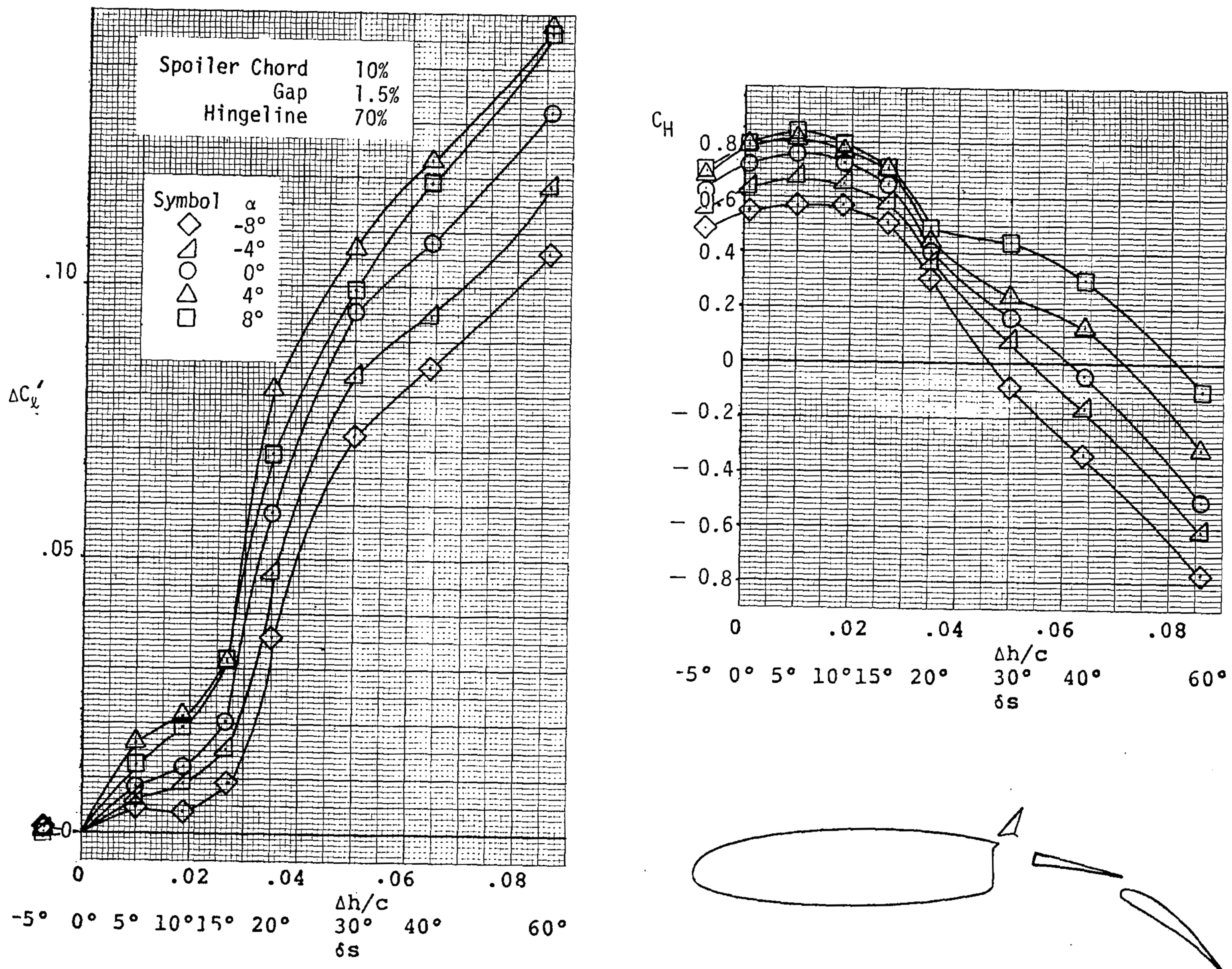

(a) Rolling Moments and Hinge Moments

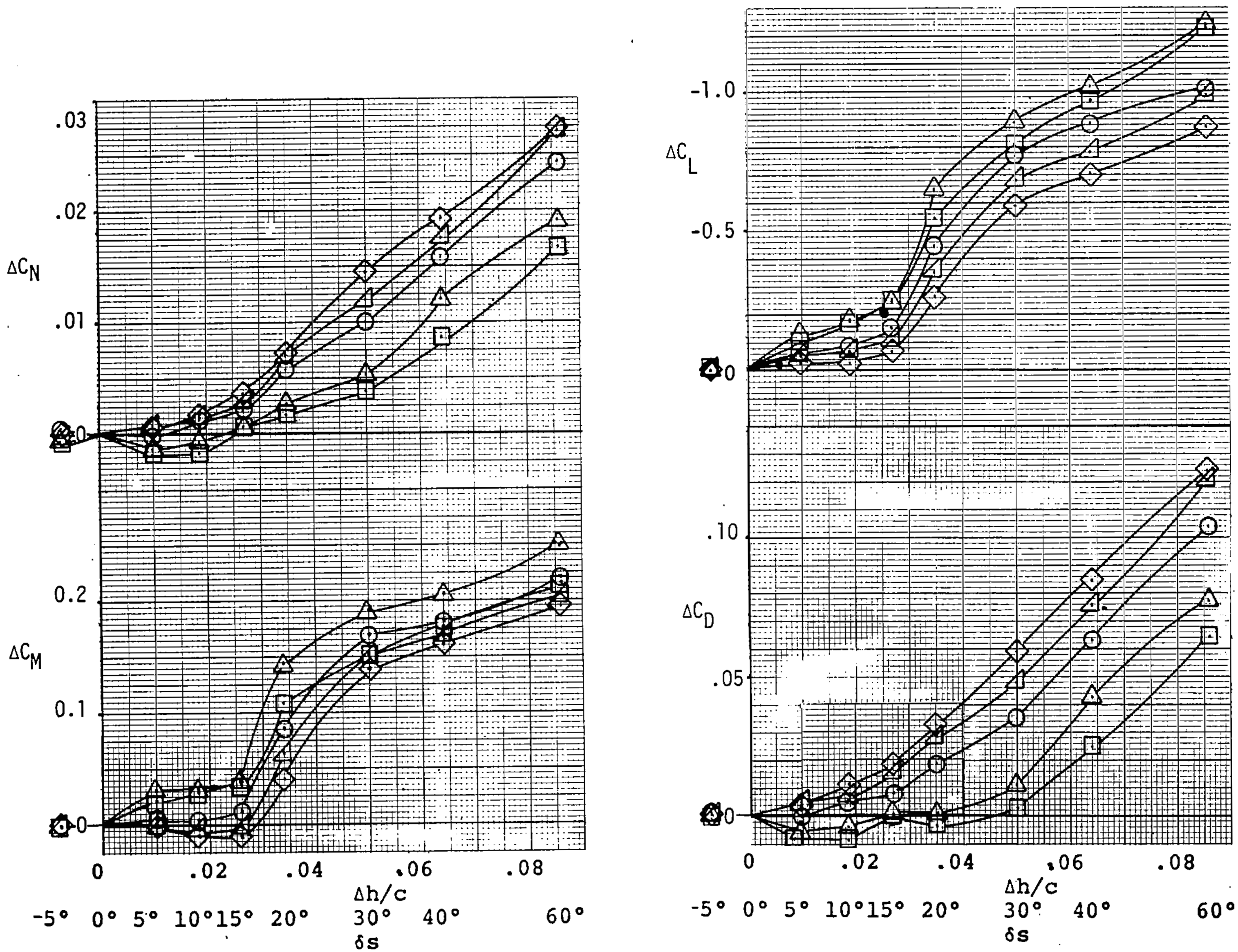

(b) Yawing Moments, Pitching Moments, Lift, and Drag.

Figure 24 - Effects of Sharp Triangle Spoiler. Flap 40^0.

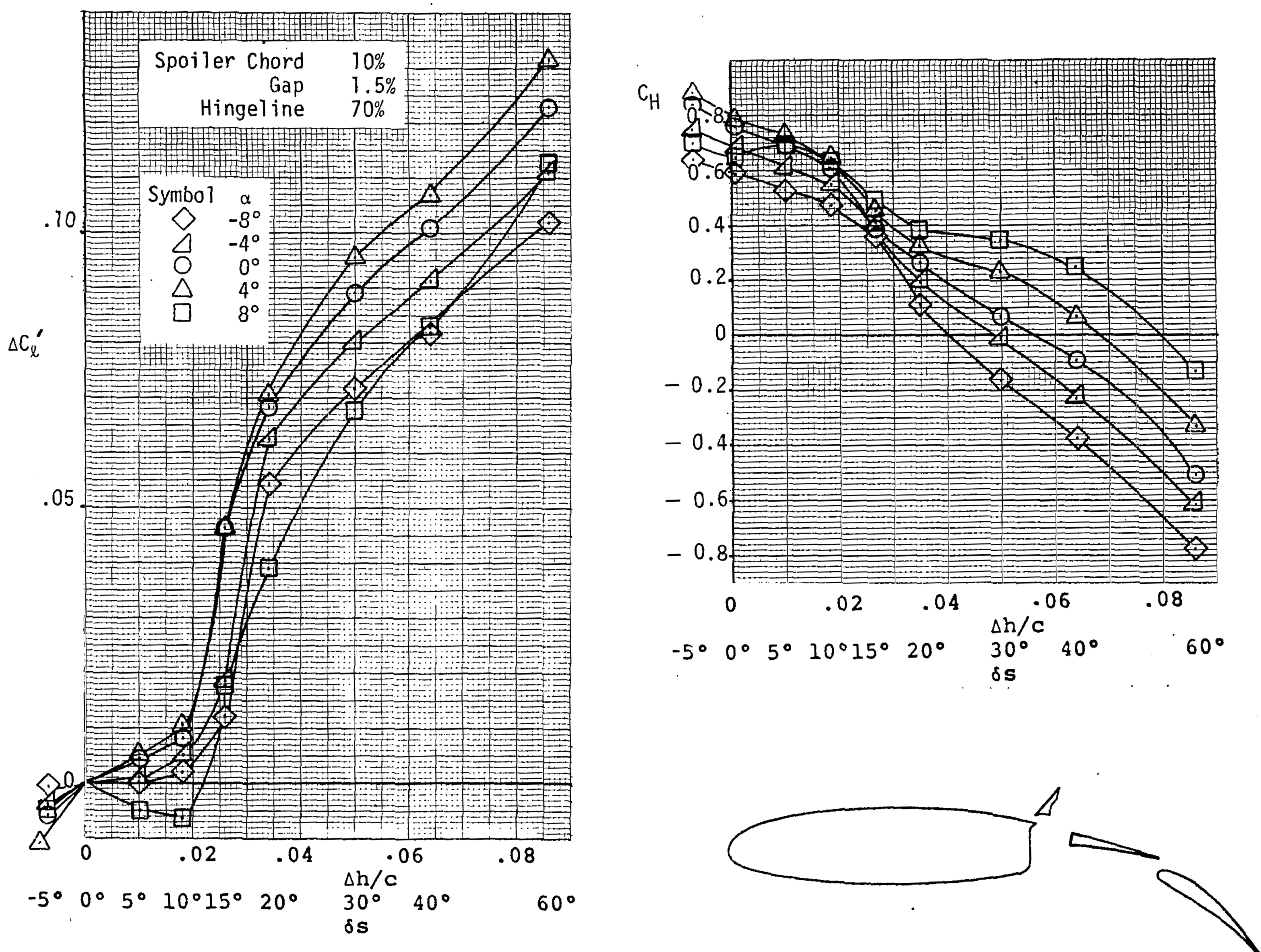

(a) Rolling Moments and Hinge Moments

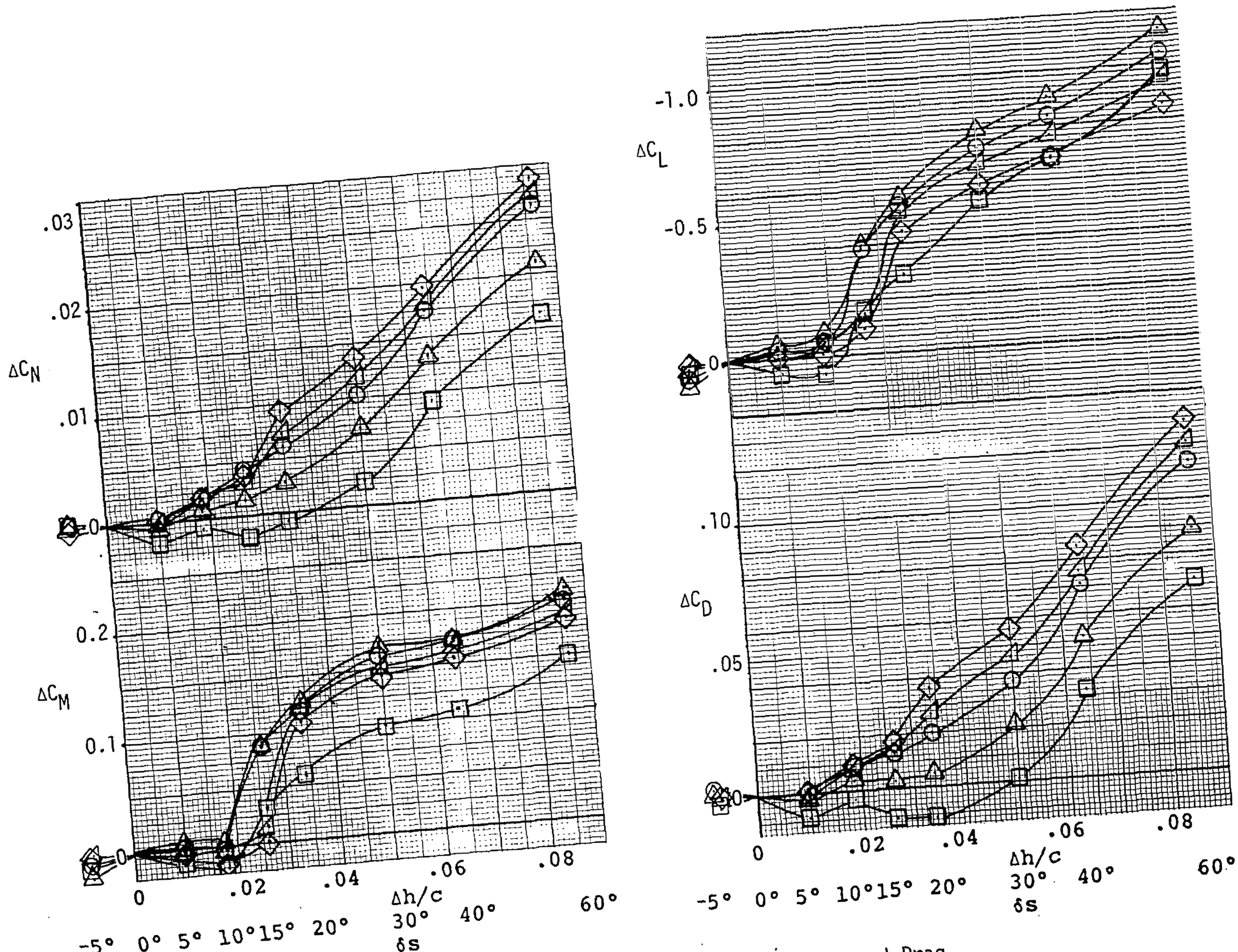

b) Yawing Moments, Pitching Moments, Lift, and Drag.

Figure 25 - Effects of MU-2 Spoiler. Flap 40°.

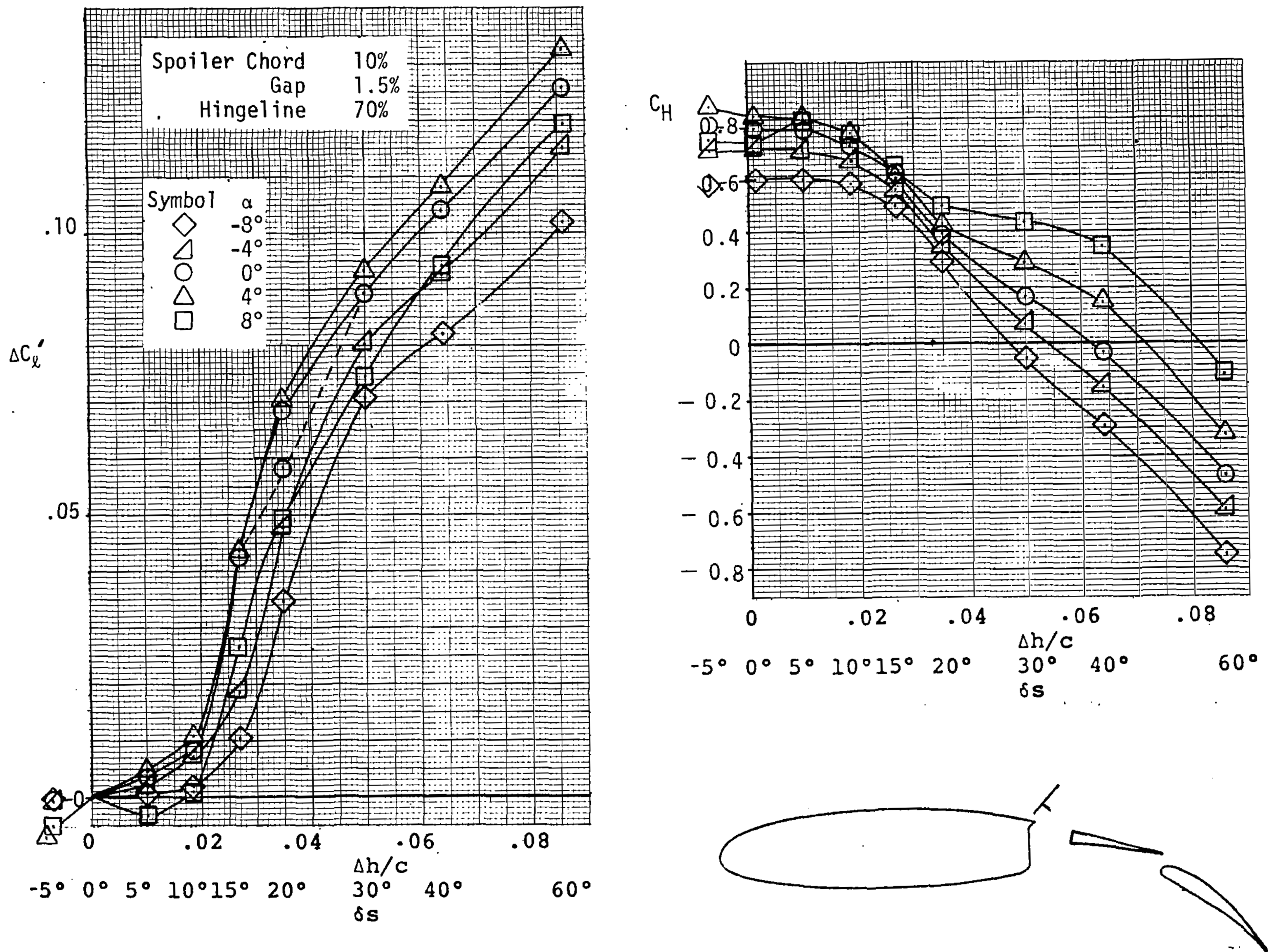

(a) Rolling Moments and Hinge Moments

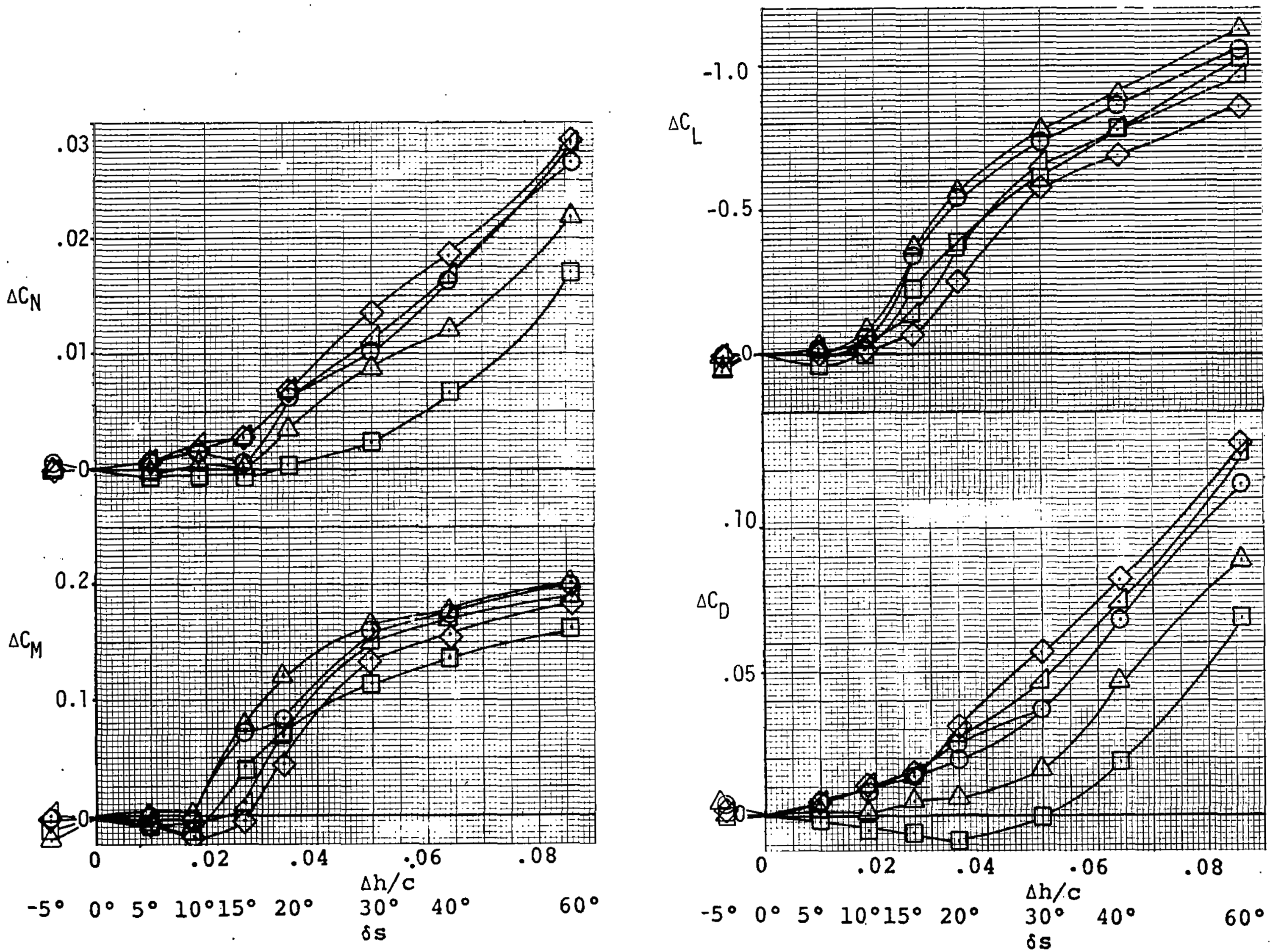

(b) Yawing Moments, Pitching Moments, Lift, and Drag.

Figure 26 - Effects of Tee Spoiler. Flap 40°.

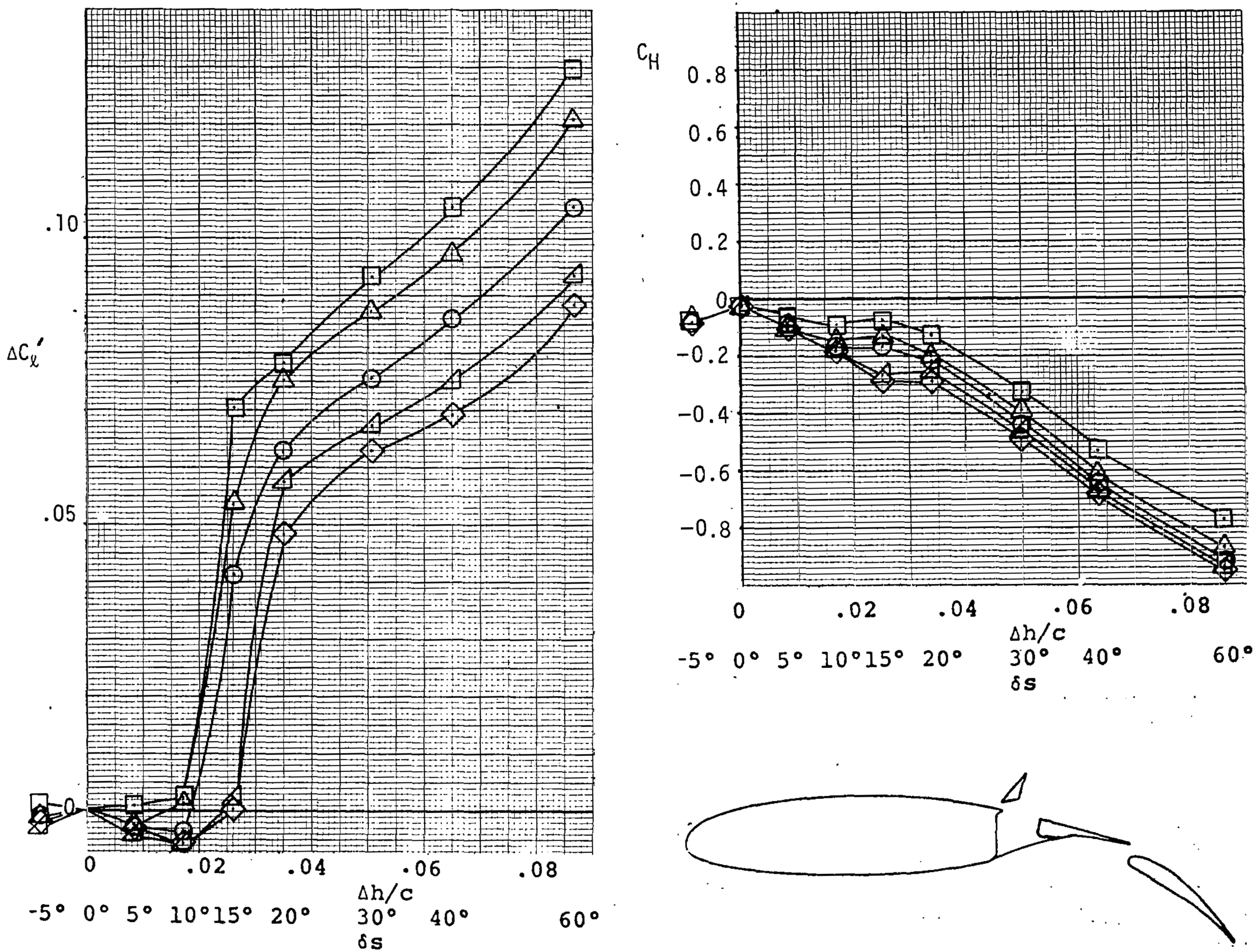

(a) Rolling Moments and Hinge Moments

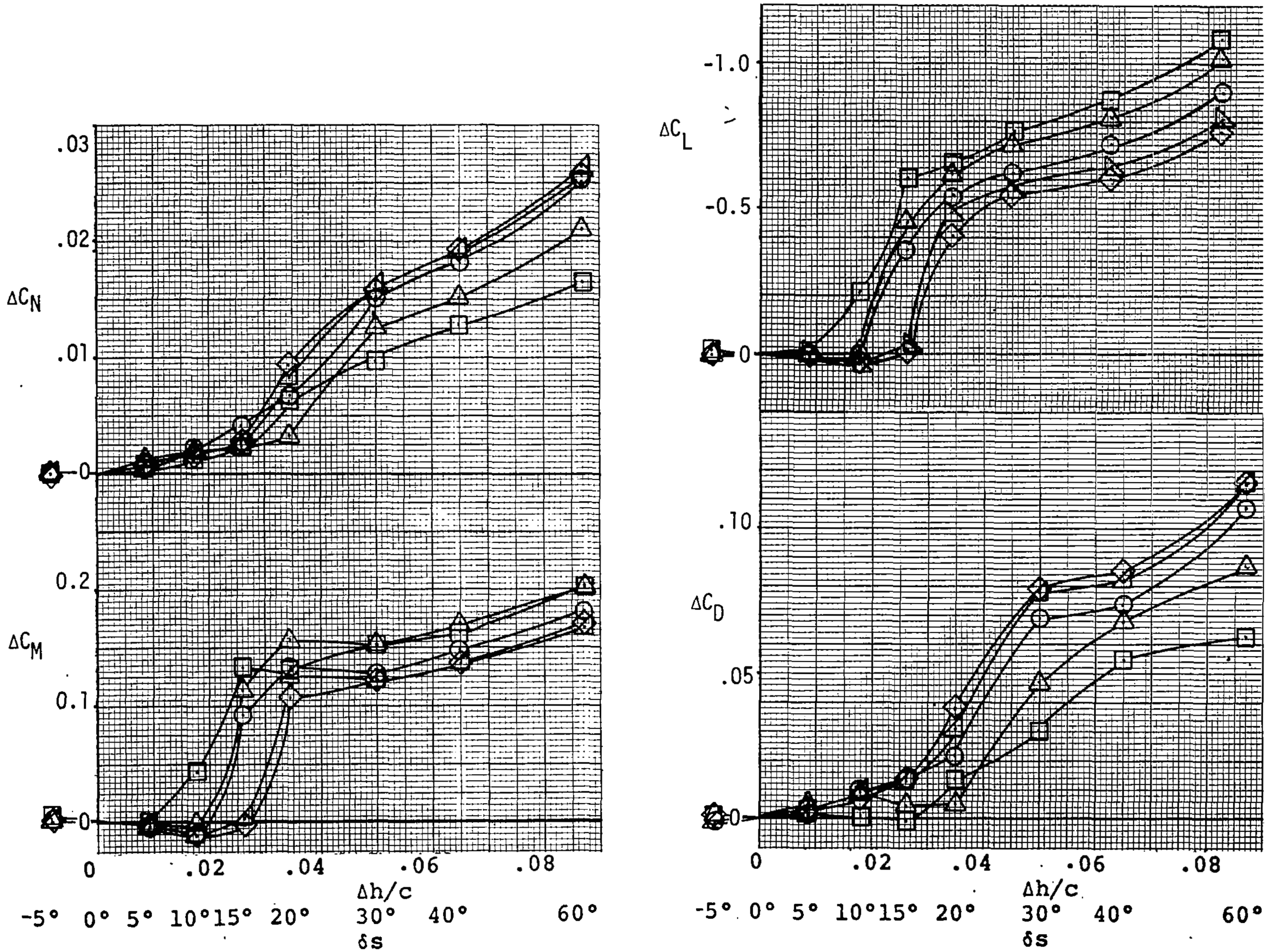

(b) Yawing moments, Pitching moments, Lift and Drag.

Figure 27 - Effects of Triangle Spoiler, with cavity sealed. Flap 40^0.

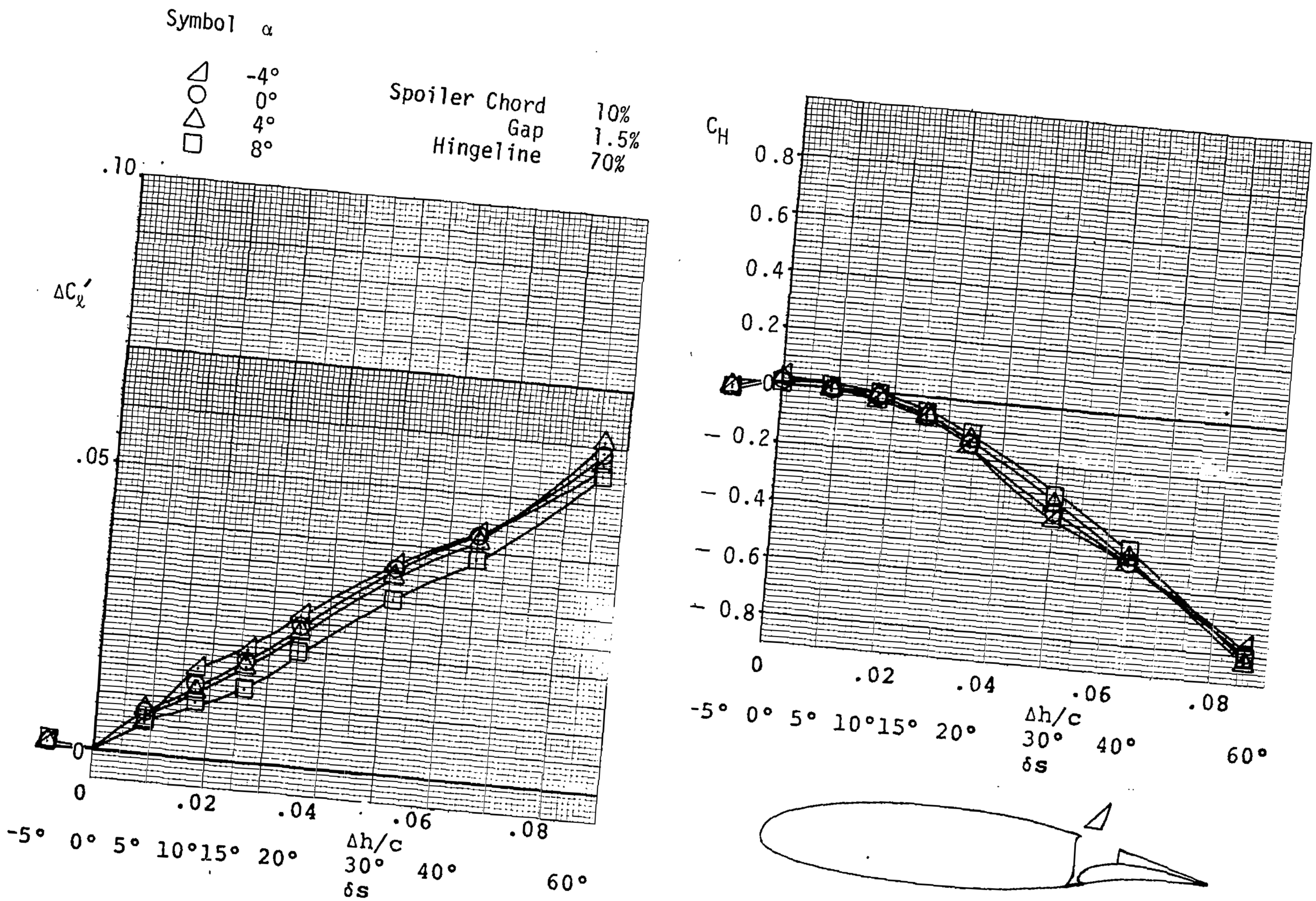

(a) Rolling Moments and Hinge Moments

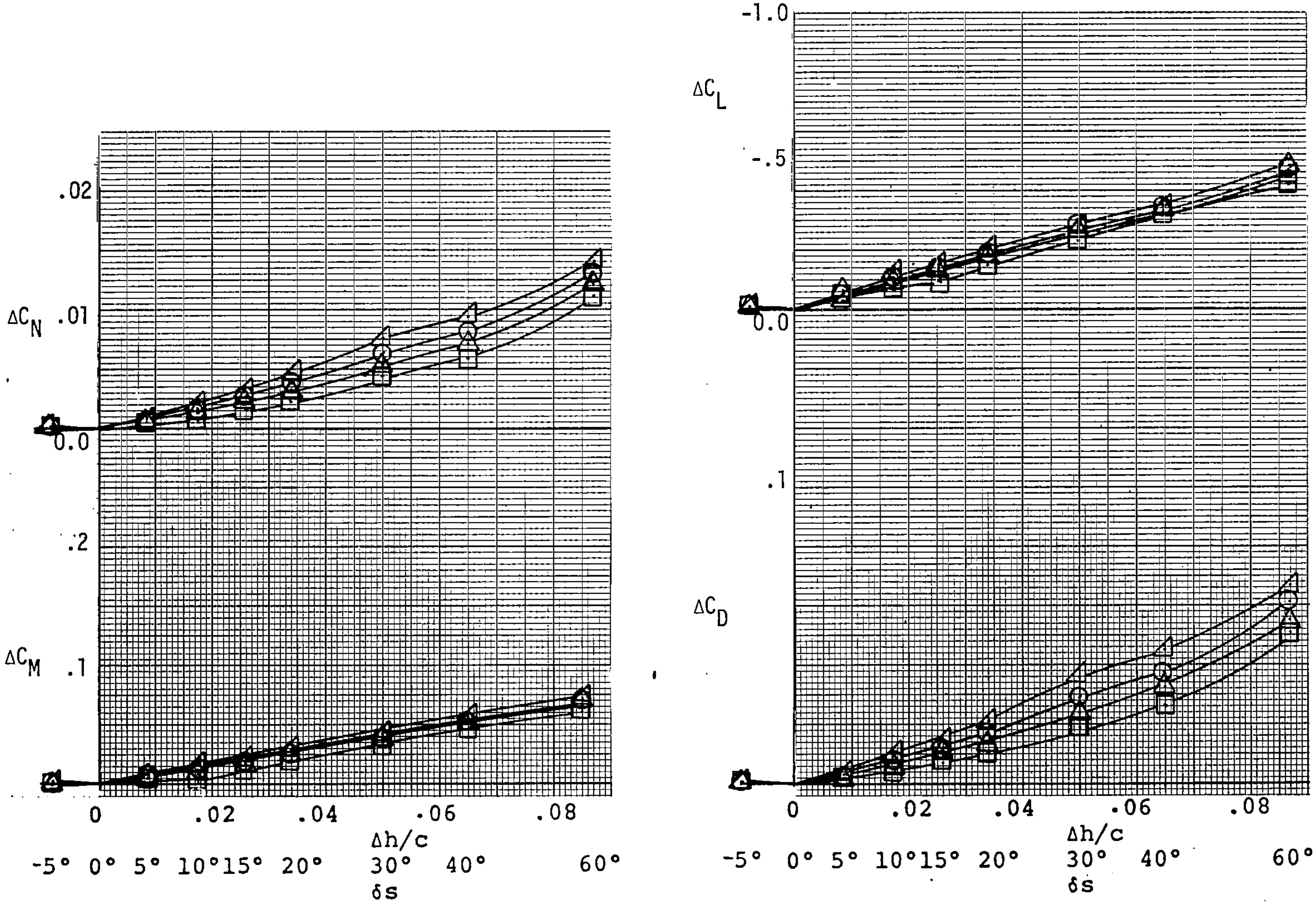

(b) Yawing Moments, Pitching Moments, Lift, and Drag.

Figure 28 - Effects of Sealing Flap. Triangle Spoiler. Flap Nested.

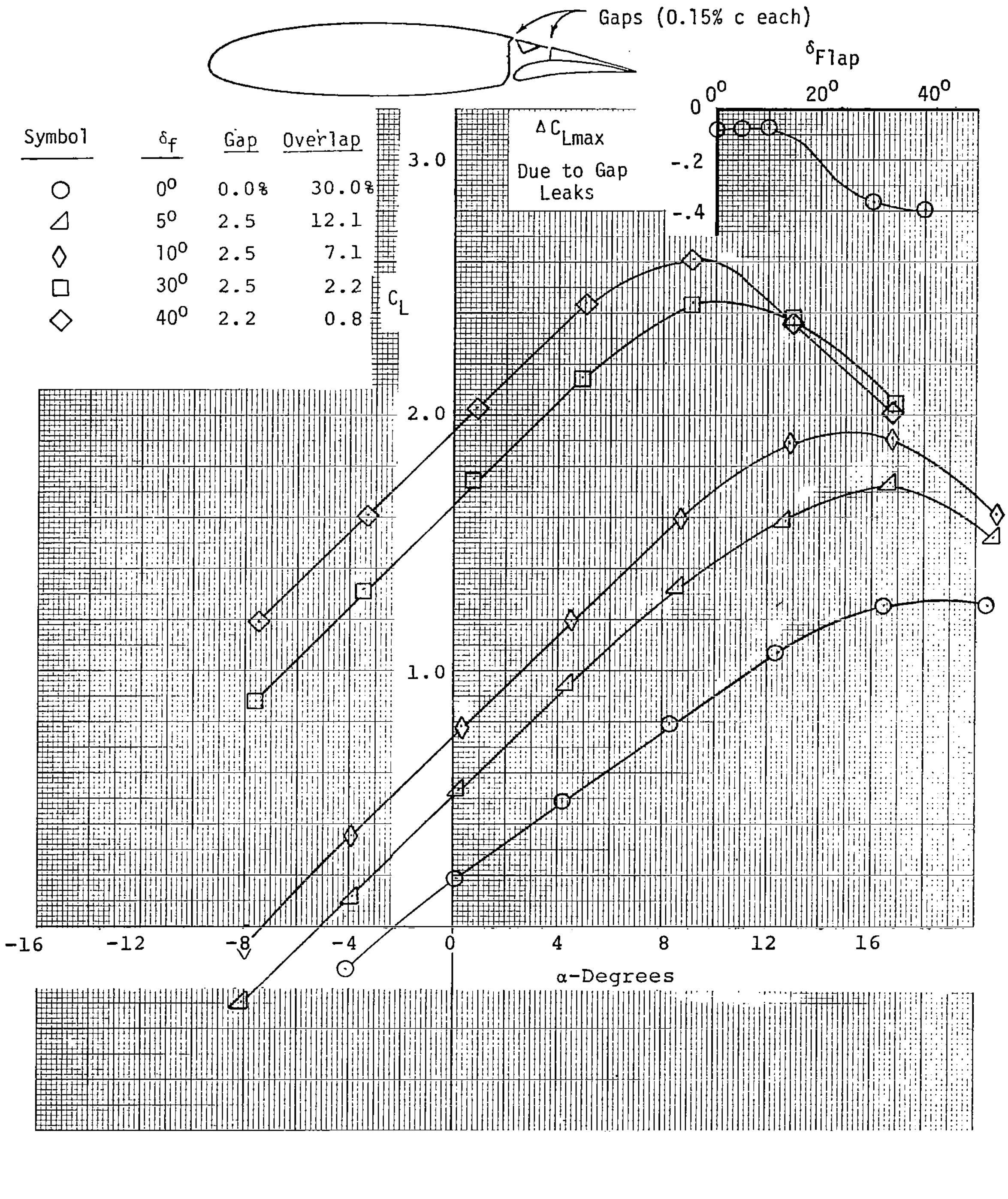

Figure 29 - Lift for various flap settings. Normal (0.3%) gap leaks.

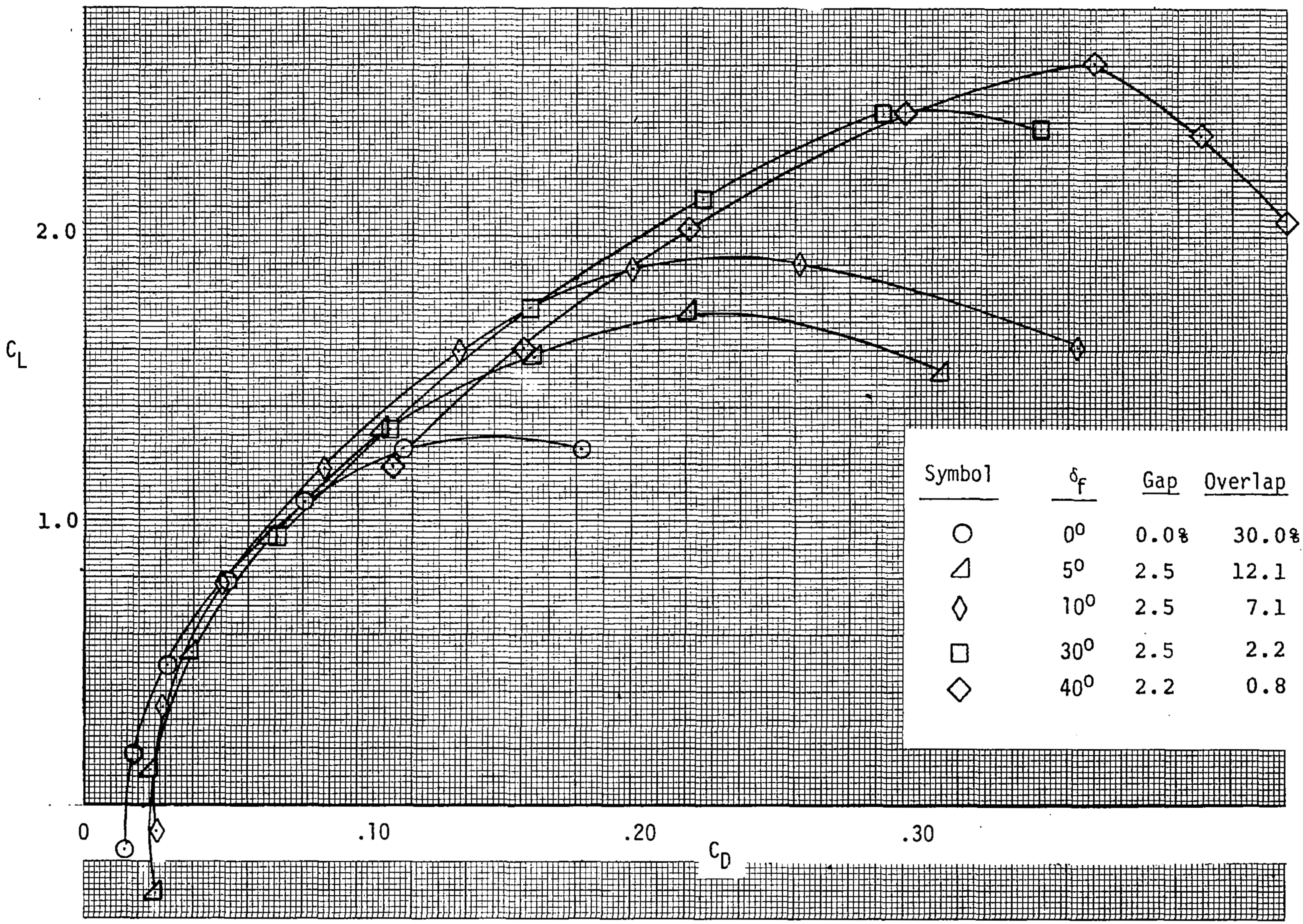

Figure 30 - Drag with normal (0.3%) gap leaks.

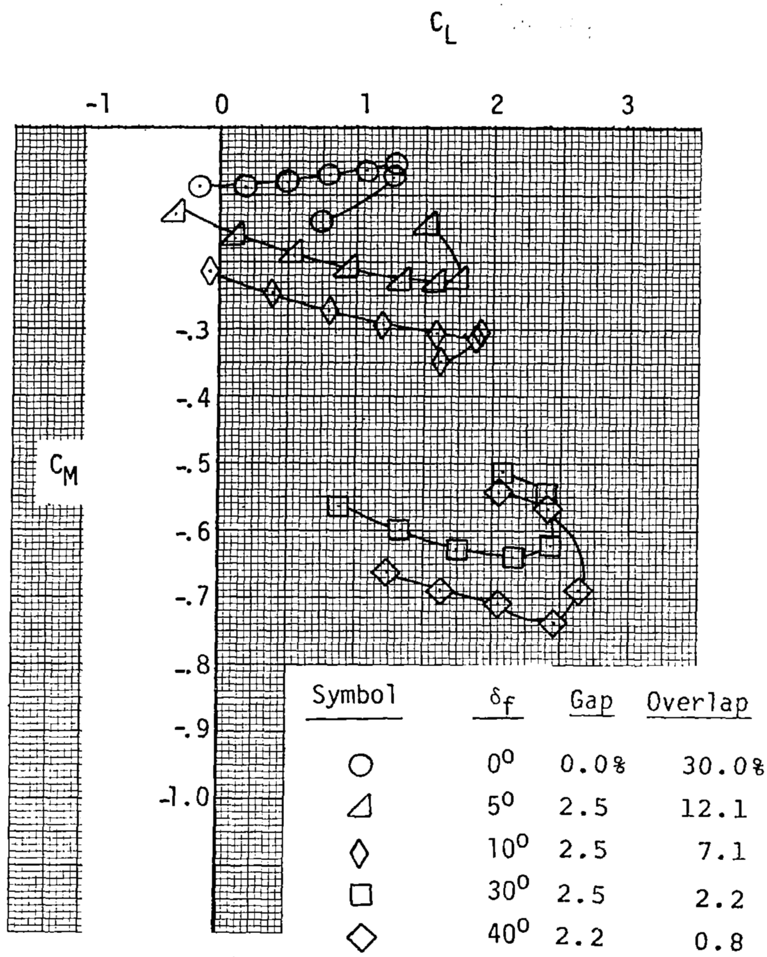

Figure 31 - Moments with normal (0.3%) gap leaks.

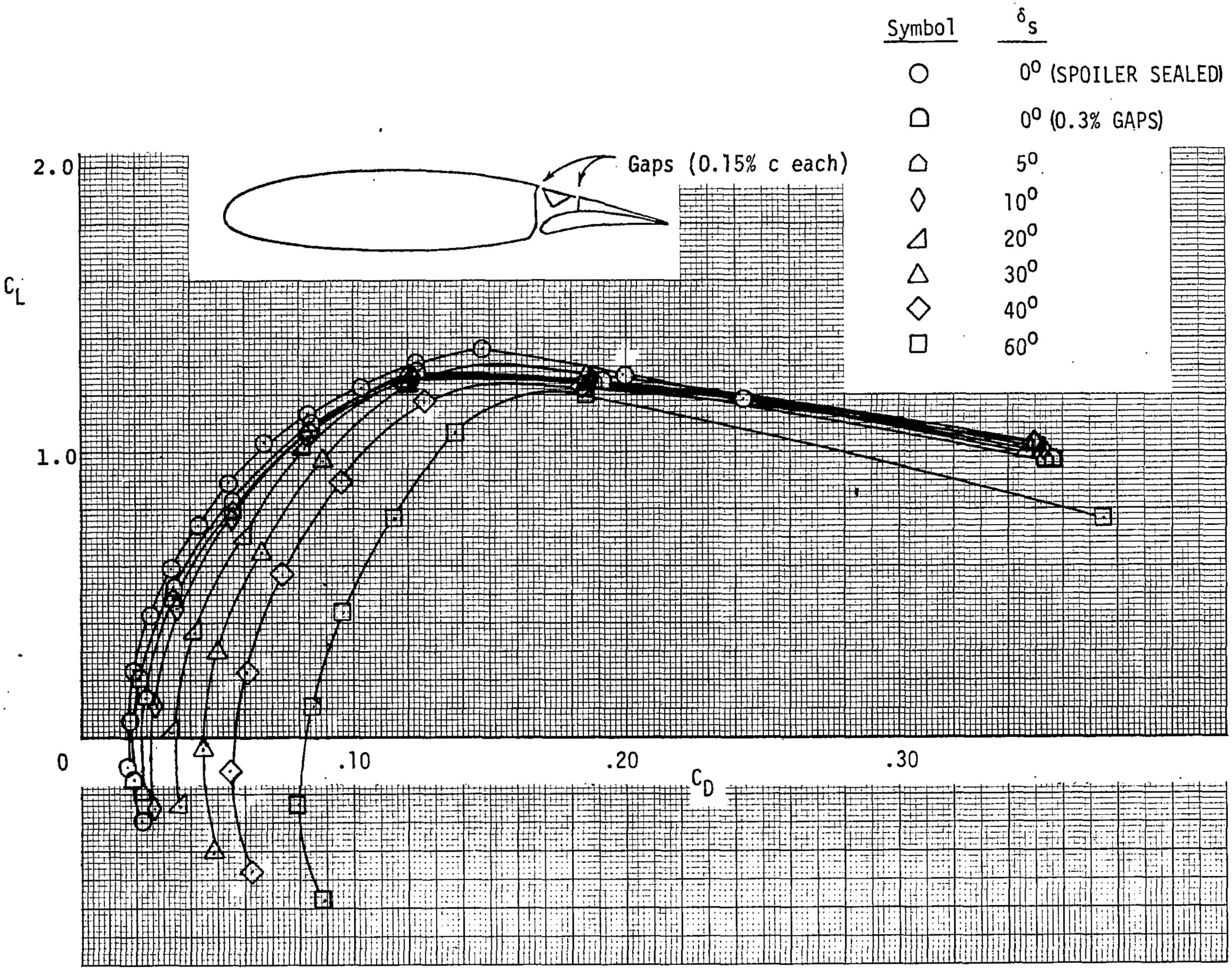

Figure 32 – Effects of Gap Leaks and Spoiler Opening on Drag. Flap Nested.

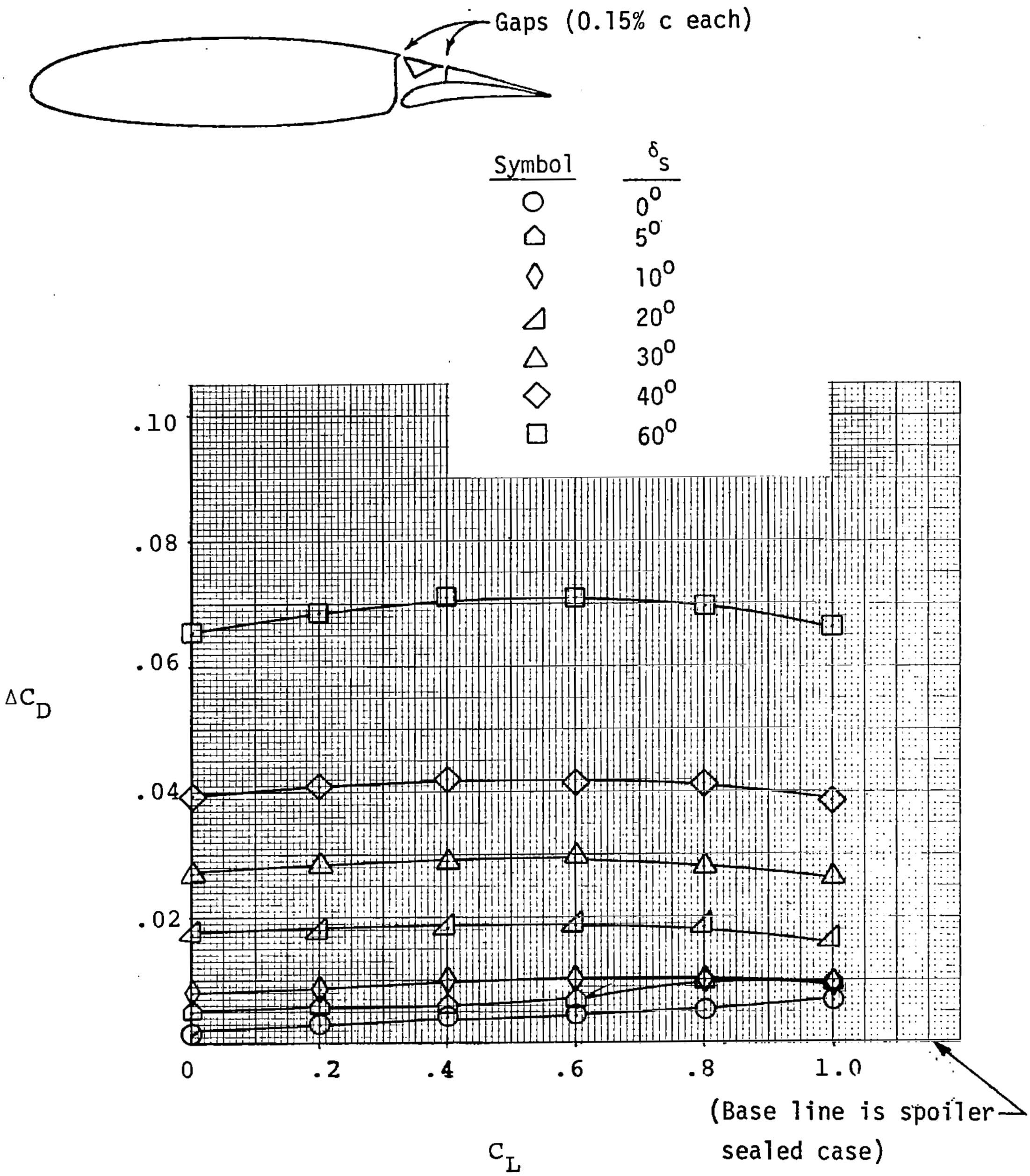

Figure 33 - Spoiler Gap Leak Drag. Flap Nested.0.30% Gap Leaks.

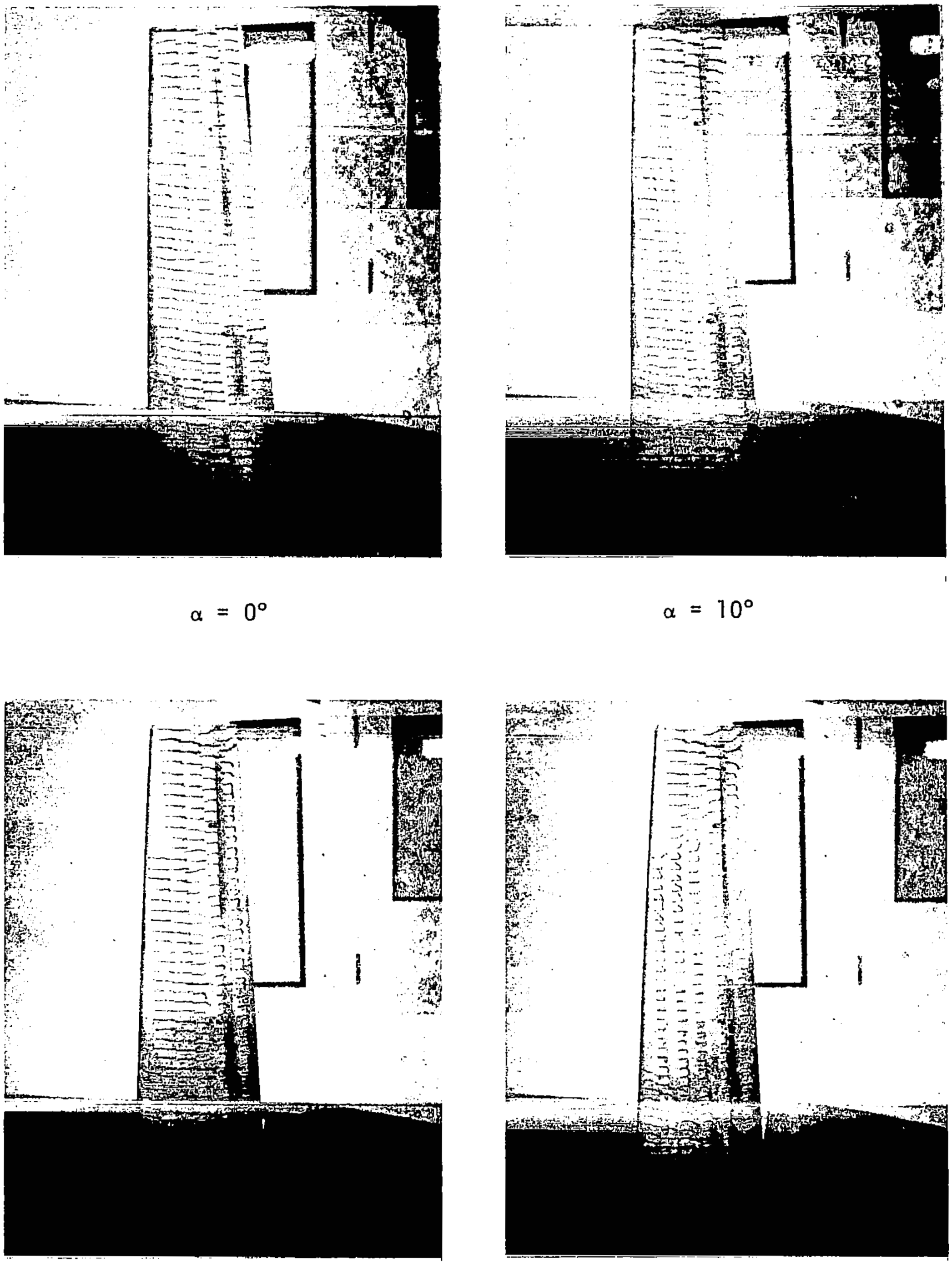

α = 0° α = 10°

α = 17.5° α = 20°

Figure 34 - Tuft photos. Flap nested.

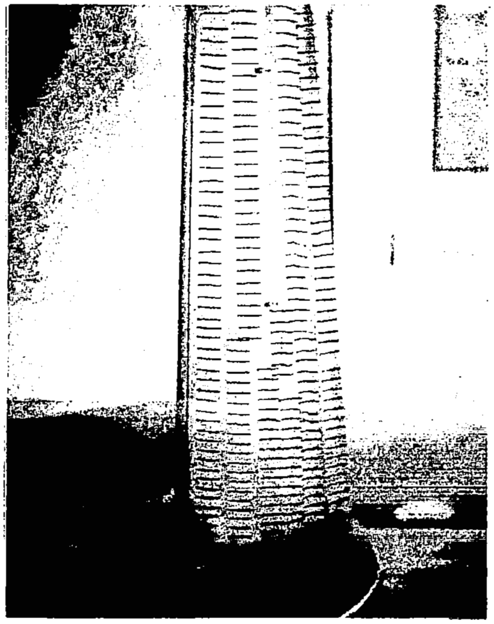

α = 4°

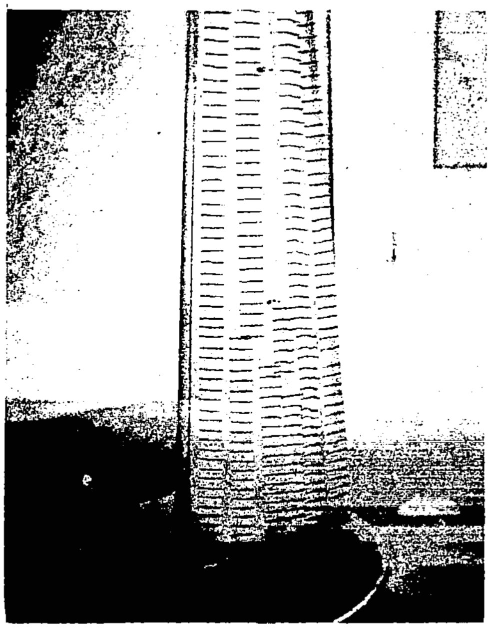

α = 8°

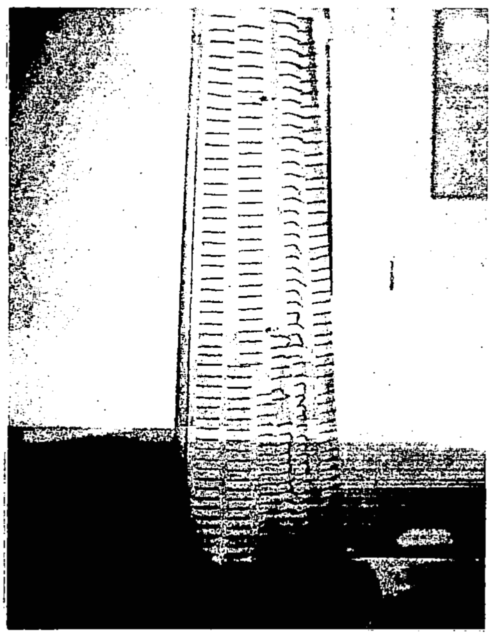

α = 12°

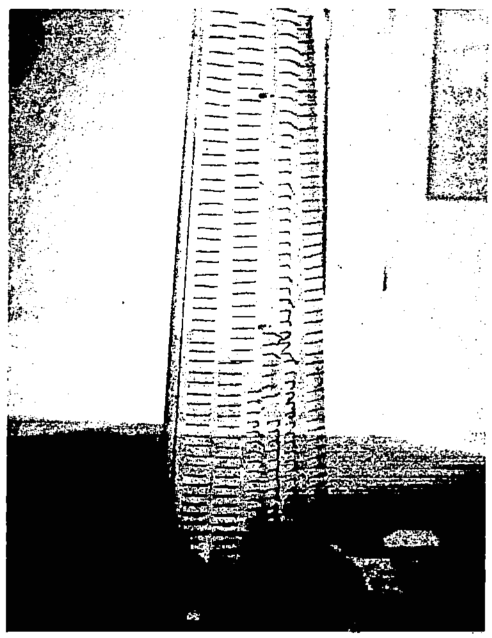

α = 14°

Figure 35 - Tuft photos . Flap 5°

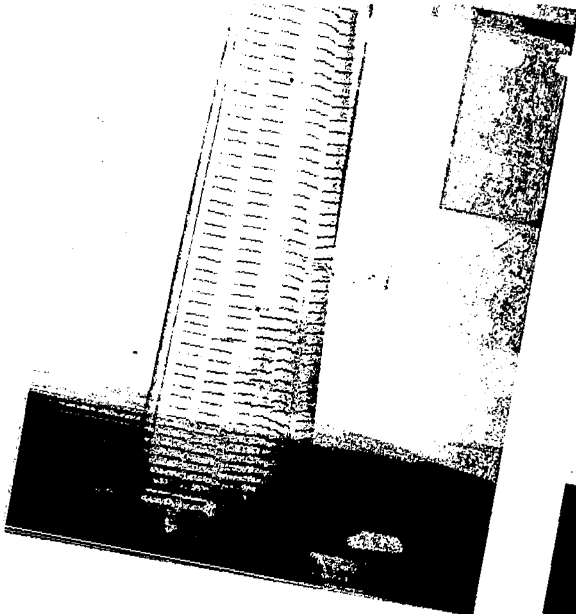

α = 10°

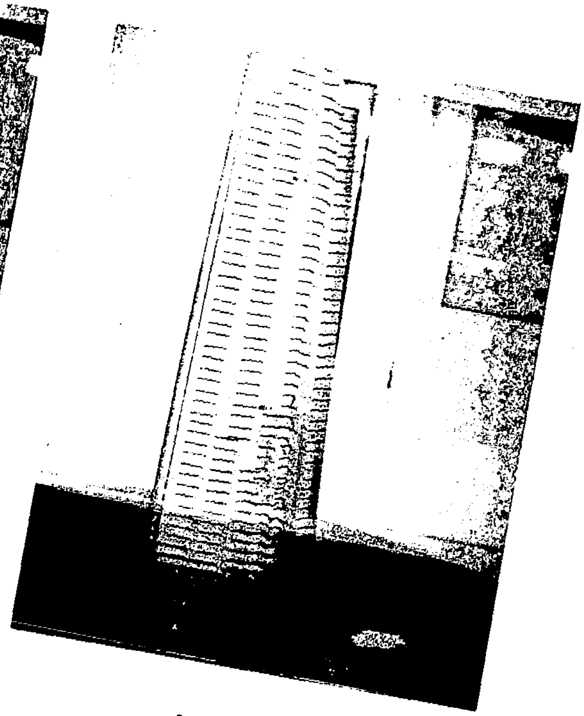

α = 12°

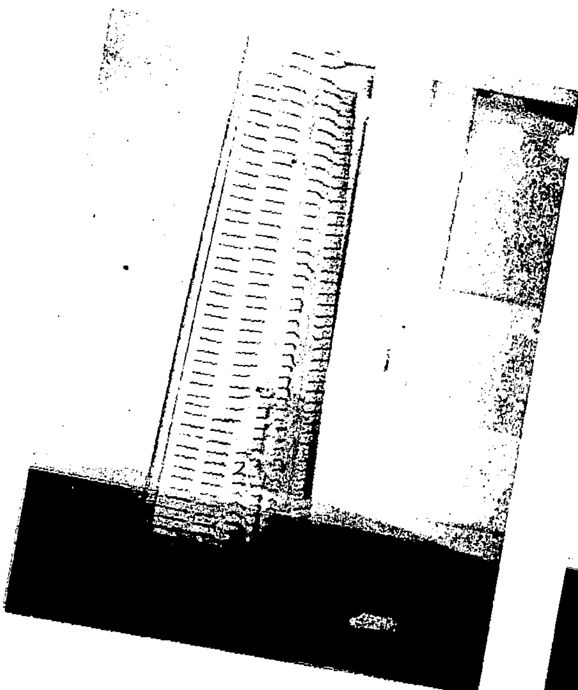

α = 14°

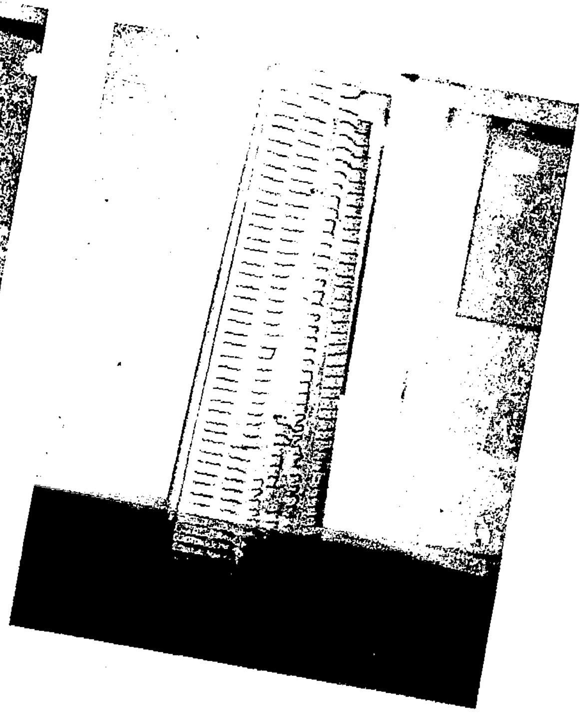

α = 16°

Figure 36 - Tuft photos. Flap 10°

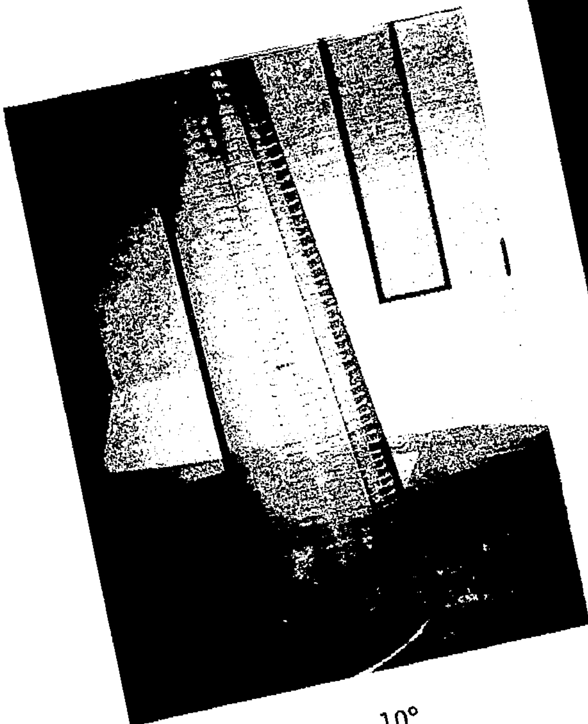

α = 10°

α = 12°

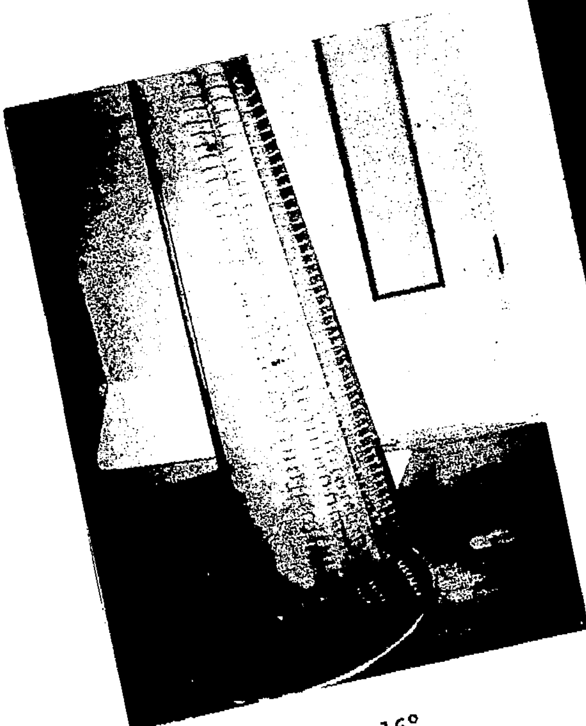

α = 16°

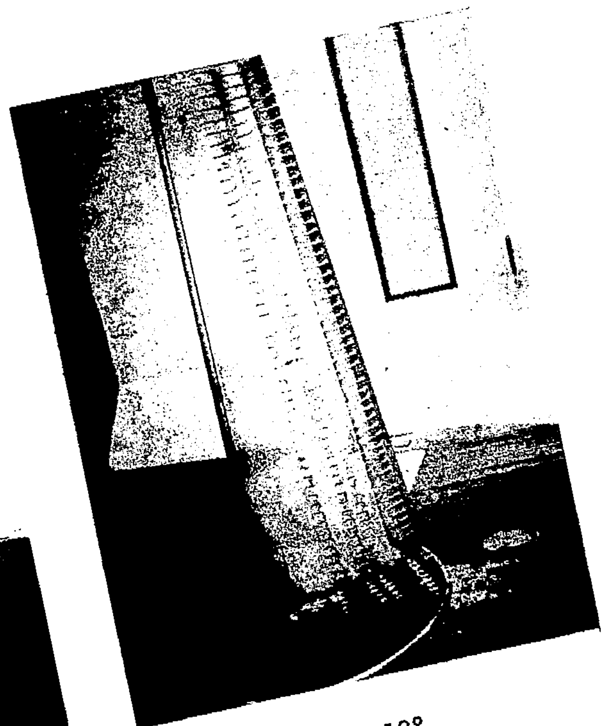

α= 18°

37 - Tuft photos. Flap 30°

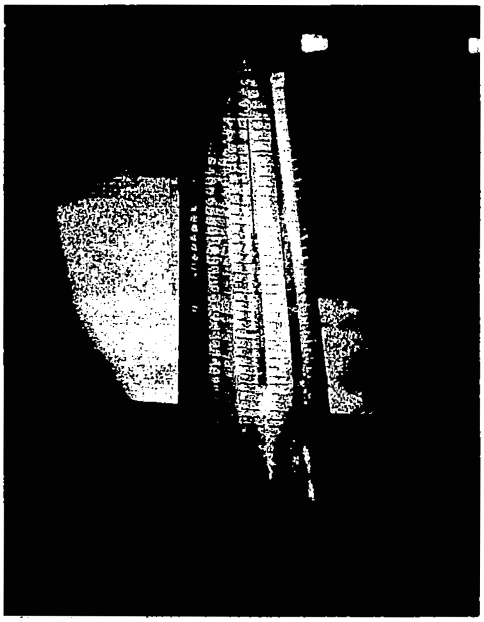

α = 0°

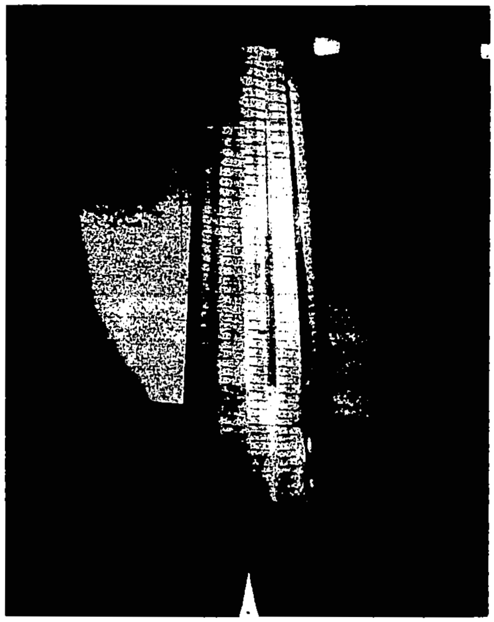

α = 8°

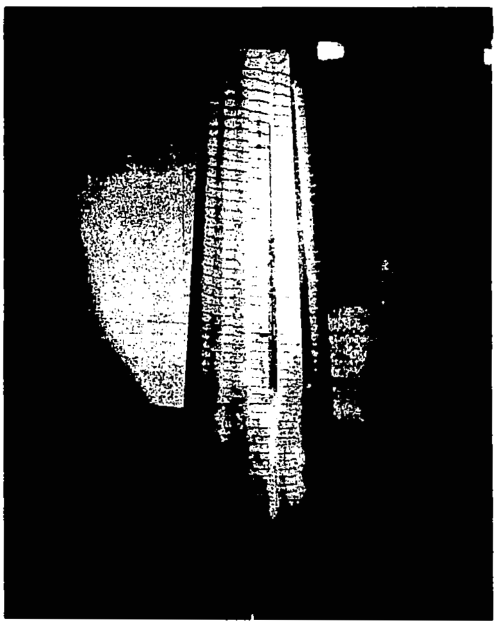

α = 10°

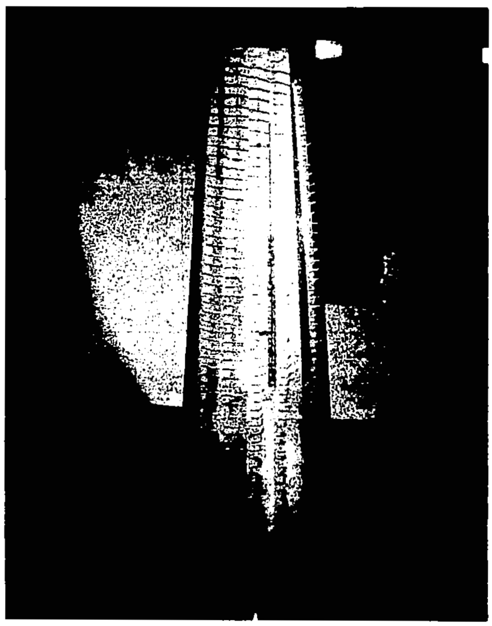

α = 12°

Figure 38 - Tuft photos. Flap 40°, gap 2.2%c, overlap +.8%c

APPENDICES

APPENDIX I - FORCE DATA REDUCTION PROGRAM

The 7-component force data reduction program calculates force coefficients for lift, drag, pitching moment, sideforce, yawing moment, rolling moment and spoiler hinge moment.

The model incorporated a disk end plate which necessitated the use of a dynamic tare of the disk alone for drag correction. The program utilizes a linear interpolation-extrapolation scheme for the static tare data to permit analysis of wind-on data at angles of attack between or beyond the measured static tare points.

After reading and storing the static tare values, the program is prepared to read wind-on data. First, a card bearing general run title information is read. Then a wind-off card is read followed by the wind-on data with 3 data samples per angle of attack. The three wind-on values are averaged and checked for the correct number of cards. Next, the tare values are looked up and subtracted followed by the subtraction of the wind-off values. (These latter values are zero or very small.) Measured forces are then corrected for solid blockage, wake blockage, downwash effects and streamline curvature. Next, using a corrected dynamic pressure value, all force coefficients are calculated and written out along with corrected angle of attack, Reynolds number, and $\Delta h/c$ (a measure of spoiler deflection).

Program listing and sample output are given on the pages which follow.

```
PAGE   1    01/02/76    1105    GAR,001,RINCKER

// JOB T

LOG DRIVE   CART SPEC   CART AVAIL  PHY DRIVE
  0000        0001        0001        0000

V2 M08   ACTUAL  8K  CONFIG  8K

// FOR
*LIST SOURCE PROGRAM
      FUNCTION TABL(X,NX,Y,XVAL)
      DIMENSION X(1),Y(1)
      DO 3 I=1,NX
      IF (X(I)-XVAL) 3,10,5
    3 CONTINUE
      JX=NX
      GO TO 8
    5 JX=I
      IF(JX-1)6,6,8
    6 JX=2
    8 PC=(XVAL-X(JX-1))/(X(JX)-X(JX-1))
      TABL=Y(JX-1)+PC*(Y(JX)-Y(JX-1))
      RETURN
   10 TABL=Y(I)
      RETURN
      END

FEATURES SUPPORTED
 ONE WORD INTEGERS

CORE REQUIREMENTS FOR TABL
 COMMON      0  VARIABLES     10  PROGRAM    126

RELATIVE ENTRY POINT ADDRESS IS 000C (HEX)

END OF COMPILATION

// DUP

*STORE      WS  UA  TABL
CART ID 0001   DB ADDR  2CB0   DB CNT   000A

// FOR
*IOCS (CARD, 1132 PRINTER,PLOTTER)
*LIST SOURCE PROGRAM
      INTEGER TN
      REAL CONFI (10)
      DIMENSION        ZL(30),ZD(30),ZP(30),ZR(30),ZS(30),ZA(30),ZY(30)
      DIMENSION EQ(3),ED(3),ER(3),ES(3),EP(3),EY(3),EA(3),EL(3)
C
C
C     ATLIT I    FORCE DATA REDUCTION
C
C
      IN=5
      IO=6
      READ(IN,1)AREA,AEROC,SCORD,SAREA,SPAN
    1 FORMAT(5F10.5)

C     READ TARE NUMBER AND NUMBER OF POINTS
```

```
      2 READ(IN,3)TN,NPTS
      3 FORMAT(I1,I2)
        IF (NPTS) 99,99,4

C       READ TARE ZERO

      4 READ(IN,8)ZQ,TZS,TZR,TZY,TZD,TZP,TZL,TZA
      8 FORMAT(10X,F3.0,1X,F5.0,1X,F5.0,1X,F5.0,1X,F5.0,1X,F5.0,1X,F5.0,5X
       1,F3.0)

C       READ TARE DATA
        DO 9 I=1,NPTS
        READ(IN,10)ZQ,ZS(I),ZR(I),ZY(I),ZD(I),ZP(I),ZL(I),ZA(I)
     10 FORMAT(10X,F3.0,1X,F5.0,1X,F5.0,1X,F5.0,1X,F5.0,1X,F5.0,1X,F5.0,5X
       1,F3.0)
      9 CONTINUE
        DO 11 I=1,NPTS
        ZL(I)=ZL(I)-TZL
        ZD(I)=ZD(I)-TZD
        ZP(I)=ZP(I)-TZP
        ZR(I)=ZR(I)-TZR
        ZS(I)=ZS(I)-TZS
        ZA(I)=ZA(I)-TZA
        ZY(I)=ZY(I)-TZY
     11 CONTINUE

C       READ INFO,WIND OFF AND TUNNEL DATA

     26 CONTINUE
        READ(IN,37)DELF,DELS,CONFI
     37 FORMAT(2F10.5,10A4)
        READ(IN,21)WQ,WS,WR,WY,WD,WP,WL,RUN
     21 FORMAT(10X,F3.0,1X,F5.0,1X,F5.0,1X,F5.0,1X,F5.0,1X,F5.0,1X,F5.0,23
       1X,F3.0)
        IF (RUN) 2,2,22
     22 CONTINUE

C       READ DATA

        WRITE(IO,72)
     72 FORMAT('1','1',T45,'WICHITA STATE UNIVERSITY'/)
        WRITE(IO,73)
     73 FORMAT(T44,'WALTER H BEECH WIND TUNNEL',/)
        WRITE(IO,74)
     74 FORMAT(T32,'EFFECTIVENESS OF SPOILERS ON NASA-ATLIT SEMISPAN MODEL
       1',/)
     75 FORMAT(T52,'JULY 1975',//)
        WRITE(IO,75)
        WRITE(IO,92)CONFI
     92 FORMAT(T40,10A4,/)
        WRITE(IO,71)RUN,DELF,DELS
     71 FORMAT(T8,'RUN NO',1X,F4.0,T25,'FLAP DEFLECTION',1X,F3.0,'DEG',8X,
       1'SPOILER DEFLECTION',1X,F3.0,'DEG.',//)
        WRITE(IO,76)
     76 FORMAT(4X,'ALPHA',4X,'CL',7X,'CD',6X,'CM',6X,'CR',6X,'CS',6X,'CY',
       16X,'CH',9X,'Q',12X,'RN',13X,'H/C',/)
     23 DO 27 J=1,3
        READ(IN,25)EQ(J),ES(J),ER(J),EY(J),ED(J),EP(J),EL(J),EA(J),EST,BP,
```

```
      1T,RNO
   25 FORMAT(T11,F3.0,6F6.0,T54,F4.0,T59,F4.0,T64,F4.2,T69,F3.0,T73,F3.0
     1)
      IF (RNO) 26,26,27
   27 CONTINUE
      DELS=DELS
   28 IF (RUN-RNO) 99,29,99
   29 ALPHA=(EA(1)+EA(2)+EA(3))/3.
      IF (ALPHA-EA(1)) 31,32,31
   31 WRITE(IO,66)
   66 FORMAT(10X,'ERROR')
      GO TO 23
   32 XL=(EL(1)+EL(2)+EL(3))/3.
      XD=(ED(1)+ED(2)+ED(3))/3.
      XP=(EP(1)+EP(2)+EP(3))/3.
      XR=(ER(1)+ER(2)+ER(3))/3.
      XS=(ES(1)+ES(2)+ES(3))/3.
      XY=(EY(1)+EY(2)+EY(3))/3.
      Q=(EQ(1)+EQ(2)+EQ(3))/3.
      XD=(XD-TABL(ZA,NPTS,ZD,ALPHA))
      XL=(XL-TABL(ZA,NPTS,ZL,ALPHA))
      XR=(XR-TABL(ZA,NPTS,ZR,ALPHA))
      XP=(XP-TABL(ZA,NPTS,ZP,ALPHA))
      XY=(XY-TABL(ZA,NPTS,ZY,ALPHA))
      XS=(XS-TABL(ZA,NPTS,ZS,ALPHA))
      Q=Q/10.
      Q=Q*.987

C     SUBTRACT WIND OFF AND DIVIDE BY SCALE FACTOR

      XS=(XS-WS)/5.
      XR=XR-WR
      XP=XP-WP
      XD=(XD-WD)/40.
      XY=XY-WY
      XL=(XL-WL)/10.

C     CALCULATE UNCORRECTED COEFFICIENTS

      Z=Q*AREA
      CLU=-XL/Z
      CDU=XD/Z

C     WING VOLUME IS 2131.236 SQ IN
C     K1=1.044  T2=.21   T1=.87  C=136  DELTA=.116
      ESB=(1.044*.87*1.233)/1586.
      PI=3.14159
      A=9.5
      CDUP=CDU-(CLU*CLU)/(PI*A)
      EWB=(8.22*CDUP)/544.
      DALF=0.413*CLU
      DECL=-0.00167*CLU
      DECM=-.25*DECL
      DECD=.00689*CLU*CLU

      EPS=EWB+ESB

      Q=Q*((1.+EPS)**2.)
```

```
      ZC=Q*AREA
      CD=XD/ZC
      CL=-(XL/ZC)
      CS=-(XS/ZC)
      CM=-(XP/(ZC*11.52))
      CR=XR/(Q*9.688*120.)
      CY=XY/(Q*9.688*120.)
      EST=-EST
C  USE CAL1 FOR APRIL TESTS
C  USE CAL2 FOR JULY TESTS
C  CALIBRATION 14 JULY 75
C  CAL2
C     CH=((EST-12.)/184.615)/(Q*32.64*1.02)                              CAL2
      CH=(EST/266.66)/(Q*24.64*1.02)                                     CAL1
      CH=CH*144.
      CL=CL+DECL
      CD=CD+DECD
      CM=CM+DECM
      CD=CD-.0079
      CR=-CR
      CRC=(((CL*48.5)/120.)*.4244)
      CR=CR-CRC
      CY=CY+(((CD*48.5)/120.)*.4244)
      ALPHA=ALPHA/10.
      DELT=DELS+(((EST-12.)/184.615)*.238)
      DELT=DELT/57.3
      HC=(SIN(DELT)*1.02)/10.2
      TR=T+459.6
      VISC=.0000118 +(.000000016*(TR-500.))
      RHO=(.041206*BP/TR)
      VEL=((2.*Q)/RHO)**.5
      VS=49.02*SQRT(TR)
      XMACH=VEL/VS
      RNFT=32.174*VEL*RHO/VISC
      TURF=((-.00000043294)*(RNFT-794300.))+1.296
      IF (TURF-1.)94,95,95
   94 TURF=1.
   95 CONTINUE
      REY=RNFT*TURF*(11.5/12.)
      RN=REY
  200 ALPHA=ALPHA+DALF
      WRITE(IO,67)ALPHA,CL,CD,CM,CR,CS,CY,CH,Q,RN,HC
   67 FORMAT(3X,F7.3,2X,F6.3,2X,F7.5,2X,F6.3,2X,F6.3,2X,F6.3,2X,F6.4,2X,
     1F6.3,3X,F5.2,4X,E15.7,5X,F8.5)
      GO TO 23
   99 CALL EXIT
      END

UNREFERENCED STATEMENTS
 28       200

FEATURES SUPPORTED
 ONE WORD INTEGERS
 IOCS

CORE REQUIREMENTS FOR
 COMMON       0  VARIABLES     638  PROGRAM    1352

END OF COMPILATION
```

WICHITA STATE UNIVERSITY

WALTER H BEECH WIND TUNNEL

EFFECTIVENESS OF SPOILERS ON NASA-ATLIT SEMISPAN MODEL

JULY 1975

TRIANGLE SPOILER

RUN NO 16. FLAP DEFLECTION 5.DEG SPOILER DEFLECTION 10.DEG.

ALPHA	CL	CD	CM	CR	CS	CY	CH	Q	RN	H/C
-7.972	-0.328	0.03303	-0.134	0.029	-0.109	0.0110	0.042	19.75	0.9368840E 06	0.01741
-4.007	0.083	0.03050	-0.166	-0.009	-0.077	0.0093	0.190	19.79	0.9374463E 06	0.01761
-0.041	0.490	0.04257	-0.185	-0.046	-0.050	0.0113	0.274	19.79	0.9375760E 06	0.01771
3.925	0.878	0.06443	-0.199	-0.080	-0.031	0.0159	0.366	19.81	0.9378112E 06	0.01783
7.894	1.249	0.09656	-0.212	-0.115	-0.022	0.0233	0.448	19.83	0.9381571E 06	0.01794
11.865	1.586	0.13981	-0.219	-0.146	-0.023	0.0332	0.471	19.85	0.9386238E 06	0.01797
15.850	1.765	0.18892	-0.221	-0.164	-0.019	0.0449	0.506	19.88	0.9376160E 06	0.01802
19.868	1.542	0.29045	-0.264	-0.150	0.019	0.0700	0.507	19.98	0.9393085E 06	0.01802

APPENDIX II - SPOILER INCREMENTAL EFFECTS PROGRAM

In order to permit rapid evaluation of aerodynamic increments provided by deflecting spoilers, a special computer program was written. This program calculates and stores a set of baseline data (for zero spoiler deflection) in corrected coefficient form, and subtracts these baseline values from coefficients calculated from measurements made for non-zero spoiler deflections.

A signal card in the data deck identified a baseline run. The force coefficients are calculated and corrected for wall effects, etc. by the same procedure as the basic force program. The calculated baseline values for each angle of attack are then stored. (At this stage the angle of attack has not been corrected). The program then loops back to read data which is not signaled as baseline data. Increment values are then obtained by subtracting the stored baseline values from the freshly calculated coefficients. Increment values were calculated at uncorrected angles of attack of -8°, -4°, 0°, 4°, and 8°. The angle of attack corrections are then applied and the incremental values written out. These values then yield a direct measure of the effects of spoiler deflection upon the aerodynamic coefficients.

Program listing and sample output from this computing routine are shown on the pages which follow.

```
PAGE   1    01/02/76    1106    GAR,001,RINCKER

// JOB T

LOG DRIVE   CART SPEC   CART AVAIL  PHY DRIVE
  0000        0001        0001        0000

V2 M08   ACTUAL  8K  CONFIG  8K

// FOR
*LIST SOURCE PROGRAM
      FUNCTION TABL(X,NX,Y,XVAL)
      DIMENSION X(1),Y(1)
      DO 3 I=1,NX
      IF (X(I)-XVAL) 3,10,5
    3 CONTINUE
      JX=NX
      GO TO 8
    5 JX=I
      IF(JX-1)6,6,8
    6 JX=2
    8 PC=(XVAL-X(JX-1))/(X(JX)-X(JX-1))
      TABL=Y(JX-1)+PC*(Y(JX)-Y(JX-1))
      RETURN
   10 TABL=Y(I)
      RETURN
      END

FEATURES SUPPORTED
 ONE WORD INTEGERS

CORE REQUIREMENTS FOR TABL
 COMMON      0  VARIABLES     10  PROGRAM    126

RELATIVE ENTRY POINT ADDRESS IS 000C (HEX)

END OF COMPILATION

// DUP

*STORE      WS  UA  TABL
CART ID 0001   DB ADDR  2CB0   DB CNT   000A

// FOR
*LIST SOURCE PROGRAM
*IOCS  (CARD, 1132 PRINTER)
      INTEGER TN
      REAL CONFI (10)
      DIMENSION        ZL(30),ZD(30),ZP(30),ZR(30),ZS(30),ZA(30),ZY(30)
      DIMENSION EQ(3),ED(3),ER(3),ES(3),EP(3),EY(3),EA(3),EL(3)
C
C
C     ATLIT II     INCREMENTAL DATA REDUCTION
C
C
      IN=5
      IO=6
      READ(IN,800)SF
      READ(IN,1)AREA,AEROC,SCORD,SAREA,SPAN
    1 FORMAT(5F10.5)
```

```
C       READ TARE NUMBER AND NUMBER OF POINTS

      2 READ(IN,3)TN,NPTS
      3 FORMAT(I1,I2)
        IF (NPTS) 99,99,4

C       READ TARE ZERO

      4 READ(IN,8)ZQ,TZS,TZR,TZY,TZD,TZP,TZL,TZA
      8 FORMAT(10X,F3.0,1X,F5.0,1X,F5.0,1X,F5.0,1X,F5.0,1X,F5.0,1X,F5.0,5X
       1,F3.0)

C       READ TARE DATA
        DO 9 I=1,NPTS
        READ(IN,10)ZQ,ZS(I),ZR(I),ZY(I),ZD(I),ZP(I),ZL(I),ZA(I)
     10 FORMAT(10X,F3.0,1X,F5.0,1X,F5.0,1X,F5.0,1X,F5.0,1X,F5.0,1X,F5.0,5X
       1,F3.0)
      9 CONTINUE
        DO 11 I=1,NPTS
        ZL(I)=ZL(I)-TZL
        ZD(I)=ZD(I)-TZD
        ZP(I)=ZP(I)-TZP
        ZR(I)=ZR(I)-TZR
        ZS(I)=ZS(I)-TZS
        ZA(I)=ZA(I)-TZA
        ZY(I)=ZY(I)-TZY
     11 CONTINUE

C       READ INFO,WIND OFF AND TUNNEL DATA

     97 READ(IN,800)BRUN
    800 FORMAT(F10.5)
     26 CONTINUE
        READ(IN,37)DELF,DELS,CONFI
     37 FORMAT(2F10.5,10A4)
        IF (DELF-1.)57,97,57
     57 READ(IN,21)WQ,WS,WR,WY,WD,WP,WL,RUN
     21 FORMAT(10X,F3.0,1X,F5.0,1X,F5.0,1X,F5.0,1X,F5.0,1X,F5.0,1X,F5.0,23
       1X,F3.0)
        IF (RUN) 2,2,22
     22 CONTINUE

C       READ DATA

        WRITE(IO,72)
     72 FORMAT('1','1',T45,'WICHITA STATE UNIVERSITY'/)
        WRITE(IO,73)
     73 FORMAT(T44,'WALTER H BEECH WIND TUNNEL',/)
        WRITE(IO,74)
     74 FORMAT(T32,'EFFECTIVENESS OF SPOILERS ON NASA-ATLIT SEMISPAN MODEL
       1',/)
        WRITE(IO,75)
     75 FORMAT(T49,'MARCH-APRIL 1975',//)
        WRITE(IO,92)CONFI
     92 FORMAT(T40,10A4,/)
        WRITE(IO,71)RUN,DELF,DELS
     71 FORMAT(T8,'RUN NO',1X,F4.0,T25,'FLAP DEFLECTION',1X,F3.0,'DEG',8X,
       1'SPOILER DEFLECTION',1X,F3.0,'DEG.',//)
        WRITE(IO,76)
```

```
   76 FORMAT( T8,'ALPHA',6X,'H/C',5X,'DCROLL',6X,'DCD',7X,'DCM',6X,'DCYA
     1W',4X,'DCSIDE',6X,'DCL',7X,'DCH',8X,'Q',10X,'RN'/)
   23 DO 27 J=1,3
      READ(IN,25)EQ(J),ES(J),ER(J),EY(J),ED(J),EP(J),EL(J),EA(J),EST,BP,
     1T,RNO
   25 FORMAT(T11,F3.0,6F6.0,T54,F4.0,T59,F4.0,T64,F4.2,T69,F3.0,T73,F3.0
     1)
      IF (RNO) 26,26,27
   27 CONTINUE
      DELS=DELS
   28 IF (RUN-RNO) 99,29,99
   29 ALPHA=(EA(1)+EA(2)+EA(3))/3.
      IF (ALPHA-EA(1)) 31,32,31
   31 WRITE(IO,66)
   66 FORMAT(10X,'ERROR')
      GO TO 23
   32 XL=(EL(1)+EL(2)+EL(3))/3.
      XD=(ED(1)+ED(2)+ED(3))/3.
      XP=(EP(1)+EP(2)+EP(3))/3.
      XR=(ER(1)+ER(2)+ER(3))/3.
      XS=(ES(1)+ES(2)+ES(3))/3.
      XY=(EY(1)+EY(2)+EY(3))/3.
      Q=(EQ(1)+EQ(2)+EQ(3))/3.
      XD=(XD-TABL(ZA,NPTS,ZD,ALPHA))
      XL=(XL-TABL(ZA,NPTS,ZL,ALPHA))
      XR=(XR-TABL(ZA,NPTS,ZR,ALPHA))
      XP=(XP-TABL(ZA,NPTS,ZP,ALPHA))
      XY=(XY-TABL(ZA,NPTS,ZY,ALPHA))
      XS=(XS-TABL(ZA,NPTS,ZS,ALPHA))
      Q=Q/10.
      Q=Q*.987

C     SUBTRACT WIND OFF AND DIVIDE BY SCALE FACTOR

      XS=(XS-WS)/5.
      XR=XR-WR
      XP=XP-WP
      XD=(XD-WD)/40.
      XY=XY-WY
      XL=(XL-WL)/10.

C     CALCULATE UNCORRECTED COEFFICIENTS

      Z=Q*AREA
      CLU=XL/Z
      CDU=XD/Z
      CMU=XP/(Z*11.5)
      CRU=XR/(Q*9.688*120.)
      CSU=XS/Z
      CYU=XY/(Q*9.688*120.)

C     WING VOLUME IS 2131.236 SQ IN
C     K1=1.044   T2=.21   T1=.87   C=136   DELTA=.116
      ESB=(1.044*.87*1.233)/1586.
      EWB=(8.22*CDU)/544.
      DALF=.21*.116*.0604*CLU
      DECL=-DALF*.00139
      DECM=-.25*DECL
```

```
      EPS=EWB+ESB
      Q=Q*((1.+EPS)**2.)
      ZC=Q*AREA
      CD=XD/ZC
      CL=-(XL/ZC)
      CS=-(XS/ZC)
      CM=-(XP/(ZC*11.52))
      CR=XR/(Q*9.688*120.)
      CY=XY/(Q*9.688*120.)
C     USE SF= 266.66 FOR APRIL DATA, SF= 184.615 FOR JULY DATA.
      CH=(EST/SF)/(Q*32.64*1.02)
      CH=CH*144.
      CL=CL+DECL
      CM=CM+DECM
      CD=CD-.0079
      CR=-CR
      CRC=(((CL*48.5)/120.)*.4244)
      CR=CR-CRC
      CY=CY+(((CD*48.5)/120.)*.4244)
      ALPHA=ALPHA/10.
      DELT=DELS+((EST/SF)*.238)
      DELT=DELT/57.3
      HC=(SIN(DELT)*1.02)/10.2
      TR=T+459.6
      VISC=.0000118 +(.000000016*(TR-500.))
      RHO=(.041206*BP/TR)
      VEL=((2.*Q)/RHO)**.5
      VS=49.02*SQRT(TR)
      XMACH=VEL/VS
      RNFT=32.174*VEL*RHO/VISC
      TURF=((-.00000043294)*(RNFT-794300.))+1.296
      IF (TURF-1.)94,95,95
   94 TURF=1.
   95 CONTINUE
      REY=RNFT*TURF*(11.5/12.)
      RN=REY
      IF(RUN-BRUN)111,499,111
  499 IF (ALPHA-8.)632,620,199
  632 IF (ALPHA-4.)633,621,199
  633 IF (ALPHA-0.)634,622,199
  634 IF (ALPHA+4.)635,623,199
  635 IF (ALPHA+8.)199,624,199
  620 CLBAE=CL
      CDBAE=CD
      CMBAE=CM
      CSBAE=CS
      CYBAE=CY
      CRBAE=CR
      CHBAE=CH
      GO TO 23
  621 CLBBE=CL
      CDBBE=CD
      CMBBE=CM
      CSBBE=CS
      CYBBE=CY
      CRBBE=CR
      CHBBE=CH
```

```
      GO TO 23
  622 CLBCE=CL
      CDBCE=CD
      CMBCE=CM
      CSBCE=CS
      CYBCE=CY
      CRBCE=CR
      CHBCE=CH
      GO TO 23
  623 CLBDE=CL
      CDBDE=CD
      CMBDE=CM
      CSBDE=CS
      CYBDE=CY
      CRBDE=CR
      CHBDE=CH
      GO TO 23
  624 CLBEE=CL
      CDBEE=CD
      CMBEE=CM
      CRBEE=CR
      CSBEE=CS
      CYBEE=CY
      CHBEE=CH
      GO TO 23
  111 IF (ALPHA-8.)132,120,199
  132 IF (ALPHA-4.)133,121,199
  133 IF ( ALPHA-0.)134,122,199
  134 IF (ALPHA+4.)135,123,199
  135 IF (ALPHA+8.)199,124,199
  120 DCL=CL-CLBAE
      DCD=CD-CDBAE
      DCR=CR-CRBAE
      DCM=CM-CMBAE
      DCS=CS-CSBAE
      DCY=CY-CYBAE
      DCH=CH-CHBAE
      GO TO 200

  121 DCL=CL-CLBBE
      DCD=CD-CDBBE
      DCR=CR-CRBBE
      DCM=CM-CMBBE
      DCS=CS-CSBBE
      DCY=CY-CYBBE
      DCH=CH-CHBBE
      GO TO 200

  122 DCL=CL-CLBCE
      DCD=CD-CDBCE
      DCR=CR-CRBCE
      DCM=CM-CMBCE
      DCS=CS-CSBCE
      DCY=CY-CYBCE
      DCH=CH-CHBCE
      GO TO 200

  123 DCL=CL-CLBDE
      DCD=CD-CDBDE
```

```
      DCR=CR-CRBDE
      DCM=CM-CMBDE
      DCS=CS-CSBDE
      DCY=CY-CYBDE
      DCH=CH-CHBDE
      GO TO 200
  124 DCL=CL-CLBEE
      DCD=CD-CDBEE
      DCR=CR-CRBEE
      DCM=CM-CMBEE
      DCS=CS-CSBEE
      DCY=CY-CYBEE
      DCH=CH-CHBEE
      GO TO 200

  200 ALPHA=ALPHA+DALF
      WRITE(IO,89)ALPHA,HC,DCR,DCD,DCM,DCY,DCS,DCL,DCH,Q,RN
   89 FORMAT(4X,10F10.5,E15.5)
  199 GO TO 23
   99 CALL EXIT
      END

UNREFERENCED STATEMENTS
 28

FEATURES SUPPORTED
 ONE WORD INTEGERS
 IOCS

CORE REQUIREMENTS FOR
 COMMON      0  VARIABLES    726  PROGRAM   1824

END OF COMPILATION

// XEQ

// EOJ
```

WICHITA STATE UNIVERSITY

WALTER H BEECH WIND TUNNEL

EFFECTIVENESS OF SPOILERS ON NASA-ATLIT SEMISPAN MODEL

MARCH-APRIL 1975

TRIANGLE SPOILER

RUN NO-- 72. FLAP DEFLECTION 0.DEG SPOILER DEFLECTION 30.DEG.

ALPHA	H/C	DCROLL	DCD	DCM	DCYAW	DCSIDE	DCL	DCH
-3.96464	0.04939	0.03448	0.03467	0.04380	0.00719	-0.03432	-0.26515	-0.45875
0.00541	0.04945	0.03268	0.02597	0.03838	0.00534	-0.02875	-0.25210	-0.45939
3.97614	0.04952	0.03043	0.02014	0.03381	0.00412	-0.02537	-0.23124	-0.44074
7.94774	0.04959	0.02629	0.01461	0.02739	0.00298	-0.02291	-0.19763	-0.42409